Deanship of Graduate Studies

Al-Quds University

Low density polyethylene/zinc peroxide composite and nanocomposite prepared by cast solution: Thermal, mechanical and morphological characterization

Hanibal Mousa Issa Mansour

M.Sc. Thesis

Jerusalem - Palestine

2023 \1444

Low density polyethylene/zinc peroxide composite and nanocomposite prepared by cast solution: Thermal, mechanical and morphological characterization

Prepared By:

Hanibal Mousa Issa Mansour

M.S. Applied Industrial Technology. Al-Quds University.

Jerusalem- Palestine

Supervisor: Dr. Ahmad Al-Jabareen

Co-Supervision: Prof. Dr. Fuad Al-Rimawi

A Thesis Submitted in Partial Fulfillment of the requirement for the degree of Master of Applied Industrial Technology.

Al-Quds University- Palestine

2023\1444

Al-Quds University
Deanship of Graduate Studies
Applied and Industrial Technology Program

Thesis Approval

Low density polyethylene/zinc peroxide composite and nanocomposite prepared by cast solution: Thermal, mechanical and morphological characterization

Prepared by: Hanibal Mousa Issa Mansour
Registration Number: 21920273

Supervisor: Dr. Ahmad Al-Jabareen

Co-Supervisor: Prof. Dr. Fuad Al-Rimawi

Master thesis submitted and accepted, Date 06/05/2023

The names and signatures of the examining committee are as follows:

1. Dr. Ahmad Al-Jabareen:	Committee Member,	Signature: .....
2. Prof. Fuad Al-Rimawi:	Co-supervisor,	Signature: .....
3. Dr. Raed Mali	Internal Examiner,	Signature: .....
4. Dr. Yaseen Qawasmi	External Examiner,	Signature: .....

Jerusalem/ Palestine

1444/2023

Dedication

Thank and blessing for Allah

I dedicate this thesis to my dear parents who gave me the best assistance at this journey and their full support. They planted the seed of love for learning and knowledge inside me. I also would like to dedicate this work to my brother and lovely sisters Al-Moez, Aseel and Adeel who are a piece of my heart and who have always been a major source of support and encouragement. In the end, I dedicate this thesis to my friends and to every staff member in Al-Quds University who helped me with patience and love.

Thank you very much.

Hanibal Mousa Issa Mansour

Declaration

I certify that this thesis submitted for the degree of master is my own research, except where otherwise acknowledged, and that this thesis (or any part of the same) has not been submitted for higher degree to any other university or institution.

Signed: .....

Hanibal Mousa Issa Mansour

Date: 06/05/2023

Acknowledgments

After all these long years, ambition never comes to an end. A journey of thousand begins with a step. I finally achieved this dream.

At the outset, I thank and extend gratitude to God almighty, thank you for the blessings you have bestowed on my life. You have provided me with more than I could ever have imagined.

I would like to express my deepest appreciation and thanks to my supervisor Dr. Ahmad Al-Jabareen for giving me the opportunity to work with him, many thanks to his kindness and knowledge I acquired from his huge experience.

I would like also to thanks to my Co-supervisor Prof. Fuad Al-Rimawi for standing by me and providing all possible facilities for the completion of this research and helping me in this thesis.

A special thanks to Prof. Omar Ayyad, for standing beside me throughout my years of university, and I do not forget the credit given to me with support and encouragement.

I also extend my thanks to all laboratory technicians in the faculties of engineering, especially Mrs. Mariam Faroun and Eng. Mohammed AL-Bawwab and extend my thank to Al-Makassed Hospital medical labs, especially Mrs. Suzan Idkeidek, you have been like my family in standing and supporting me to reach where I am now. Thank you very much

In addition, thanks to all my gratitude and appreciate to everyone, who supported me and stood by me during this stage of my life

Hanibal Mousa Issa Mansour.

Abstract

Polymer composite and nanocomposite materials with inorganic filler like metal oxides such as zinc oxide, magnesium oxide and zinc peroxide are motive fields of research due to the innovative combination of properties between the polymer and filler, arising from the application of inorganic filler and nanofiller within polymer matrix. The present study investigated the influence of different concentration of zinc peroxide (ZnO_2) particles and nanoparticles on the thermal, mechanical, morphological, and antibacterial properties of low-density polyethylene (LDPE)/ZnO_2 composite and nanocomposite. Different compositions of LDPE/ZnO_2 and LDPE/nano ZnO_2 composites were prepared by solution cast technique with ZnO_2 concentration of (1wt%, 3wt % and 5wt%) for composite and (0.5wt%, 1wt%, 1.5wt%, 3wt% and 5wt %) for nanocomposite. Firstly, ZnO_2 nanoparticles were synthesized using three different methods, the first one reflux reaction method used polyethyleneimine (PEI) as capping agent and the second one reflux reaction method without capping agent and the last one sol-gel method. Reflux reaction method without capping agent was chosen for preparing nanocomposite, because it has the good reaction percentage yield compared to the other methods. The synthesized ZnO_2 nanoparticles were characterized by X-Ray Diffraction (XRD), Scanning electron microscope (SEM), Fourier-transform infrared spectroscopy (FTIR) and Differential scanning calorimetry (DSC). Highly crystalline cubic-ZnO_2 nanoparticles grown in a near- spherical shape were obtained with average size about 82 nm ,48 nm and 55 nm for reflux without PEI, reflux with PEI and sol-gel respectively, based on SEM and XRD analysis. It was found by DSC that the synthesized ZnO_2 samples decomposes into zinc oxide (ZnO) at about 230-238 ^oC. The observed vibrational modes by FTIR in the ZnO_2 nano-powder are discussed and compared with previous reports and suggest the purity of the ZnO_2 particles that synthesized from the reactants. The results of the morphological analyses of composite shows a distribution of ZnO_2 in the LDPE matrix with little signs of agglomerates and the particles were embedded in the matrices of the composite but they don't appear well on the surface of composite. For the nanocomposite, The SEM micrographs show that the nanoparticles are well distribution within the whole polymer matrix. The micrograph of the nanocomposite with ZnO_2 nanoparticles filler showed a distinct dispersion behavior as that of the composite containing the ZnO_2 filler. The addition of ZnO_2 filler in the composite and nanocomposite imparted slight variations in the melting temperature of

different concentration of composite and nanocomposite samples and gave significant improvements in the degree of crystallinity since the filler could act as a nucleating agent. The results of mechanical characterization showed that the tensile properties of LDPE/ZnO_2 nanocomposites are higher than those of LDPE/ZnO_2 composites except yield strength which mean that the composite can withstand high stress without a permanent plastic deformation as compared to nanocomposite. It was found that LDPE without any filler achieved a tensile strength of 4.94 MPa and the tensile strength of ZnO_2 /LDPE nanocomposites increased with increasing ZnO_2 nanoparticles concentration until reaching the highest value of tensile strength 5.28 MPa at 5wt% of nanoparticles, while the tensile strengths of the composites decreased with increased concentration of ZnO_2 powder and dropped to 4.35 MPa at 5wt% ZnO_2 particles. The elastic modulus of ZnO_2 /LDPE composite and nanocomposite was found to increase progressively with ZnO_2 concentration, the highest set of values was obtained for 5 % concentration of ZnO_2 for nanocomposite with the modulus value 0.124 GPa compared to pure LDPE with modulus value 0.103 GPa. As well the fracture strength increased as the nanofiller size decreased to nano sized as compare to composite, so the nanocomposite has higher ability to resist failure than composite. Moreover, the elongation at fracture decreased steadily with increasing in ZnO_2 concentration for the composite from 36 % to 29 % and for nanocomposite from 48 % to 42 %. Unfortunately, the antibacterial characterization of composite and nanocomposite did not show any zone of inhibition on agar plates for composites and nanocomposite against aerobic and anaerobic bacterias.

Table of content

- Declaration i
- Acknowledgment ii
- Abstract iii
- Table of the Content v
- List of Table viii
- List of figures ix
- List of abbreviation, symbols and terminology xiii

Chapter one: Introduction 1

1.1 Plastic materials 2

1.1.1 Thermoplastic polyethylene (PE) 3

1.2 Composite materials 5

1.2.1 Polymer matrix composites 7

1.2.2 Polymer matrix nanocomposites 8

1.3 Inorganics metal oxides filler 9

1.3.1 Zinc peroxide filler 9

1.3.2 Zinc peroxide nanofiller 9

1.4 Antimicrobial activity of ZnO_2 nanoparticles 11

1.5 Plastic composite/nanocomposite processing 14

1.6 Research questions 16

1.7 Research aims and objectives 16

Chapter 2: literature Review 17

2.1 Synthesis of zinc peroxide nanoparticles 18

2.2 Antibacterial activity of synthesized zinc peroxide nanoparticles 19

2.3 Metal oxides nanocomposite 21

Chapter Three: Material and Methodology **23**

3.1 Materials 24

3.1.1 Low density polyethylene 24

3.1.2 Xylene 26

3.1.3 Zinc peroxide 27

3.1.4 Zinc Peroxide nanoparticles. 28

3.1.4.1 Zinc acetate dihydrate 28

3.1.4.2 Hydrogen peroxide 29

3.1.4.3 Polyethyleneimine 30

3.2 Preparation of Samples 31

3.2.1 Synthesis of zinc peroxide nanoparticles: 31

3.2.1.1 Synthesis of zinc peroxide NP's by refluxing method. 32

3.2.1.2 Synthesis of zinc peroxide by a Sol-gel method. 33

3.2.2 Preparation of LDPE/ZnO_2 composite and nanocomposite. 34

3.3 Experimental methods. 36

3.3.1 X-Ray diffraction. 36

3.3.2 Scanning Electron Microscopy. 36

3.3.3 Fourier-Transform Infrared Spectroscopy. 37

3.3.4 Differential Scanning Calorimetry. 38

3.3.5 Tensile properties test 40

3.3.6 Antibacterial activity Test. 44

3.3.6.1 Antibacterial test for composite and nanocomposite. 44

Chapter Four: Result and Discussions **45**

4.1 Physico-chemical Characterization **46**

4.1.1 X-ray Diffraction analysis 46

4.1.1.1 Zinc peroxide purchased material 46

4.1.1.2 Synthetized zinc peroxide nanoparticles (ZnO_2 NP's) 47

4.1.2 Morphological characterization 48

4.1.2.1	Zinc peroxide purchased material	48
4.1.2.2	Synthetized zinc peroxide nanoparticles (ZnO_2 NP's)	49
4.1.2.3	Composite and nanocomposite	53
4.1.3	Fourier-transform infrared spectroscopy analysis	61
4.1.3.1	Synthetized zinc peroxide nanoparticles (ZnO_2 NP's)	61
4.2	**Thermal Characterization**	**62**
4.2.1	Zinc peroxide (ZnO_2) used material	62
4.2.2	Synthetized zinc peroxide nanoparticles (ZnO_2 NP's)	63
4.2.3	Composite and nanocomposite	65
4.3	**Mechanical characterization**	**71**
4.3.1	Tensile strength	73
4.3.2	Elastic modulus	76
4.3.3	Yield strength	78
4.3.4	Fracture strength	80
4.3.5	% Elongation at fracture	82
4.4	**Antibacterial characterization**	**85**
4.4.1	Composite and nanocomposite	85
Chapter 5: Conclusion and future work		**88**
5.1	Conclusion	89
5.2	Future work	90
References		**91**
الملخص باللغة العربية		**105**

List of Tables

Table 1.1	Some of the most popular types of thermoplastic polymers used.	2
Table 1.2	Polyethylene classification based on conformation and density	4
Table 1.3	Chemical families of reinforcements for plastic	6
Table 3.1	Properties of used low-density polyethylene	25
Table 3.2	Properties of used xylene.	26
Table 3.3	Zinc peroxide used properties	27
Table 3.4	Zinc acetate dihydrate properties.	28
Table 3.5	Hydrogen peroxide properties.	29
Table 3.6	Properties of Polyethyleneimine	30
Table 3.7	Synthesized ZnO_2 nanoparticles codes for method used	31
Table 3.8	Composite materials based on zinc peroxide / low density polyethylene codes of material used.	34
Table 4.1	Experimental X-ray diffraction pattern of purchased zinc peroxide particles.	46
Table 4.2	X-Ray diffraction analysis data of synthetized zinc peroxide nanoparticles	47
Table 4.3	Characteristic parameter of ZnO_2 NP's obtained from analysis of their SEM micrograph	50
Table 4.4	Characteristic parameter of ZnO_2 NP's and their percentage yields of reactions.	52
Table 4.5	Thermal properties of zinc peroxide obtained from differential scanning calorimetry	63
Table 4.6	Melting and crystallization temperature as a function of zinc peroxide concentration obtain from DSC curves for composite and nanocomposite.	67
Table 4.7	Particle size histograms obtained from image analysis of the SEM micrograph, where A1: reflux without PEI, A2: reflux with PEI and B: sol-gel method.	68
Table 4.8	Tensile properties of composites materials.	72
Table 4.9	Tensile properties of nanocomposites materials.	72

List of Figures

Figure 1.1	Addition polymerization of Polyethylene with one of the possible termination steps.	3
Figure 1.2	Reinforcements forms	6
Figure 1.3	Composite material that contains particle as reinforcement in polymer matrix.	7
Figure 1.4	Nanocomposite material based on nanoparticles with polymer matrix.	8
Figure 1.5	Scheme of top-down and bottom-up synthesis of nanoparticles (NPs).	10
Figure 1.6	Schematic of zinc peroxide nanoparticles and the resulting antibacterial effect.	11
Figure 1.7	Mechanisms of action of the bactericidal effect from metal oxides nanoparticles.	12
Figure 1.8	Solution casting technique of Composite samples	15
Figure 3.1	Low density polyethylene structure and ethylene monomer.	24
Figure 3.2	Low density polyethylene pellets obtained from the Materials Engineering faculty, Al-Quds University.	25
Figure 3.3	Three structural of xylene, A: (Ortho-xylene), B: (meta-xylene) and C: (para-xylene).	26
Figure 3.4	Zinc peroxide structure.	27
Figure 3.5	Zinc Acetate Dihydrate structure	28
Figure 3.6	Hydrogen peroxide structure.	29
Figure 3.7	Repeating unit of liner and branched Polyethylenimine.	30
Figure 3.8	Synthesized of zinc peroxide NP's by refluxing.	32
Figure 3.9	Steps of Preparation of LDPE/ZnO_2 composite and nanocomposite.	35
Figure 3.10	Dogbone samples of each concentration for tests.	35
Figure 3.11	Fourier-transform infrared spectroscopy at Pharmacy laboratory at Al-Quds University-East Jerusalem.	37
Figure 3.12	Differential Scanning Calorimetry (DSC) peak analysis.	38
Figure 3.13	Differential scanning calorimeter (DSC) at the nanotechnology research laboratory at Al-Quds University-East Jerusalem.	39
Figure 3.14	Preparation of composite and nanocomposite samples for DSC.	39

Figure 3.15	Industrial plastic center machine amatrol T9013-p	40
Figure 3.16	A: Universal testing machine of polymer (tensile test) B: Tensile specimens during testing	40
Figure 3.17	Tensile bar dimensions type IV ASTM D638.	41
Figure 3.18	Yield Point and Yield strength.	42
Figure 3.19	Engineering stress-strain curve	43
Figure 3.20	Antimicrobial Activity of composite and nanocomposite.	44
Figure 4.1	Experimental X-ray diffraction pattern of zinc peroxide (C).	46
Figure 4.2	X-ray diffraction pattern of synthesized zinc peroxide nanoparticles.	47
Figure 4.3	SEM images of the purchased zinc peroxide particles.	48
Figure 4.4	SEM images of the ZnO_2 nanoparticles by reflux method without PEI, (Scale bar 500 nm).	49
Figure 4.5	SEM images of the ZnO_2 nanoparticles by reflux method with PEI. (Scale bar 500 nm).	49
Figure 4.6	SEM images of the ZnO_2 nanoparticles by Sol-gel method (B). (Scale bar 500 nm).	50
Figure 4.7	Particle size histograms obtained from image analysis of the SEM micrograph.	51
Figure 4.8	SEM micrographs from the surface of pure LDPE prepared by solution method.	53
Figure 4.9	SEM micrographs from the surface of the LDPE composite with 1% concentration of ZnO_2 particles.	54
Figure 4.10	SEM micrographs from the surface of the LDPE composite with 3% concentration of ZnO_2 particles.	55
Figure 4.11	SEM micrographs from the surface of the LDPE composite with 5% concentration of ZnO_2 particles.	55
Figure 4.12	SEM micrographs from the surface of the LDPE nanocomposite with 0.5% concentration of ZnO_2 NP's.	56
Figure 4.13	SEM micrographs from the surface of the LDPE nanocomposite with 1% concentration of ZnO_2 NP's.	57
Figure 4.14	SEM micrographs from the surface of the LDPE nanocomposite with 1.5% concentration of ZnO_2 NP's.	58

Figure 4.15	SEM micrographs from the surface of the LDPE nanocomposite with 3% concentration of ZnO_2 NP's.	59
Figure 4.16	SEM micrographs from the surface of the LDPE nanocomposite with 5% concentration of ZnO_2 NP's.	60
Figure 4.17	Fourier-transform infrared spectrum of the synthetized ZnO_2 -NPs.	61
Figure 4.18	Differential scanning calorimetric curve of used zinc peroxide.	62
Figure 4.19	Differential scanning calorimetric curves of the synthetized ZnO_2	63
Figure 4.20	DSC scans of composites where (A): Heating 1st scan, (B): Heating 2nd scan, (C): Cooling 1st scan and (D) Cooling 2nd scan.	65
Figure 4.21	DSC scans of nanocomposites where (A): Heating 1st scan, (B): Heating 2nd scan, (C): Cooling 1st scan and (D) Cooling 2nd scan.	66
Figure 4.22	% Degree of crystallinity trend for: (a) Composite, (b) Nanocomposite.	69
Figure 4.23	Stress-strain curves behavior, where (A): composite samples and (B): nanocomposite samples.	71
Figure 4.24	Tensile strength of nanocomposite, with different concentration of zinc peroxide NP's.	73
Figure 4.25	Ultimate tensile strength of composite, with different concentration of zinc peroxide.	74
Figure 4.26	Ultimate tensile strength of composite and nanocomposite, with different concentration of zinc peroxide.	75
Figure 4.27	Elastic modulus of composite and nanocomposite, with different concentration of ZnO_2.	76
Figure 4.28	Elastic modulus of composite and nanocomposite, with different concentration of ZnO_2.	77
Figure 4.29	Yield strength of composite and nanocomposite, with different concentration of ZnO_2.	78
Figure 4.30	Yield strength of composite and nanocomposite, with different concentration of ZnO_2.	79
Figure 4.31	Fracture strength of nanocomposite with different concentration ZnO_2.	80
Figure 4.32	Fracture strength of composite, with different concentration ZnO_2.	81
Figure 4.33	Fracture strength of composite and nanocomposite, with different concentration ZnO_2.	81
Figure 4.34	% Elongation at fracture of composite, with different concentration ZnO_2.	82

Figure 4.35	% Elongation at fracture of nanocomposite, with different concentration ZnO_2 NP's.	83
Figure 4.36	% Elongation at fracture of composite and nanocomposite, with different concentration ZnO_2.	84
Figure 4.37	Disc diffusion tests for the evaluation of antimicrobial activity of different concentration of composite against aerobic strains where (A): Staphylococcus aureus, (B): Escherichia coli and (C): pseudomonas aeruginosa.	85
Figure 4.38	Disc diffusion tests for the evaluation of antimicrobial activity of different concentration of nano composite against aerobic strains where (A): Staphylococcus aureus, (B): Escherichia coli and (C): pseudomonas aeruginosa.	86
Figure 4.39	Disc diffusion tests for the evaluation of antimicrobial activity of different concentration of composite against anerobic bacteria strain where (A): anerobic gram-positive streptococcus and (B): anaerobic gram-negative bacilli.	86
Figure 4.40	Disc diffusion tests for the evaluation of antimicrobial activity of different concentration of nanocomposite against anerobic bacteria strain where: (C): anerobic gram-positive streptococcus and (D): anaerobic gram-negative bacilli.	87

Abbreviations, symbols and terminology

Abbreviation	Description
PE	Polyethylene
LDPE	Low density polyethylene
HDPE	High density polyethylene
PP	Polypropylene
PEC	Polyethylene composite
PEN	Polyethylene nanocomposite
ZnO_2	Zinc peroxide
NP's	Nanoparticles
ZnO_2-NP's	Zinc peroxide nanoparticles
ZnO	Zinc oxide
H_2O_2	Hydrogen peroxide
ROS	Reactive oxygen species
PEG	Polyethylene glycol
PVP	Polyvinylpyrrolidone
PEI	Polyethyleneimine
TEM	Transmission electron microscopy
SEM	Scanning electron microscope
TGA	Thermogravimetric analysis
DSC	Differential scanning calorimetry
XRD	X-Ray diffraction
FTIR	Fourier-transform infrared spectroscopy
rpm	Round per minute
Rv	Volume average radius
(Nv)i	The number of particles
PDI	Polydispersity index
Tg	Glass transition temperature
Tm	Melting point

Tc	Crystallization temperature
ΔH_c	Change in heat of crystallization
ΔH_f	Change in heat of melting
Xc	Degree of crystallinity
ΔH_m	Change in enthalpy of the final melting
ΔH_{fo}	Change in heat of fusion
ASTM	American Society for testing and Materials
UTS	Ultimate tensile strength
E	Elastic modulus
ε	Strain
σ	Stress
L	Length after load is applied
L_0	Original length
2θ Deg	Two theta degree
nm	Nanometer
MPa	Mega pascal
GPa	Giga pascal
S. aureus	Staphylococcus aureus
MRSA	Methicillin-resistant Staphylococcus aureus
E. coli	Escherichia coli

Chapter One

Introduction

1.1 Plastic Materials

The plastics industry is considered as one of the greatest industries in the world in the twenty first century, and includes global production, synthesis, recycling and sale of plastic products. Plastics are a broad group of synthetic and semi-synthetic materials in which a polymer is the main component, it's produced in chemical factories by the polymerization of its starting materials that called monomers, which are almost petrochemical in nature. (Klein, 2012)

In general, petrochemical plastics are categorized into thermoplastics, thermosets and elastomers, including flexible and rigid form. Thermoplastics are either amorphous or semi-crystalline, amorphous are disordered oriented macromolecules whereas semi-crystalline macromolecules are nearly ordered since they are embedded with crystalline phases. Thermoplastic can be processed and recycled using heat, the ability to reprocess this group of plastics makes them recyclable and it can be used again, as they can be easily molded into different shapes. This is different from thermosets and elastomers; these polymers are cross-linked and so cannot be melted for recycling purpose. (Scharff, 2012)

Thermoplastics are seen as superior to thermoset polymers as a result of its distinctive properties, that involves no chemical bonding and they can be poured into a mold to cool and solidify into the desired shape in contrast to the thermoset, commonly used thermoplastics are shown in table (1.1) with their properties and monomers. (Lagaron, et al, 2008)

Table (1.1): Some of the most popular types of thermoplastic polymers used.

Name(s)	Formula	Monomer	Properties
Low density polyethylene (LDPE)	$-(CH_2-CH_2)_n-$	$CH_2=CH_2$	Soft, waxy solid
High density polyethylene (HDPE)	$-(CH_2-CH_2)_n-$	$CH_2=CH_2$	Rigid, translucent solid
Polypropylene (PP)	$-[CH_2-CH(CH_3)]_n-$	$CH_2=CHCH_3$	Atactic: soft, elastic, solid Isotactic: hard, strong solid
Poly vinyl chloride (PVC)	$-(CH_2-CHCl)_n-$	$CH_2=CHCl$	Strong rigid solid
Polystyrene (PS)	$-[CH_2-CH(C_6H_5)]_n-$	$CH_2=CHC_6H_5$	Hard, rigid, clear solid, soluble in organic solvent

1.1.1 Thermoplastic Polyethylene (PE)

Thermoplastic polyethylene is one of the most investigated polymers used in application, which are used in this study, owing to its low density, low cost, easiness in process by commonly used equipment for manufacturing plastic materials, such as injection molding, blown film extrusion, compression molding, casting, and extrusion, its chemical resistance, and also good mechanical properties. (Almaadeed, et al, 2013)

Polyethylene is a petrochemical product that is derived from the monomer ethylene. The polyethylene polymer is produced through a process of monomer link called addition polymerization. In this process, heat and an initiator or a catalyst are added to combine monomers together. Thus, ethylene molecules are polymerized into very long polymer molecules or chains as showed in figure (1.1). (Ebewele, 2000)

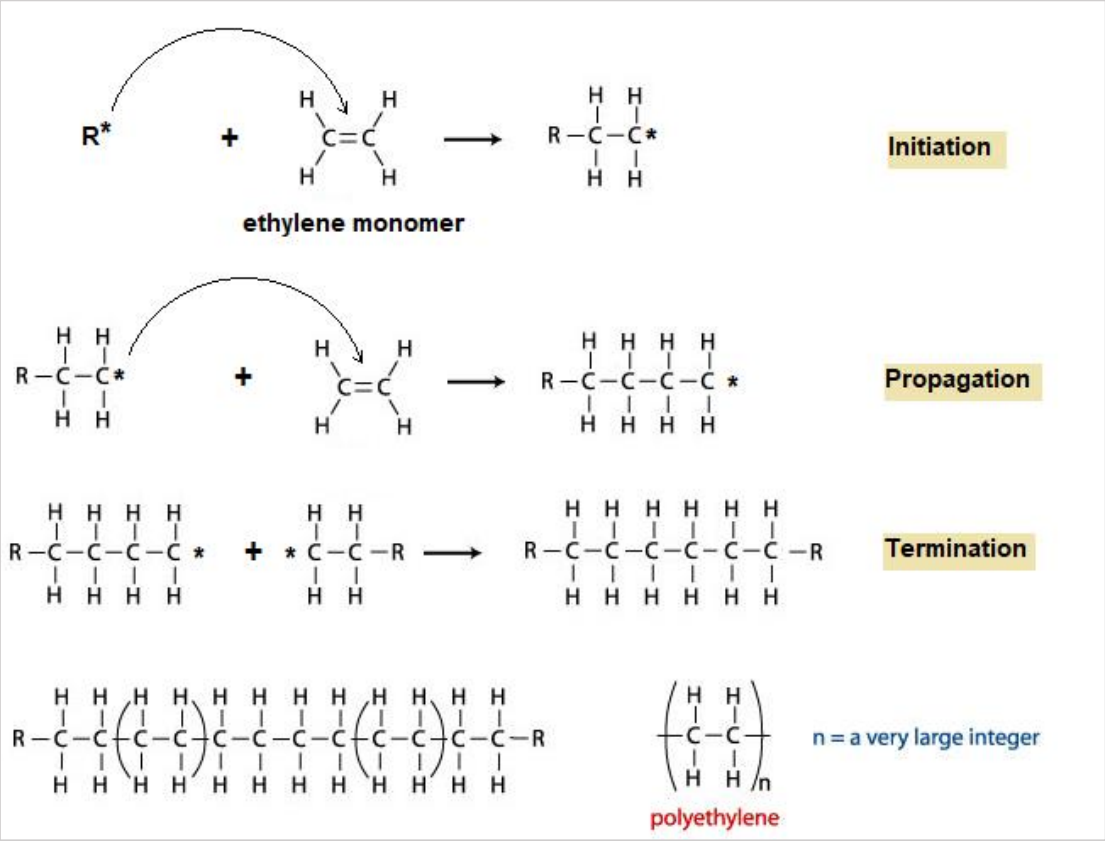

Figure (1.1): Addition polymerization of polyethylene with one of the possible termination steps.

According to other studies (Brown, et al, 2007) and (Omar, et al, 2012) polyethylene is characterized primarily based on the density and the degree of molecule branching, LDPE is a flexible polymer with long branch that do not pack well as the HDPE that its liner with packed more closely and this was proved by the density of both types, polyethylene classification shown in table (1.2).

Table (1.2): Polyethylene classification based on conformation and density. (Jordan, et al, 2016)

Polymer	**Confirmation**	**Density (g/ cm^3)**
Low density polyethylene (LDPE)	Long branches do not pack into crystal well	0.910–0.925
Liner low density polyethylene (LLDPE)	shorter branches than LDPE	0.915–0.925
High density polyethylene (HDPE)	Linear chains increase crystal packing	0.941–0.965
Ultra-high molecular weight polyethylene (UHMWPE)	Long, linear chains effectively transfer load to polymer backbone	0.930–0.935
Cross linked polyethylene (PEX)	Cross linked chains	0.940

Many studies on composite materials with different polymer matrices, such as high-density polyethylene (HDPE) (Mwafy, et al, 2015), polystyrene (PS) (Chae, et al, 2005), poly(methyl methacrylate)(PMMA)(Zeng, et al, 2010) and polypropylene carbonate (Seo, et al, 2011), aim to upgrade polymer properties to match the profile of a typical engineering plastic and also to give some of the advantages, such as high resistance to abrasion and corrosion and high stiffness and strength, the studies selected a polymer matrix for polymer/filler composites and used them in appropriate applications, as our study did. (Khashaba, 2013)

1.2 Composite materials:

Currently, materials that consist multiple materials with at least two properties are widely used in daily life. These materials are often called composite, which is the common name, because they combine two or more constituent materials, due to the fact that the properties of the composites are better than those of the original components individually and the different materials in the composite work together to give the composite unique properties. (Rajak, 2019)

Composite materials are usually classified by the type of material that used for the matrix; however, the matrix materials are generally ceramics, metals, and polymers, this gives the ability to create a limitless number of new material systems which have unique properties that cannot be obtained with any single material and the matrices hold and protect the reinforcing material from environmental and physical damage. The classification of composite based on the matrix materials are: (Sharma, et al, 2020)

- Polymer Matrix Composites (PMC's).
- Metal Matrix Composites (MMC's).
- Ceramic Matrix Composites (CMC's).

The most common type of composite is PMC's, also known as fiber reinforced polymers (FRP). They are used in the largest quantities due to their good room temperature properties, ease of manufacture and low cost, while the metal matrices have a high working temperature range and the most commonly metal used as matrices are light weight alloys such as, magnesium, aluminum and titanium. (Roylance, 2000)

MMC's are used in several application such as car engines and turbine blades. However, due to processing complexity and higher density of metal matrix as compared to polymer matrices, they are less commonly used. CMC's these materials use a ceramic as the matrix and reinforce it with short fibers. These composites are used in very high temperature environments and are not as commonly used as polymers, because they are brittle and difficult to process, the main matrices used are alumina (Al_2O), silica (SiO_2). Categories of composites have very different properties and applications. Understanding the performance differences can help to make better sourcing decisions and help in product designs as composite. (Cantor, et al, 2003) (Zhang, 2014)

The strength, density and most of the properties of the composite material are very dependent on the reinforcing material. The additives that improve the properties of composite may be continuous, e.g., long fibers or ribbons and these are incorporated into the matrix with regular arrangements that extend throughout the dimensions of the composite or particles and discontinues (short) such as short fibers, flakes, platelets or spheres and these are dispersed throughout the continuous matrix without specific arrangement. Figure (1.2) showed the reinforcement forms that used in composite materials. (Kutz, 2015)

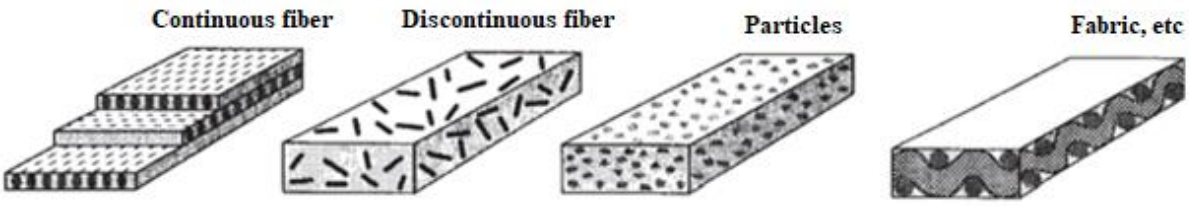

Figure (1.2): Reinforcement forms. (Kutz, 2015)

There is a wide variety in the chemical structures, forms, shapes and sizes, of the various organic and inorganic reinforcement that are used as fillers. According to (Wypych and George, 2016) in their book, fillers may be classified as inorganic or organic materials as showed in Table (1.3).

Table (1.3): Chemical families of reinforcements for plastics. (Wypych and George, 2016)

Chemical family	**Examples**
Inorganics	
Oxides	Glass (fibers, spheres, hollow spheres, flakes), MgO, SiO_2, Al_2O_3.
Hydroxides	$Al(OH)_3$, $Mg(OH)_2$.
Salts	$CaCO_3$, $BaSO_4$, $CaSO_4$, phosphates
Silicates	Talc, mica, kaolin, wollastonite, montmorillonite, nanoclays, feldspar
Metals	Boron, steel
Organics	
Carbon, graphite	Carbon fibers, graphite fibers and flakes, carbon nanotubes, carbon black
Natural polymers	Cellulose fibers, wood flour and fibers, flax, cotton, sisal, starch
Synthetic polymers	Polyamide, polyester, aramid, polyvinyl alcohol fibers

1.2.1 Polymer matrix composites:

Recently, PMCs, as engineering materials, are the research interest of scientists around the world for many applications in daily life. PMCs are mixtures of polymers with inorganic or organic additives, in which the polymer is continuous phase and the reinforced filler is the dispersed phase, where the continuous phase serves to adhere the reinforcement together for the efficient transfer of load between them. PMCs are by far the most widely used type of composites at this time. (Sharma, et al, 2020) Figure (1.3) showed polymer composites with combination of fillers, particulates or powders within polymer matrix.

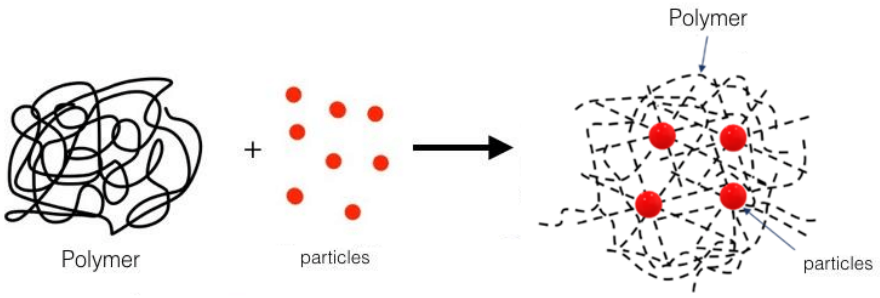

Figure (1.3): Composite material that contain particles as reinforcement in polymer matrix.

There are different polymer matrices which can be used in composite materials, one of the PMCs, thermoset matrix composites are the most common than thermoplastic matrix composites. Thermosets are matrix that undergo a chemical reaction or curing and normally transform from a liquid to a solid while thermoplastics matrix are melt-process able plastics that the materials are processed with heat. Both thermoset and thermoplastic matrix composite materials have manufacturing differ. (Davim and Reis, 2003)

In general, application of inorganic filler into polymer matrix leads to improve the mechanical properties of composite such as the elastic modulus and tensile strength, hardness and wear resistance and may be also introduce or enhance additional functions and new functions attained but causing an overall reduction in the matrix strain, especially in the particle/matrix interface due to the inorganic reinforcing fillers. Which are stiffer than the matrix and deform less, composite material properties also depend on the size, shape, concentration and composition of the filler particles, and even their bond with the matrix. (Rastelli, et al, 2012)

1.2.2 Polymer matrix nanocomposites

A nanocomposite material is a composite material, in which one of the components has at least one dimension that is nanometer in size that is around 10^{-9} m. Nano-composite materials are made of nanoobjects embedded within an organic matrix as shown in figure (1.4), these new composites material will exhibit unexpected properties, which greatly differ from that of conventional materials and shown great potential in many fields. (Khan, et al, 2016)

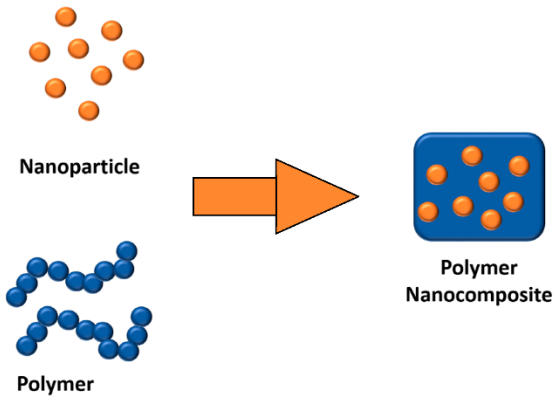

Figure (1.4): Nanocomposite material based on nanoparticles with polymer matrix.

Polyethylene, being a useful and versatile commodity polymer, has also been one of the most popular matrices for nanocomposite studies. Nanocomposites are a special class of materials having unique properties and a wide application potential in diverse areas, the use of nano-fillers in polymers opens up new pathways for engineering flexible composites that exhibit advantageous electrical, antibacterial, or mechanical properties. (Gul, et al, 2016)

Typically, nanocomposites are classified as inorganic nanocomposite where the matrix and reinforcement are inorganic. And organic nanocomposite where organic filler within organic matrix or hybrid materials such as our study, i.e., inorganic ZnO_2 in organic polyethylene matrix. Using inorganic ZnO_2 NP's in polymer matrix to produce nanocomposite is a strategy to enhance the biological activity properties of nanocomposite. However, the standard material, low-density polyethylene, has its drawbacks in terms of its activity against bacteria; it is not considered one of the substances that have an effect on killing bacteria when it is alone, so it is reinforced with ZnO_2 to improve its biological activity properties. (Patel, et al, 2006)

1.3 Inorganics metal oxides filler

Traditionally, inorganic fillers were considered as additives and reinforcements, which, due to their unfavorable features, improved the properties of polymers and to reduce the cost of materials. Several types and size with different volume fraction and distribution of inorganic filler are used in products and these affect all materials properties. The most common used type inorganic fillers are glass (fibers, spheres, hollow spheres, flakes), MgO, SiO_2, ZnO, Al_2O_3 and ZnO_2. (Xanthos, 2005)

1.3.1 Zinc peroxide filler

ZnO_2 has attracted the attention of scientists for many and several decades, it's an inorganic compound appears as a yellowish-white crystalline powder at room temperature, ZnO_2 is mostly used in many applications in the field of industries as accelerator in the vulcanization of the rubber industry (L. Ibarra, et al, 2002) and plastic processing (Ohno, et al, 1980). It can be used as an oxidizing agent for explosives and pyrotechnic mixtures (Hagel, et al, 1981), Recently, many of studies have shown that ZnO_2 has anti-bacterial properties. (Hussein, et al, 2021)

The development of plastic composite based on metal oxide fillers is one of the most important applications for polymer chemistry and physics, as well as in the fields of materials applications. Zinc oxides are one of the fillers that are used in polymer composites to a lesser extent in research compared to other high strength fillers such as alumina, silicon carbide. Therefore, the mechanical and thermal properties of the polymer may be change significantly after the incorporation of the ZnO_2 filler. Moreover, it has been reported that ZnO_2 fillers has antibacterial activity.

1.3.2 Zinc peroxide nanofiller

Recent advances in the field of nanotechnology particularly the ability to prepare highly ordered nano particulates of any shape and size up to about 100 nm, nano objects can be distinguished into three nanoscale dimensions as nanoparticles, two nanoscale dimensions as nanofibers and one nanoscale dimension as nanoplatelets, while the nanoscale dimensions are normally in a range between 1 and 100 nm , particles in these size ranges have been used by several industries such as nanocomposite and materials applications. (Bergs, 2017)

Nanoparticles are often synthesized from a top-down or bottom-up approach as shown in figure (1.5). A bottom-up approach relies on nucleating atomic-sized materials and build up to nanostructures, this method has the potential of creating less waste and hence the more economical, include organometallic chemical route, sol-gel synthesis, revers-micelle route, hydrothermal synthesis, colloidal precipitation. While top-down methods, where a bulk material is physically broken down to make smaller molecules, include milling, laser ablation, and spark ablation. (Ealia, et al, 2017)

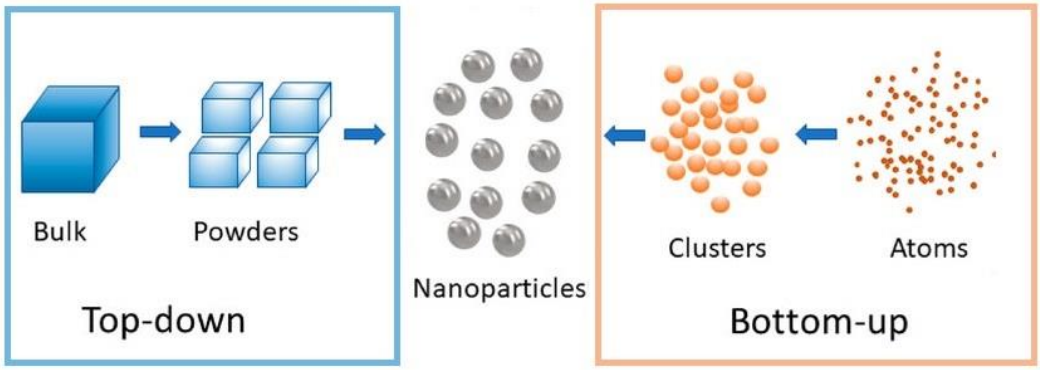

Figure (1.5): Scheme of top-down and bottom-up synthesis of nanoparticles (NPs).

Metal oxides nanoparticles are one of the most families of NP's that have been discovered and studied because of their unique properties, such as antibacterial (Bergs, et al, 2017), antifungal (Ali, et al, 2017), wound healing (Kaushik, et al, 2019) and low toxicity (Padmavathy, 2008), it is known that they effectively inhibit and resist the growth of a wide range of different types of bacteria, emerging as hopeful candidates to challenge antimicrobial resistance. (Kadiyala, et al, 2018)

ZnO_2 crystallizes in a cubic structure with the space group Pa3. (Chen, et al, 2009) It's widely used in many common applications. Furthermore, ZnO_2 NP's is extensively used as crosslinker for the production of carboxylated nitrile butadiene rubbers (XNBR) (Brown, 1963) and used as a “green” precursor for the synthesis of zinc oxide nanoparticles (Uekawa, et al, 2003), additionally ZnO_2 NP's used in cosmetic (Rosenthal-Toib, et al, 2008).

1.4 Antimicrobial activity of ZnO_2 nanoparticles:

Metal oxides have been used as an antimicrobial agent for thousands of years, dating back to 1,500 BP where Egyptians first recorded the use of copper salts as an astringent (Lemire, et al, 2013). Increasing bacterial poisoning has generated scientific interest to synthesize novel antimicrobial agents with broad spectrum activities to eliminate this problem. There are two main classes of antimicrobial agents, organic and inorganic. Over the past decade, inorganic materials, like metal and metal oxides such as zinc oxide, magnesium oxide and others have attracted additional attention as they found to be safe for citizenry and animals and conjointly had the potency to face up to harsh conditions. (Aoki, et al, 2013)

Engineering and nanotechnology are among the most important sciences used in bacterial activity applications, the nanoparticles are fighting against microorganisms, they are a safe potential antimicrobial alternative for use. The antibacterial activity of the nanoparticles depends primarily on the size and shape; so, it requires of nanometer-scale materials. (Guzmán, et al, 2009)

The antibacterial activity of ZnO_2 has been referred to a variety of issues, but the exact mechanism is not completely elucidated and still controversial, distinctive mechanisms that have been put forward in this study are listed as shown in figure (1.6).

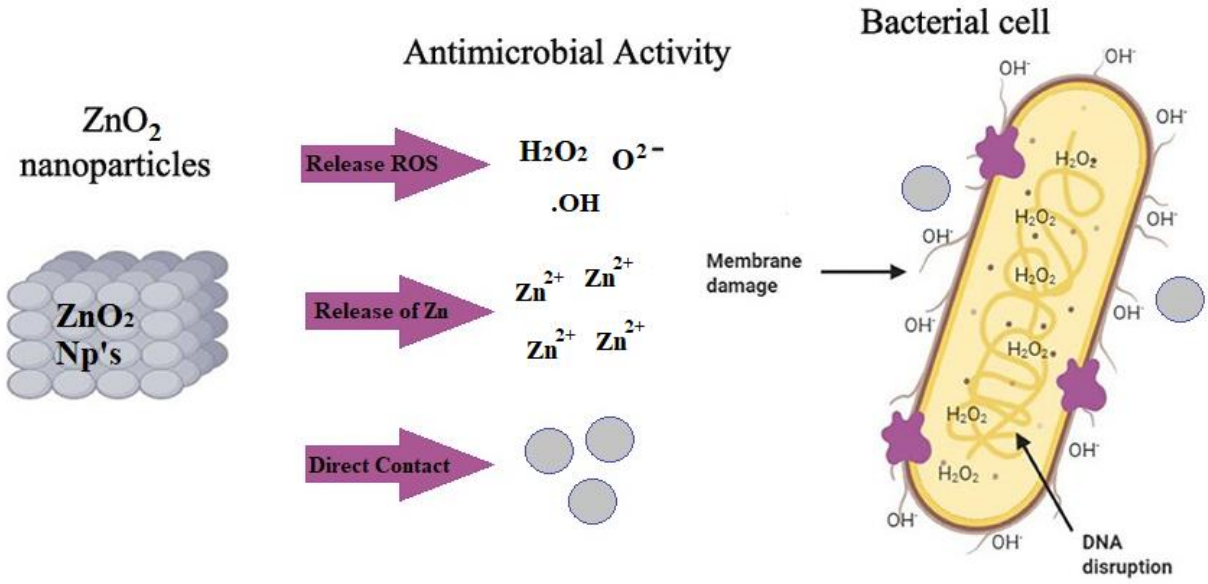

Figure (1.6): Schematic of zinc peroxide nanoparticles and the resulting antibacterial effect.

The mechanism of antimicrobial activity of ZnO_2 is related to the electrostatic interaction with the membrane. ZnO_2 nanoparticles attach to the bacterial membrane, pitting occurs in the membrane due to the production of ROS with oxygen free radicals or by release of Zn^{+2} ions or when the nanoparticles directly contact with cell membrane which fatally damages the cell. (Dimapilis, et al, 2018)

A mechanism by which nanoparticles kill bacteria when the surface of ZnO_2 release ROS or oxygen free radicals, such as the superoxide anion O^{2-} which is a powerful oxidizing agent very reactive with water. Hydrogen peroxide H_2O_2 and the hydroxyl radical (•OH) which these ROS cause fatal damage to microorganisms because ROS produce disruption of DNA, damage by oxidation of polyunsaturated fatty acids and amino acids as shown in figure (1.7).

The cell wall ruptures when exposed to ROS due to the surface activity of ZnO_2 and thus leads to the decomposition of the cell wall, the decomposition of its membrane, the leakage of the contents of the cell, and eventually to cell death (Gold, et al, 2018). Previous studies verified that the bacteria concentration in infected tissues minimized perpetually with increasing oxygen concentration. (Yamamoto, 2001)

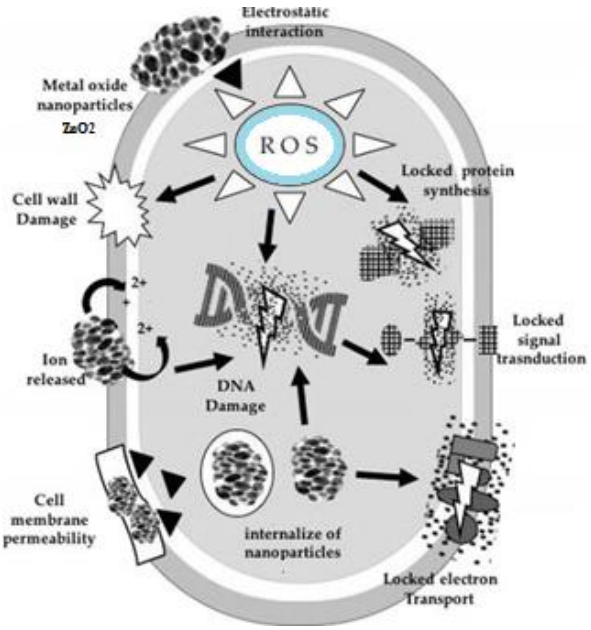

Figure (1.7): Mechanisms of action of the bactericidal effect from metal oxides nanoparticles.

(Vega-Jiménez, et al, 2019)

ZnO_2 NP's releases of zinc ions Zn^{+2} that damages the cell, for example the toxicity of nanoparticles against Escherichia coli was attributed mainly to the released Zn^{+2} ions according to (Kasemets, et al , 2009), the release of Zn^{+2} ion causes the damage of the cell membrane and penetrate the intracellular contents and the ions of metal oxides might also cause the decomposition of bacterial cells due to the diffusion of metal ions by generating large amounts of hydroxyl radicals and diffusion in bacterial cells.(Vega-Jiménez, et al, 2019)

The mechanism of ZnO_2 NP's as antibacterial agents is dependent not only as mentioned above, but is strongly correlated to the nanoparticle's physical properties, such as its shape, size, solubility, agglomeration, and surface charge. (Sirelkhatim, et al, 2015)

The antimicrobial activity of ZnO_2 nanoparticles depends on their size and concentration. The effect of size and concentration was successfully analyzed by a work carried by (N. Padmavathy, et al ,2008). Specifically, the highest antibacterial activity is achieved at the smallest particle size, it's more likely to penetrate bacterial cell walls due to the increase surface area to volume ratio thus enhancing their antibacterial efficient and the better antibacterial activity can obtain with higher concentration of NP's. (Jones, et al ,2008)

The direct contact of nanoparticles plays important roles in the antibacterial activity. Contact of nanoparticles with the cell membrane causes changes in microenvironment within the contact area of the organism and particle so the bacterial cell walls were damaged and disorganized and the nanoparticles cause increased membrane permeability leading to subsequent cellular internalization of the nanoparticles. (Dimapilis, et al ,2018)

Further suggestion and some studies have shown that the biological activity of zinc oxides nanoparticles related to the changing in the methods of synthesis and chemical modification in the surface of nanoparticles as capping agent such as PEG and PVP, leads to as well as joint use with other nanomaterials affects the physical and morphological characteristics of nanoparticles, which, in turn, leads to a change in their antibacterial properties and positively or negatively affect in the efficiency of activity of NP's against bacteria . (Javed, et al, 2016)

1.5 Plastic Composite/Nanocomposite Processing

Plastic processing is the conversion of plastic materials into useful forms that are used in many applications, these bulk plastics come in resin, granules, pellets, powders, sheets, preforms, or fluids and are converted into formed shapes or parts. Plastic manufacturing processes have been developed over time to cover many applications that we use every day. From packaging to toys, plastic products are everywhere. Plastic is also very versatile because it can be molded into almost any shape. (Harper, 2006)

In general plastic materials are manufactured in many ways that differ from each other based on the cost of equipment, production rate, tool cost and construction size. One of the most common methods used in the manufacturing process: compression molding, transfer molding, injection molding, extrusion, rotational molding, blow molding, thermoforming, casting, and foam molding. (Spaak, 1975)

Several technologies are used to produce composite and nanocomposite materials, but some methods produce better quality products than others because they introduce fewer defects, or allow better control over fiber placement and orientation or enable a higher volume fraction of fiber reinforcement to be used, or lend themselves to better quality control monitoring. The main methods used in the manufacturing process of composite and nanocomposite according to starting methods and processing techniques are: (Pavlidou, et al, 2008)

- Solution induced intercalation method.
- In situ polymerization method.
- Melting processing method.

Solution induced intercalation method where is consists of solubilizing the polymer in a suitable solvent, then the particles are dispersed in the solution to prepare a homogeneous mixture, then the solvent is evaporated to obtain the particle-polymer mixture. And the second method in situ polymerization method where is one or more monomer were mixed with the catalyst and the initiator then the particles are dispersed in the system to produce a homogeneous mixture and in the end the monomers were polymerized or crosslinked, it is still widely used especially in thermosetting nanocomposite. (Shen, et al, 2002)

The last method is melting processing method where's the particles dispersed into polymer during the melting process. The melt interaction method allows the use of polymer which were not suitable for polymerization and solution intercalation method. The processing temperature must be optimized to obtain a suitable melt viscosity during the process in order to produce a well dispersed system. (Shen, et al, 2002)

In our study solution casting techniques is used for preparation composite and nanocomposite samples, it's one of the oldest technologies used in polymer processing, it's easy and versatile method as showed in figure (1.8).

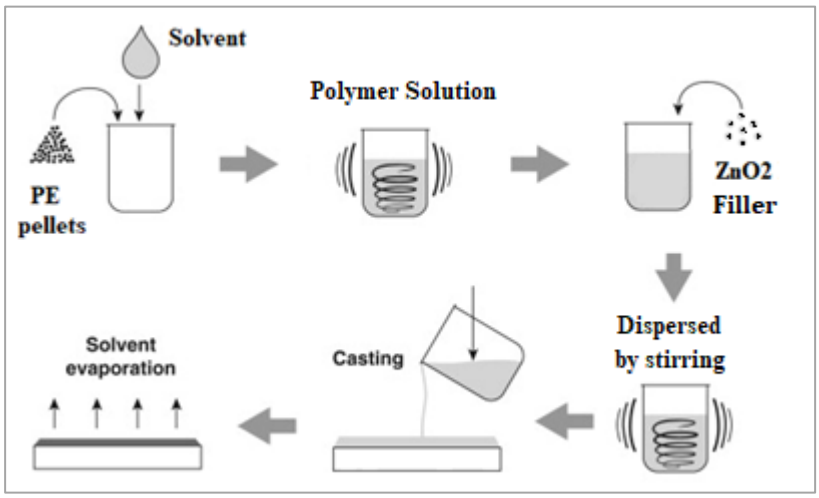

Figure (1.8): Solution casting technique of Composite samples

In the solution casting of polymer composite and nanocomposites, the polymer phase is dissolved in water or a non-aqueous solvent and mixed with particles or nanoparticles fillers in the same solvent medium prior to casting on a surface, then solvent phase is removed by evaporation and then the dried composite is released from the substrate. Unlike in melt intercalation, the driving force behind exfoliation adsorption is the entropy gained by the desorption of solvent. (Ray, et al, 2003)

According to (Araby, et al, 2014) the solution mixing technique achieved better dispersion compared with the melt method. This is because more interlayer spacing is available for polymer to intercalate. This was validated with the lower percolation threshold and higher mechanical properties obtained through their study.

1.6 Research Questions

- Does the ZnO_2 particles and nanoparticles improve the mechanical, thermal, and antibacterial properties of composites and nanocomposite?
- Does the composite and nanocomposite that contains ZnO_2 fillers have antibacterial properties against bacteria?
- Do the ZnO_2 nanoparticles enhance the properties of the nanocomposite better than the ZnO_2 composite?
- Does the ZnO_2 particles and nanoparticles change the morphology and degree of crystallinity of composite and nanocomposite?

1.7 Research aims and objectives.

The specific aim of this research is:

To investigate the effect of ZnO_2 particles and nanoparticles with different size and concentration on the thermal, mechanical, morphological and antibacterial properties of composite and nanocomposite.

The main objectives of this study are

- To synthesize and characterize ZnO_2 nanoparticles by XRD, SEM, FTIR and DSC.
- To characterize composite and nanocomposite mechanical properties, thermal properties, and morphology as a function of ZnO_2 concentration.
- To characterize composite and nanocomposite antibacterial properties as a function of ZnO_2 concentration against different types of bacteria.
- To compare the mechanical, thermal, morphological, and antibacterial properties of the composite and the nanocomposite materials.

Chapter two

Literature review

Recently, the use of inorganic filler as reinforcement and antibacterial agent in polymers opens up new pathways for engineering flexible composites and nanocomposite that exhibit big advantageous. The application of metal oxides in polymer matrices has been looked at for the production of composite and nanocomposite with new properties that can withstand to extreme and critical conditions resulted to their engineering performance. There are several scientific studies that discuss the syntheses of ZnO_2 NP's with their novel properties, in addition to articles that incorporated this metal oxide within the polymer to obtain distinctive properties.

2.1 Synthesis of zinc peroxide nanoparticles:

ZnO_2 NP's were synthesized by chemical method. (Chen, et al, 2009) The purpose of the study was to investigated the structure, structural stability, and magnetic and optical properties of ZnO_2 nanoparticles by experiments and first-principles calculations, the results revealed that the ZnO_2 nanoparticles with an average particle size of 3.1 nm which has a cubic structure with space group Pa3. This cubic ZnO_2 nanocrystalline is stable up to 230 °C and above this temperature it decomposes into ZnO and it is an indirect semiconductor.

Furthermore, ZnO_2 NP's were synthesized from zinc acetate and hydrogen peroxide using the sol-gel method under ultrasound assistance by (Ramírez, et al, 2020). The synthesized nanoparticles have a particles size of ~6 nm which cluster to form particles of 100 nm, with good dispersion in water.

(Escobedo-Morales, et al, 2011) reported and synthesized of ZnO_2 NP's through hydrothermal method, they studied the thermal stability, morphology, structural and vibrational properties of the ZnO_2 nanoparticles by thermogravimetry/differential scanning calorimetry, X-ray diffraction, low- and high-resolution transmission electron microscopy, infrared spectroscopy and Raman spectroscopy, The study results showed that the synthesized nanoparticles have an average size of 15 nm with highly crystalline cubic and they found that the synthesized ZnO_2 sample decomposes into ZnO at about 250 C^o.

In addition, ZnO_2 NP's have been synthesized by surfactant free method by (Hussein, et al, 2021). They synthesized nanoparticles by reduction of methanolic solution of zinc ions using $NaBH_4$ as a reducing agent, followed by oxidation using hydrogen peroxide and the nanosized ZnO_2 were characterized by TEM, SEM, TGA, DSC, Raman, XRD, FTIR, UV– Vis absorption spectroscopy, The results showed that the mean average size of the nanoparticles was around 15 nm with high antibacterial effect of the prepared ZnO_2 against multi-resistant bacteria and antifungal pathogen that used in their study.

(Colonia, et al, 2013) were synthesized ZnO_2 nanoparticle by a sol–gel method using zinc acetate and hydrogen peroxide in an aqueous solution with exposed to ultrasound irradiation, and the nanoparticles of ZnO_2 were characterized by XRD and SEM. The bactericidal activity of the ZnO_2 nanoparticles was tested by the well diffusion agar method against B. subtilis, E. coli and S. aureus. The result showed that the ZnO_2 NP's have an average particle size of 98 and 134 nm with narrow size distribution and the antibacterial activity showed that the ZnO_2 NP's shows inhibition zones against all type of bacteria that used in study and this indicate that the ZnO_2 has antibacterial properties.

2.2 Antibacterial activity of synthesized zinc peroxide NP's:

The antibacterial activity of the synthesized ZnO_2 NP's was investigated against seven clinical multiple drug resistance pseudomonas aeruginosa strains using disc diffusion assays on Muller-Hinton agar by (El-Shounya, et al, 2019), the bactericidal activity of ZnO_2 -NPs against tested strains was exhibited, with inhibition against P. aeruginosa strain at a concentration of 300µg/m ,the result of ZnO_2 -NPs exhibited a significant anti-biofilm activity by inhibiting bacterial biofilm formation and showed that the antimicrobial activities of ZnO_2 – NPs increased with the increase of concentrations .

(Bergs ,2017) synthesized ultrasmall and uniform biofunctionalized glucose-1-phosphate (Glc1P)-coated ZnO_2 NP's. Using a one-step reaction procedure, and investigated the antimicrobial activity of ZnO_2 against anaerobic bacteria such as Enterococcus faecalis, Aggregatibacter actinomycetemcomitans, Porphyromonas gingivalis and Prevotella intermedia, the result showed that the ZnO_2 NP's have tunable sizes (between 4.0 nm and 9.4 nm) depending on different reaction time and initial coated concentration. The antimicrobial tests performed with four bacterial species exhibiting variation on inhibition to bacteria due to the different susceptibility to oxygen cornered the antimicrobial activity of ZnO_2 nanoparticles.

The antimicrobial activity of zinc oxide against various bacterial and fungal strains was investigated by (Pasquet, et al, 2014), the study aimed to evaluation of the contribution of the soluble zinc species to the antimicrobial activity of ZnO on microbial cultures. The antimicrobial activities against the five microorganisms of the challenge tests were measured, the results show that the Zn^{2+} released in the broth brought about a significant contribution to the overall antimicrobial activity of ZnO. This led to a better antimicrobial efficacy of ZnO powders.

Furthermore, (Ali, et al, 2017) synthesized ZnO_2 NPs by used co-precipitation method, the synthesized ZnO_2 -NPs were characterized by XRD, FTIR, TEM, TGA, DSC, and UV-vis spectroscopy. The antimicrobial activity of ZnO_2 -NPs was determined against MDR Pseudomonas aeruginosa (PA) and Aspergillus niger (AN) strains isolated from burn wound infections. The characterization techniques revealed that the synthesis ZnO_2 -NPs of non-agglomerated having sizes in the range of 15–25 nm. The result, showed both strains, PA6 and AN4, were found to be more susceptible strains to ZnO_2 -NPs and in the end, they found that the synthesized ZnO_2 -NPs have demonstrated a competitive capability as antimicrobial, anti-elastase, anti-keratinase, and anti-inflammatory candidates.

2.3 Metal oxides nanocomposite:

(Anžlovar, et al, 2019) prepared composites of polyolefin matrices (HDPE and PP) with nanosized ZnO powders by melt processing and they studied the mechanical, thermal properties and antibacterial activity of composites against Staphylococcus aureus and Escherichia coli. The result showed that the zinc oxide nanoparticle (modified and nonmodified) does not enhance the mechanical properties of HDPE composites, while PP composites show slight enhancement in young modulus and tensile strength. The thermal properties revealed only a small effect of adding zinc oxide nanoparticles on the degree of crystallinity of these composites. The antibacterial tests show a high activity of polyolefin/ZnO composites against Staphylococcus aureus, while antibacterial activity against Escherichia coli shows only the composites prepared with unmodified ZnO.

In addition, (Golchha, et al, 2018) prepared thin films of low-density polyethylene with zinc oxide nanoparticles using solution casting technique at different concentration of ZnO nanoparticles (0, 0.5, 1, 3 and 5 wt. %) filler, the thin film composites were analyzed by XRD, SEM and FTIR. XRD confirms the presence of crystalline metal oxide within the polymer matrix, and absence of any extra peak in the pattern shows there is no new phase formation. The SEM images showed that the dispersion of ZnO NPs particles was relatively good and uniformly dispersed throughout the entire polymer matrix. Fourier Transform Infrared result indicates that there is no chemical bonding between the ZnO and LDPE. There is even no significant shift in the characteristic transmittance peaks indicating that LDPE did not have strong interaction with ZnO.

Another study discovered the influence of ZnO nanoparticle content on the morphology, mechanical properties, chemical structure, photocatalytic activity, and antibacterial properties of composite, the results showed that the morphological images by the SEM showed that the ZnO nanoparticles were well distributed in the PP matrix and the mechanical properties and chemical structures before and after sunlight exposure found that at the shortest exposure time, crosslinks could occur in the nanocomposites, which resulted in improved mechanical properties, but exposed for long time period caused a reduction in the mechanical properties,

the result of antibacterial tests indicated that the nanocomposites had better antibacterial properties than neat PP. (Prasert, et al, 2020)

The antibacterial activity and mechanical properties of high-density polyethylene (HDPE) composites containing ZnO nanoparticles were investigated by (Li, S.C, et al 2010), the composite films were prepared via melt blending and a hot compression-molding process, the results of study showed that the tensile strength improved when the HDPE films contain modified ZnO nanoparticles up to 0.5 wt % in contrast with the original nano-ZnO/HDPE composite films. The results of antibacterial test indicate that the HDPE films doped with modified ZnO nanoparticles showed favorable antibacterial activity, especially for Staphylococcus aureus.

Furthermore, the morphological structures, thermal properties, and antibacterial properties of the nanocomposite were investigated as a function of ZnO concentration by (Seo, et al, 2011), the nanocomposite films were prepared via a solution blending method. It was found that poor dispersion was induced in the composite films with a high ZnO content while composite films with less than 5 wt % ZnO exhibited good dispersion of ZnO in the PPC matrix and the morphological results by SEM and FTIR revealed that the blending did not lead to a strong interaction between PPC and unmodified ZnO. The results of antimicrobial analysis showed that PPC/ZnO nanocomposite films also displayed a good inhibitory effect on the growth of bacteria against E. coli than toward Lactobacillus.

Chapter Three

Materials and Methodology

3.1 Materials

Materials used to obtain composites and nanocomposites based on LDPE matrix with zinc peroxide fillers are:

3.1.1 Low density polyethylene

Low density polyethylene (Ipethene 670, Carmel Olefins). It's considered to be a thermoplastic made from the monomer ethylene. It's used in many applications due to the numerous properties that make them superior to other materials in many applications. (Koerner and Koerner, 2018) LDPE prepared by from the polymerization of ethylene (or ethene) monomer as shown in figure (3.1). Polyethylene chemical formula is $(C_2H_4)n$. Polyethylene chains are produced via free radical polymerization process. Two basic processes used for the production of low-density polyethylene: stirred autoclave or tubular routes. (Ebewele, 2000)

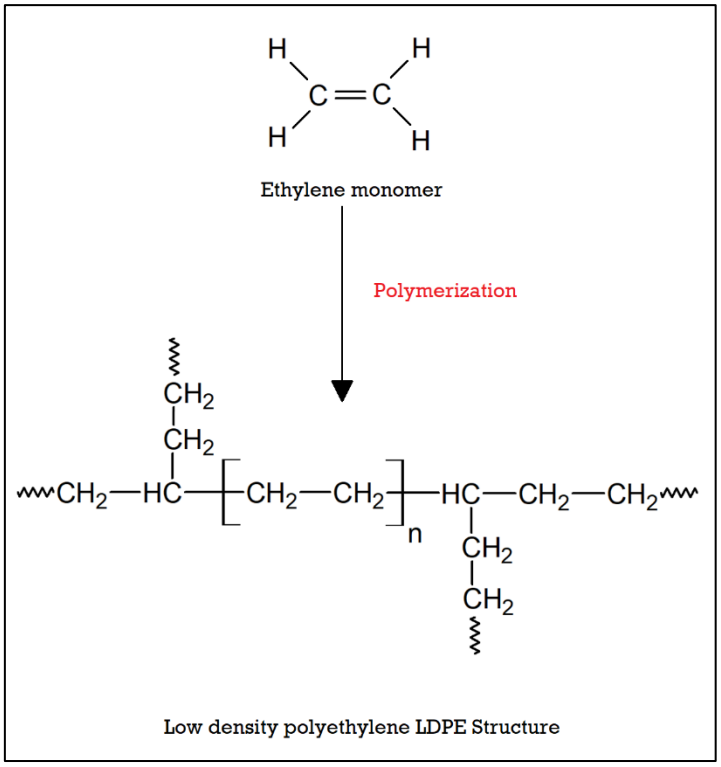

Figure (3.1): Low density polyethylene structure and ethylene monomer.

LDPE which was used in this study shown in figure (3.2), it is a soft, flexible, lightweight plastic material with no additives, good moisture barrier, with physical and thermal properties as shown in table (3.1).

Table (3.1): Properties of used low-density polyethylene

Properties	**Method**	**Typical value with unit**
Physical Properties		
Density	ISO 1183-A	0.917 g/cm^3
Melt flow index	ISO 1133	7.5 g/10 min
Hardness	ISO 868 /'D' Scale	45
Thermal properties		
Melting Temperature	ISO 11357-3/by DSC	107 ºC

Figure (3.2): LDPE pellets obtained from the Materials Engineering faculty, Al-Quds University.

3.1.2 Xylene

Xylene (98.5%, Aldrich) is organic compound with the formula $(CH_3)_2C_6H_4$. It's using as solvent for LDPE, it's obtained from the Materials Engineering department store, Al-Quds University. Xylene derived from the substitution of two hydrogen atoms with methyl groups in a benzene ring; which hydrogens are substituted determines which of three structural isomers results as shown in figure (3.3).

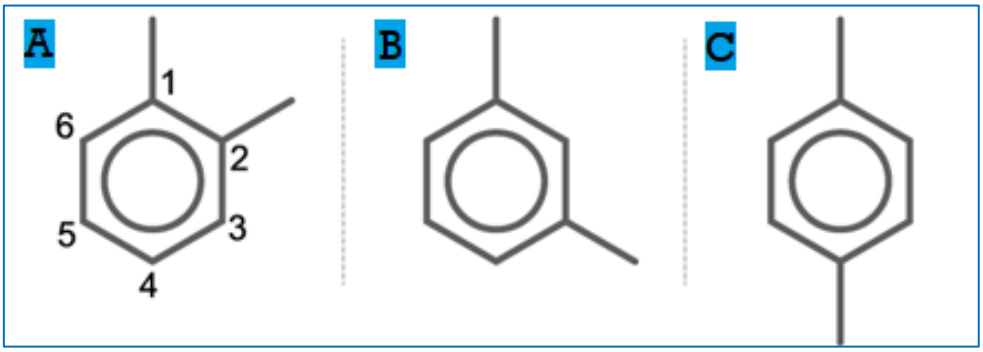

Figure (3.3): Three structural of xylene, A:1,2-dimethylebenzene (Ortho-xylene), B: 1,3-dimethylebenzene(meta-xylene) and C: 1,4-dimethylebenzene(para-xylene)

Xylene is a colorless, flammable, non-viscous, toxic liquid and its properties shown in table (3.2).

Table (3.2): Properties of used xylene.

Properties	**Specification**
Assay Total of C_8H_{10} isomers	98.5% min
Xylene formula	C_8H_{10}
IUPAC name	Dimethylbenzene
Molecular Weight	106.17 g/mol
Density	0.865 g/mL
Boiling Point	136-140 °C
Melting Point	-34 °C

3.1.3 Zinc peroxide

Zinc peroxide (ZnO_2, Aldrich) is a light, white, slightly irritative, pungent, astringent, bacteriostatic powder. Unstable in water suspensions, it readily loses part of its oxygen. For this study, ZnO_2 used as fillers in LDPE composite for improving polymer properties, it's obtained from the materials Engineering faculty store, Al-Quds University.

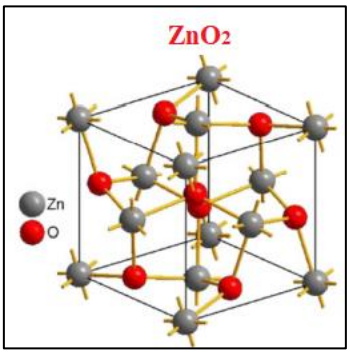

Figure (3.4): Zinc peroxide structure. (Escobedo-Morales, et al, 2011)

ZnO_2 used as a bleaching and curing agent, additive to antiseptic ointments. It can be prepared by reacting ZnO or zinc acetate with hydrogen peroxide. (https://www.worldofchemicals.com/chemical-properties/zinc peroxide.html, 08-10-2022). It has cubic crystalline structure (Bocharov, et al, 2022) and its properties shown in table (3.3).

Table (3.3): Zinc peroxide used properties.

Properties	**Specification**
Assay	50-60%
Synonym(s):	Zinc dioxide
Chemical formula	ZnO_2
Form/Appearance	Powder/ white-yellowish
Molar mass	97.408 g/mol
Density	1.57 g/cm^3 at 25 °C
Decomposition temperature	212 °C

3.1.4 Zinc peroxide nanoparticles.

Materials used for the synthesized of zinc peroxide nanoparticles are:

3.1.4.1 Zinc acetate dihydrate

Zinc acetate dihydrate (99-102 %, Aldrich) is a zinc salt of acetic acid, with the formula ($C_4H_6O_4Zn.2H_2O$) both the hydrate and the anhydrous forms are colorless solids. It's used as precursor to plays an important role in the synthesis of ZnO_2, when synthesized ZnO_2 NP's, it is considered as a source of zinc.

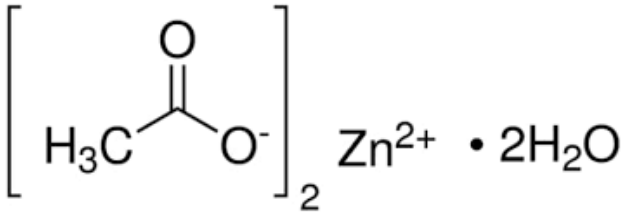

Figure (3.5): Zinc Acetate Dihydrate structure.

For synthesized ZnO_2 NP's, zinc acetate dihydrate obtained from the materials engineering faculty store, Al-Quds University. Some of properties shown in table (3.4).

Table (3.4): Zinc acetate dihydrate properties.

Properties	**Specification**
Assay	99.5-101.0%
Chemical formula	($C_4H_6O_4Zn.2H_2O$) (dihydrate)
Molar mass	219.51 g/mol (dihydrate)
Melting point	Decomposes at 237 °C
Appearance	White solid (all forms)
Density	1.74 g/cm^3 at 20 °C (dihydrate)

3.1.4.2 Hydrogen peroxide

Hydrogen peroxide (30%, Aldrich) is a chemical compound with the formula H_2O_2. In its pure form, it is a pale blue to translucent liquid, slightly more viscous than water. It's acts as a bleaching agent and is also used as a disinfectant. (Ahmad, et al, 2020) In this study it's used as an oxidizing agent for synthesized of ZnO_2 NP's according the following chemical reactions:

$$Zn(CH_3COO)_2.\ 2H_2O + H_2O_2 \rightarrow ZnO_2 + 2CH_3COOH$$

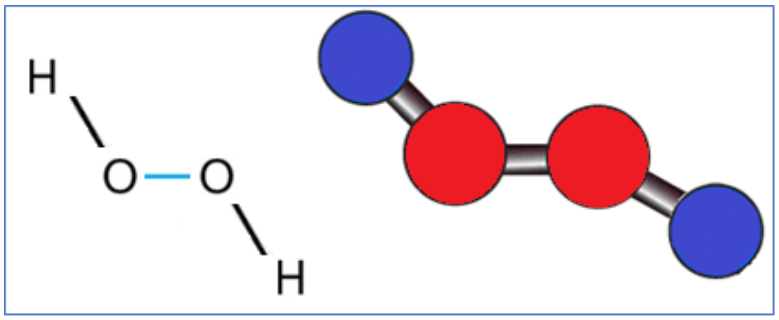

Figure (3.6): Hydrogen peroxide structure.

Hydrogen peroxide is the simplest kind of peroxide available (oxygen-oxygen single bond). It's in both acidic and basic medium acts as an oxidizing as well as a reducing agent. (Ahmad, et al, 2020) Some of properties shown in table (3.5).

Table (3.5): Hydrogen peroxide properties.

Properties	**Specification**
Assay	30%
Chemical formula	H_2O_2
pH	≤3.5 (20 °C in H_2O)
Decomposition Temperature	> 100 °C
Appearance	liquid colorless
Density	1,11 g/cm^3 at 20 °C

3.1.4.3 Polyethyleneimine

Polyethylenimine (50%, Aldrich) is a highly positive charged polymer with repeating units composed of the amine group and two carbon aliphatic CH_2CH_2 made by ring opening polymerization of aziridine. PEI is an organic polymer which can be linear or branched, the linear form contains only primary amines in the backbone whereas branched PEI also contains secondary and tertiary amines. (Jager, et al, 2012)

In this study PEI, with high cationic charge density, it's used as capping agent to synthesized PEI-functionalized ZnO_2 nanoparticles.

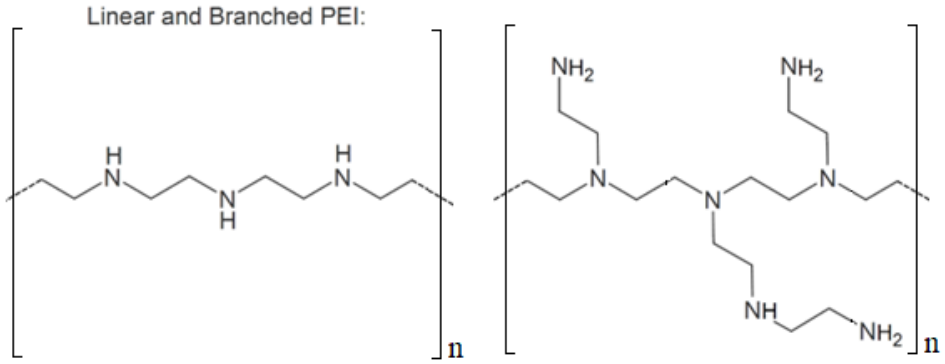

Figure (3.7): Repeating unit of liner and branched Polyethylenimine.
(http://polymerdatabase.com/Polymer/Polyethyleneimine,12/11/2022)

PEI that used in the study it's a Solution 50 % in water, viscous liquid with colorless to very light green-yellow. Some of properties shown in table (3.6).

Table (3.6): Properties of Polyethyleneimine.

Properties	**Specification**
Synonym(s)	Ethyleneimine polymer solution, PEI
Appearance (Form)	Liquid or Viscous Liquid
Concentration	~50% in H_2O
Molecular weight	600,000-1,000,000
Viscosity	18 – 40 Pas

3.2 Preparation of Samples

3.2.1 Synthesis of zinc peroxide nanoparticles:

In this part of the study, ZnO_2 nanoparticles were synthesized by three methods as showed in table (3.7) using the same materials that mentioned. One of the methods is refluxing, it was used PEI as capping agent to control the aggregation of nanoparticles and the second methods without used capping agent while the last one by sol-gel method. One of these methods were chosen for prepared nanocomposite for several reasons that were mentioned in our study.

Table (3.7): Synthesized ZnO_2 nanoparticles codes for method used.

ZnO_2 NP's method	Sample codes	Used of capping agent	Reaction Temperature
Refluxing	A1	×	150 °C
Refluxing	A2	✓ PEI	150 °C
Sol-gel	B	×	80 °C

The nanosized ZnO_2 of all the methods were characterized by SEM, DSC, XRD, FTIR. The formation of ZnO_2 nanoparticles was confirmed through visual assessment due to the white color and further confirmed throughout the characterization.

ZnO_2 -NPs was synthesized in a procedure by reaction of zinc acetate with hydrogen peroxide:

$$Zn\ (CH3COO)_2.\ 2H_2O + H_2O_2 \rightarrow ZnO_2 + 2CH_3COOH$$

According to (Escobedo-Morales, et al, 2011) study, it is proposed that the formation mechanism of the grown ZnO_2 nanoparticles is by the following chemical reactions:

$$Zn\ (CH_3COO)_2\ .2\ H_2O \rightarrow Zn^{2+} + 2\ (CH_3COO)^- + 2\ H_2O \quad (1)$$

$$CH_3COO^- + H_2O \rightarrow CH_3COOH + OH^- \quad (2)$$

$$Zn^{2+} + 2\ OH^- \rightarrow Zn\ (OH)_2 \quad (3)$$

$$Zn\ (OH)_2 + H_2O_2 \rightarrow ZnO_2 + 2\ H_2O \quad (4)$$

$$2\ H_2O_2 \rightarrow 2\ H_2O + O_2 \quad (5)$$

3.2.1.1 Synthesis of zinc peroxide NP's by refluxing method.

a) By using capping agent PEI:

ZnO_2 -NPs was synthesized in a procedure by using refluxing as shown in figure (3.8), ZnO_2 was synthesized using the following analytical grade chemicals without further purification:

- Zinc acetate dihydrate ($Zn\ [CH_3COO]_2 \cdot 2H_2O$).
- Hydrogen peroxide (H_2O_2; sol 30%).
- Distilled water.
- Polyethyleneimine (PEI; sol 50%).

The ZnO_2 nanoparticles were synthesized by refluxing; for this purpose, a precursor solution was prepared by using 5 mL of concentrated H_2O_2 30% added to 50 ml distilled water under magnetic stirring for 5 min. Elsewhere 50 ml of 5 % of PEI was prepared by used hot distilled water. Then, 1 g of zinc acetate (99.9%) was dissolved in prepared PEI solution by magnetic stirring for 5 min until a homogeneous solution is obtained, subsequently in rounded bottom flask a precursor solution was added to the PEI solution and refluxing in heat mental at 150 ^oC for 24 hours and a white precipitate was produced. This precipitate was then centrifuged at 4900 rpm for 10 minutes, then the precipitate was washed repeatedly by distilled water. The precipitate was dried at 60 ^oC in oven to obtain dry fine powder.

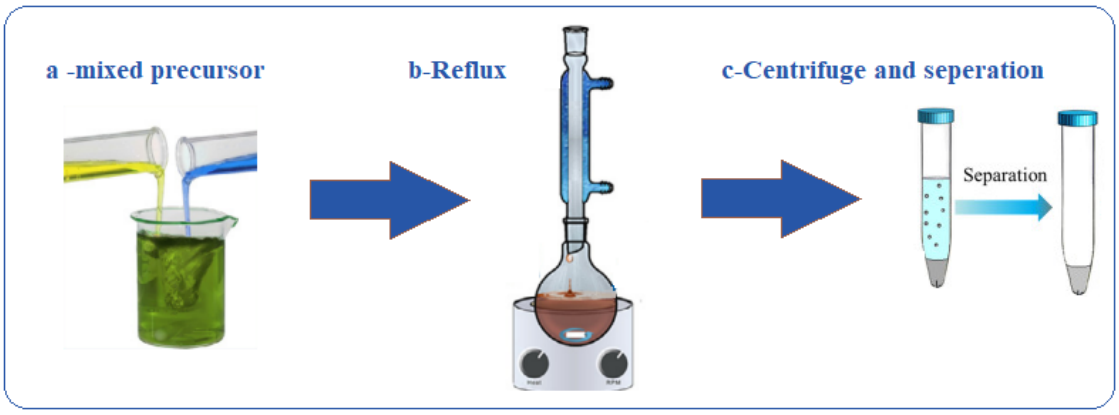

Figure (3.8): Synthesized of zinc peroxide NP's by refluxing.

b) Without using capping agent.

Nanometer-sized ZnO_2 nanoparticles were synthesized using the following analytical grade chemicals without further purification:

- Zinc acetate dihydrate (Zn $[CH_3COO]_2 \cdot 2H_2O$).
- Hydrogen peroxide (H_2O_2; sol 30%)**.**
- Distilled water.

For the refluxing reaction process, 5 mL of 30% hydrogen peroxide (H_2O_2) aqueous solution was diluted with 50 mL of deionized water under magnetic stirring for 5 min then 1 g of zinc acetate dihydrate (99.9%) was dissolved in the H_2O_2 solution with stirring for another 5 min. Then the mixture reflux in rounded bottom flask in heat mental at 150 ^oC for 24 hours and a white precipitate was produced. This precipitate was then centrifuged at 4900 rpm for 10 min, then the precipitate was washed repeatedly by distilled water. The precipitate was dried at 60 ^oC in oven to obtain dry fine powder.

3.2.1.2 Synthesis of zinc peroxide by a sol-gel method.

The ZnO_2 nanoparticles were synthesized through sol-gel method in an almost similar way according to Colonia study (Colonia, et al, 2013), the following chemicals were purchased and used without further purification:

- Zinc acetate dihydrate (Zn $[CH_3COO]_2 \cdot 2H_2O$).
- Hydrogen peroxide (H_2O_2; sol 30%)**.**
- Distilled water

In a typical synthesis of ZnO_2 nanoparticles 5 mL of 30% hydrogen peroxide (H_2O_2) aqueous solution was diluted with 50 mL of deionized water under magnetic stirring for 5 min then 1 g of zinc acetate dihydrate (99.9%) was dissolved in the H_2O_2 solution with stirring for another 5 min. Then the mixture sonication in ultra-water bath at 80 ^oC for 24 hours, after this stage it was observed that the appearance of the solution progressively turns from translucent to cloudy white. Finally, the solution was cooled freely to room temperature; then the solid material was extracted by centrifuged at 4900 rpm for 10 min and washed several times with deionized water and the precipitate was dried to obtain dry fine powder.

3.2.2 Preparation of LDPE/ZnO_2 composite and nanocomposite.

Different compositions of LDPE/ZnO_2 composite and nanocomposite as show in table (3.8), were prepared by using solution – cast technique (Golchha, et al, 2018). LDPE and xylene charged into a 500 ml round bottom flask. The mixture was refluxed at approximately 100 ^oC for 2 h. After the reflux process was completed, a hot transparent viscous solution was obtained, then ZnO_2 powder was added to the solution to dispersed it with continuous stirring for 1 hour at the same temperature.

Table (3.8): Composite materials based on zinc peroxide / low density polyethylene codes of material used.

Sample code	%wt. of LDPE	%wt. of ZnO_2	%wt. of nano ZnO_2
PE	100	0	--
PEC1	99	1	--
PEC3	97	3	--
PEC5	95	5	--
PEN0.5	99.5	--	0.5
PEN1	99	--	1
PEN1.5	98.5	--	1.5
PEN3	97	--	3
PEN5	95	--	5

To avoid agglomeration, the mixed solution was cast into a glass beaker with magnetic stirring which exists in a water bath at room temperature to immobilize ZnO_2 filler and nanofillers immediately following the heating process. Afterward, the solidified organic phase system was evaporated at room temperature in the fume hood for 48 h to evaporated xylene. After the solvent was completely removed, the composite was extracted from the beaker, and injected by industrial plastic center machine to give dogbone samples for both composites and nanocomposite then stored at room temperature for further study as shown in figure (3.9).

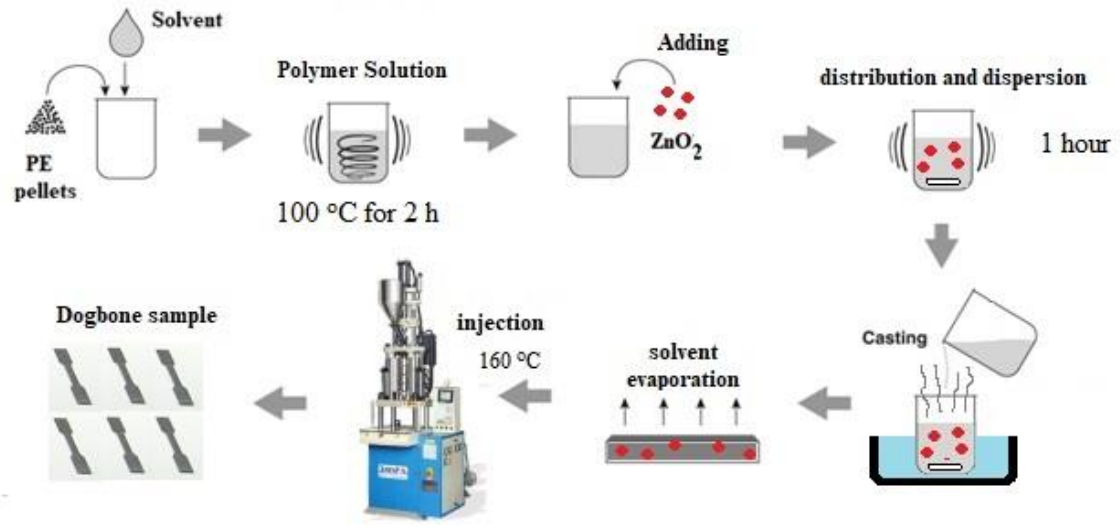

Figure (3.9): Steps of Preparation of LDPE/ZnO_2 composite and nanocomposite.

The industrial plastic center machine temperature was to set at 160 ^{o}C and the temperature of die is 165 ^{o}C and the composite was placed in the barrel for 10 minutes to melt and then injected into the mold with pressure 7 bar and then it was cooled. Six of the dogbone shape for each concentration for both composites and nanocomposite as shown in figure (3.10) were prepared for test, then the samples were characterized using DSC, SEM, UTM and antibacterial test.

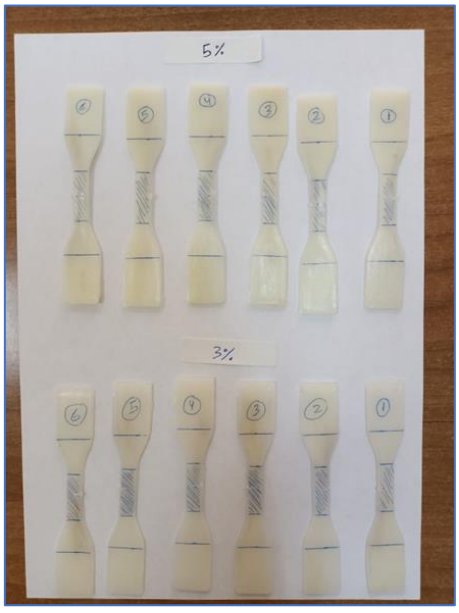

Figure (3.10): Dogbone samples of each concentration for tests.

3.3 Experimental methods.

3.3.1 X-Ray diffraction.

XRD is one of the most important and useful characterization tools used to reveal the crystallographic structure and chemical composition of solid-state crystalline material. The constituent (atoms, ion or molecules) of a solid crystalline material can form a regular three-dimensional arrangement or array of particles in space called crystal lattice or space lattice, so each crystal structure when exposed to x rays, form a characteristic pattern that can be used as a fingerprint for identifying the material. Hence, applying XRD can be source of information about lattice parameter, phase identify, phase purity, crystallinity and crystal structure (determine how the atoms pack together in the crystalline state). (Ghatage and Kanitkar, 2019)

ZnO_2 NP's were characterized by XRD (Bruker AXS, Karlsruhe, Germany). The 2θ values were set in the range of 6°–90°. Peaks on the X-ray patterns recorded for the sample were compared with standard XRD pattern of ZnO_2. The mean crystallite size was calculated using the Scherer equation by XRD software.

3.3.2 Scanning Electron Microscopy.

SEM is a type of electron microscope that images the sample surface by scanning it with a high-energy beam of electrons in a raster scan pattern. The electrons interact with the atoms that make up the sample producing signals that contain information about the sample's surface topography, composition and other properties. A scanning electron beam impinges upon the specimen surface; the signals are detected, amplified and modulated in cathode ray tube. These reflected signals are collected and constructed to form an image. The magnification of this image that appears on the screen is the ratio of a distance on the screen and the corresponding distance on the specimen. (Akhtar, et al, 2018)

In this study surface morphology and size of nanoparticles were examined via SEM (HRSEM, Sirion 200, FEI). The sizes were determined by measuring diameters of nanoparticles and calculating average size of the NP's by using (J image, 2015) software**.**

The normal distribution was used to obtain an estimate of the number average radius (Rn) and the volume average radius (Rv) according to equation 1 and 2 respective:

$$Rn = \frac{\sum(Nv)i\ Ri}{\sum(Nv)i} \tag{3.1}$$

$$Rn = \frac{\sum(Nv)i\ Ri^4}{\sum(Nv)i\ Ri^3} \tag{3.2}$$

Where (Nv)i is the number of particles having radius Ri, Also, the size polydispersity (D) was characterized by,

$$D = \frac{Rv}{Rn} \tag{3.3}$$

3.3.3 Fourier-Transform Infrared Spectroscopy (FTIR).

FTIR is the most useful technique for identifying chemical interaction, it can analyze solid, liquids and gases. It's a powerful tool to identify types of chemical bonds (functional groups). The wavelength of light absorbed is characteristics of the chemical bond, the chemical bonds in molecule can be determined by interpreting the infrared absorption spectrum. (Baudot, et al, 2010)

In this study the binding vibrations of ZnO_2 nanoparticles were examined via FTIR Spectrometer Tensor II from Bruker at Pharmacy lab in al-Quds university as shown in figure (3.11). The spectrum of the nanoparticle was obtained with in the wave number range 500 cm^{-1} to 4000 cm^{-1}. Usually approximately 100 mg of powder sample was used.

Figure (3.11): FTIR at Pharmacy laboratory at Al-Quds University-East Jerusalem.

3.3.4 Differential Scanning Calorimetry.

DSC is a thermodynamic technique that measure the difference in the amount of heat in which it is based on raising the temperature of a sample with respect to a reference as a function of time. When the sample undergoes a physical transformation such as phase transition, more or less heat will need to flow to it than the reference to maintain both at the same temperature. Whether less or more heat must flow to the sample depends on whether the process is exothermic or endothermic. (Koshy, et al, 2017)

Thermal behavior of synthetized ZnO_2 and LDPE/ZnO_2 composites and nanocomposite were analyzed using Jade DSC from Perkin Elmer with accuracy/ precision ± 2% / ± 0.1%, at the nanotechnology lab in al-Quds university as shown in figure (3.13). It's measuring the temperatures and heat flows associated with transitions in composite and nanocomposite as a function of time and temperature in a controlled atmosphere at a heating rate of 10°C/min under a nitrogen gas pressure 20ml/min at temperature range 25 to 300 ^{o}C.

DSC is widely used to get information about glass transition temperature (T_g), melting point (T_m), crystallization temperature (T_c), the heat of crystallization (ΔH_c), the heat of melting (ΔH_f) during the cure reactions or decomposition reactions as shown in figure (3.12). It is possible to calculate degree of crystallinity (Xc) and it defines as the degree of long-range order in a material, and strongly affects its properties. The more crystalline a polymer, the more regularly aligned its chains. (Schick, 2009)

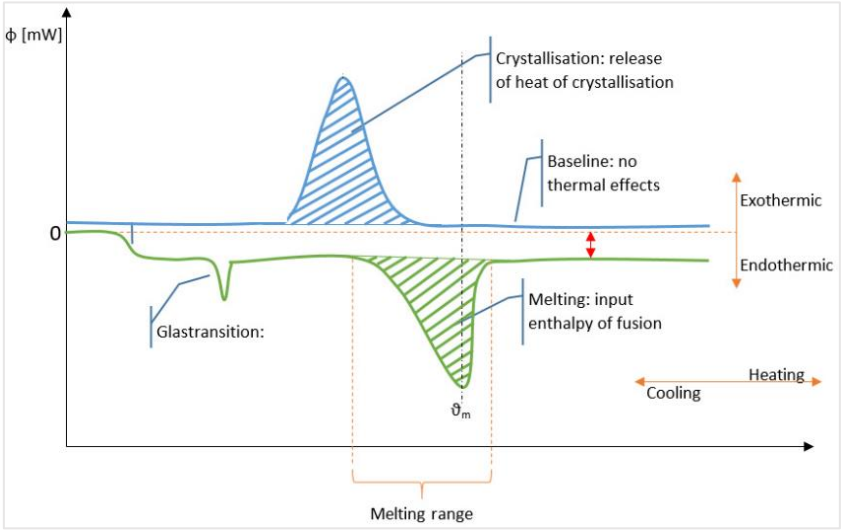

Figure (3.12): Differential Scanning Calorimetry peak analysis.

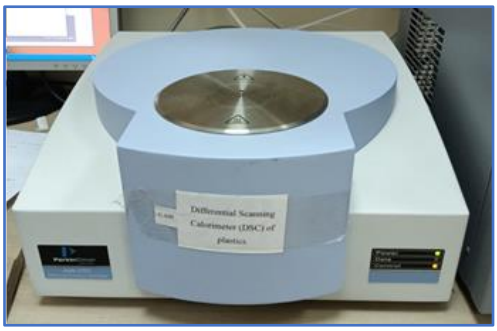

Figure (3.13): Differential scanning calorimeter at the nanotechnology research laboratory at Al-Quds University-East Jerusalem.

In this study the method for determining the degree of crystallinity of a composite and nanocomposite is shown in following equation

$$X_c = \frac{\Delta H_m - \Delta H_{cc}}{(1-\phi)\Delta H_f^o} \cdot 100\% \qquad (3.4)$$

where ΔH_m is the enthalpy of the final melting, ϕ is the weight fraction of additives in the composites, ΔH_{cc} is the enthalpy of crystallization, its value is negligible (in case crystallization peak is absent) and ΔH_f^o = 288.0 J/g is the heat of fusion of a completely crystalline LDPE. (Mirabella FM, et al 2002)

In our study, the prepared composites and nanocomposite sample were cut and weighted in milligrams (5 mg) and placed in aluminum pan (tray and a lid) then the samples within tray and a lid was pressed by used the crimper and load into the DSC machine as shown in figure (3.14) and the nitrogen gas was entered the system., DSC machines use a reference pan as a comparison during DSC analysis

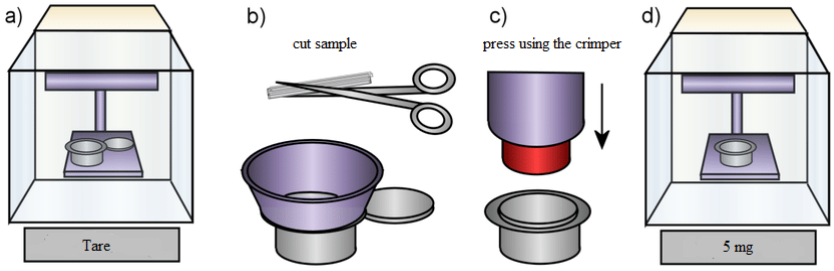

Figure (3.14): Preparation of composite and nanocomposite samples for DSC.

(Steinmann, W, et al. ,2013)

3.3.5 Tensile test

LDPE/ ZnO_2 composites and nanocomposites were prepared using solution casting method and the samples were formed to dog bone shape using industrial plastic center machine by Amatrol T9013-P at (Al-Quds-University) as shown in figure (3.15). The machine used for creating a product by forcing a material through a die to form a shape.

Figure (3.15): Industrial plastic center machine amatrol T9013-p

Six of the dog bone-shaped specimen with standard dimension was prepared to carry out tension test. All the specimens were loaded with the Universal Testing machine at (Al-Quds-University) with strain rate of 5 mm/min as specified by the American Society for testing and Materials *ASTM D638-14* to determine each specimen's tensile stress-strain relationship, two grips were fixed on each side of each dog bone specimen with a length of 60 mm as show in the following figure (3.16 B).

Figure (3.16): A: Universal testing machine of polymer (tensile test) B: Tensile specimens during testing.

Tensile specimens were made by formed to *IV ASTM D-638* type or dumbbell shape oriented parallel to the gate flow direction (MD), these specimens were defined in figure (3.17), sample dimension are:

L :25mm, Wc:7mm, T:0.7mm, L_O:115mm, D :60mm.

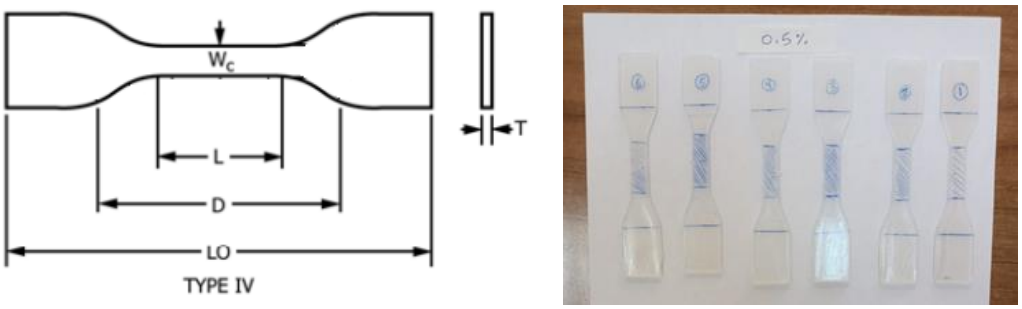

Figure (3.17): Tensile bar dimensions type *IV ASTM D638.*

The tensile properties of the composite and nanocomposite can be related to the characteristics of their stress-strain curve, after all the specimens were tested and determine each specimen's tensile stress-strain relationship, The tensile strength, elastic modulus, yield strength, fracture strength and elongation at fracture were calculated according to American specification.

Tensile strength

Ultimate tensile strength (UTS) is the maximum stress that a composite or nanocomposite specimen can withstand while being stretched or pulled before breaking, the highest point of the stress–strain curve is the ultimate tensile strength as show in figure (3.19). Tensile strengths expressed by the following equation:

$$\sigma_{\text{maximum}} = \frac{\text{F (N)}}{\text{A (mm}^2\text{)}} \tag{3.5}$$

Where: σ :Stress, F: Force (Newton) , A: Cross-sectional area (millimeter square).

Tensile strengths have dimensions, which is measured as mentioned in equation as force per unit area, according to International System of Units (SI), the unit is the pascal (Pa) or furthermore megapascals (MPa), equivalently to pascals, Newtons per square meter (N/m^2).

Elastic modulus

An elastic modulus or modulus of elasticity is the unit of measurement of a specimen of nanocomposite or composite resistance to being deformed elastically when a stress is applied to it. The elastic modulus of an object is defined as the slope of its stress–strain curve in the elastic liner deformation region as shown in figure (3.19).

$$Elastic\ modulus(E) = \frac{Stress}{Strain} \tag{3.6}$$

Where strain is the deformation or displacement of specimen that results from an applied stress:

$$\varepsilon = \frac{\Delta l}{l_o} = \frac{l_f - l_o}{l_o} \tag{3.7}$$

Where ε = strain, L_f = length after load is applied (mm), L_0 = original length (mm)

Yield strength

The yield point is the point in stress strain curve that indicate that the sample beginning of plastic behavior and the deformation will be permanent and non-reversible and is known as plastic deformation. So, the yield strength is the stress corresponding to the yield point at which the material begins to deform plastically as shown in figure (3.18).

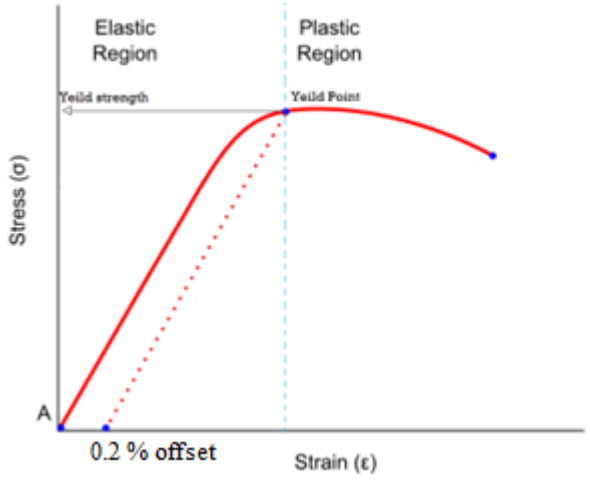

Figure (3.18): Yield Point and Yield strength

Elongation at fracture

Elongation at fracture also called “fracture strain” or “elongation at break” is the percentage increase in length that material will achieve before breaking. Elongation at fracture is measured in percentage, is the strain at fracture, expressed as a percentage = ((final gage length – initial gage length)/ initial gage length) x 100.

$$\%El = \frac{\Delta l}{l_o}.100 \tag{3.8}$$

Where is, ΔL = the change in length (mm), L_0 = original length (mm)

Fracture strength

Fracture strength is the ability of a material to resist failure so it's stress when a specimen fails or fractures, there are two types of failure mode: brittle and ductile materials respectively, failure involving fracture, the determination of the failure mode involves identifying how the crack initiated and how it subsequently extended. The final recorded point in the stress-strain curve is the fracture strength as shown in figure (3.19).

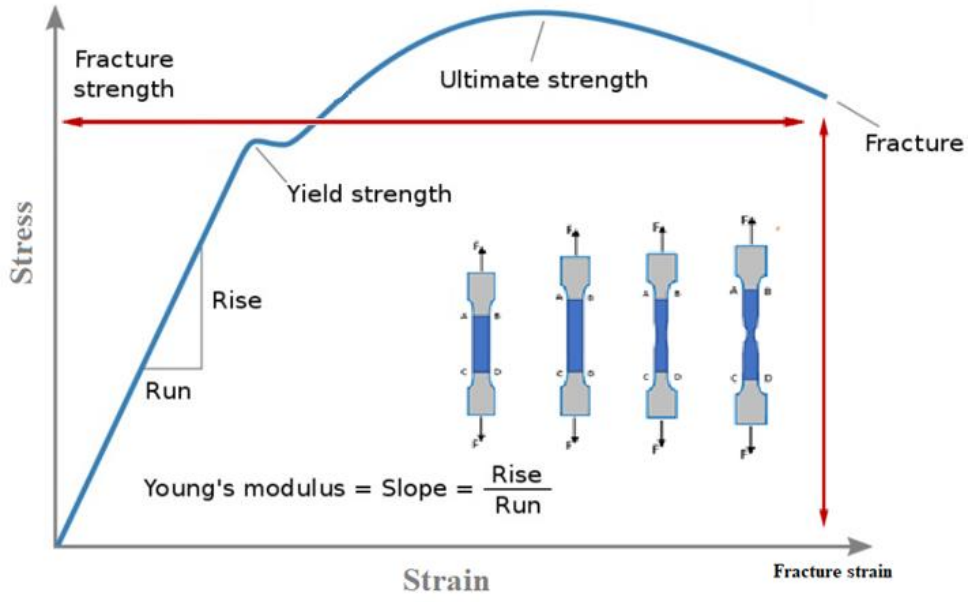

Figure (3.19): Engineering stress-strain curve.

3.3.6 Antibacterial activity Test.

3.3.6.1 Antibacterial test for composite and nanocomposite.

In our study, the disc-diffusion test was used to determine antibacterial property of the composite and nanocomposite with different concentration of ZnO_2 fillers, The antibacterial activity tested against aerobic bacteria such as Staphylococcus aureus (MRSA), Escherichia coli (E. coli) and Pseudomonas aeruginosa and against anerobic bacteria such as anerobic gram-positive streptococcus and anaerobic gram-negative bacilli that introduced to the medium surface and analyzed the results of the test as shown in figure (3.20).

In the disc-diffusion test, the different concentration of the fabricated composites and nanocomposite samples were placed on the bacteria growth medium to examine the antibacterial effect of the composite and nanocomposite. The plates then placed in incubator and left for 24 h at 37 °C for aerobic bacteria, but the anerobic bacteria the plates placed in CO_2 jar to allow the growth of bacteria in the same condition. Then the diameter measured by a precise ruler and the growing magnitude report around samples and this is called zone of inhibition as shown in figure (3.20). (Kun & Marossy, 2012).

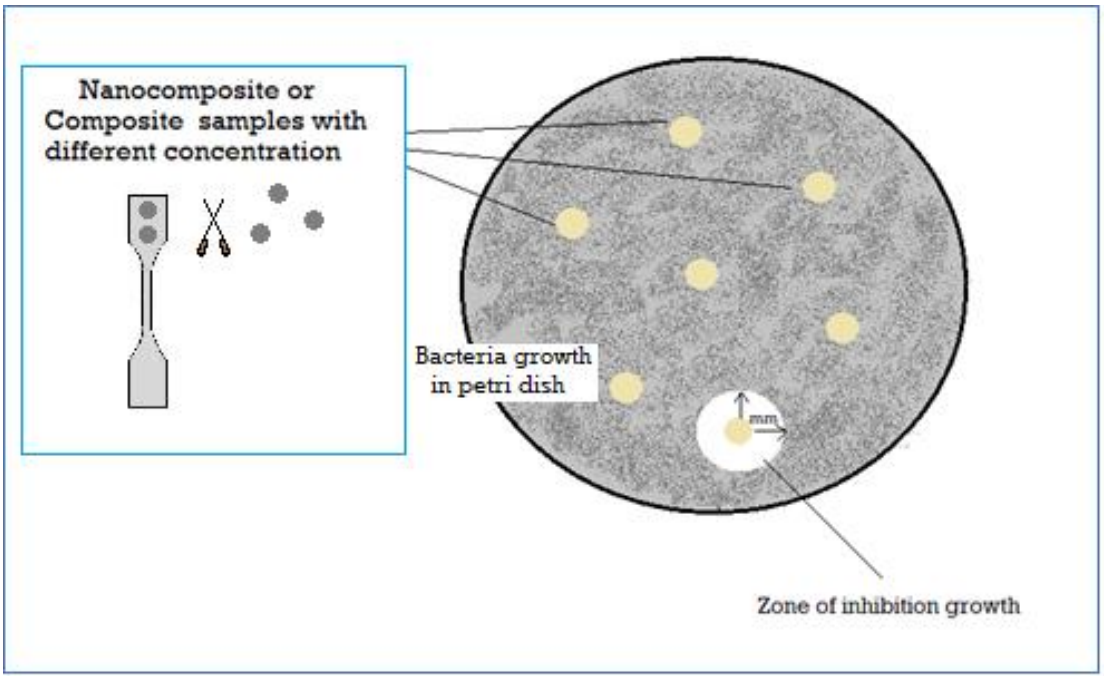

Figure (3.20): Antimicrobial activity of composite and nanocomposite.

Chapter Four

Results and Discussion

4.1 Physico-chemical Characterization

4.1.1 X-ray Diffraction Analysis

4.1.1.1 Zinc peroxide purchased material.

XRD spectrum was used to examine the crystalline forms, known as phases of compound present in powder and solid samples. The XRD pattern of the sample of zinc peroxide (50-60%, Aldrich) that used to prepare composites were shown in the figure (4.1). It's constituted by crystallites of cubic-ZnO_2 with space group $Pa3^-$ (no. 205) and crystallites of hexagonal-ZnO with space group P63mc (186) as shown in table (4.1), which indicates to zinc peroxide and zinc oxide content. The XRD analysis showed that the sample is a mixture and not a pure substance with concentration of 88.6% and 11.4% for ZnO_2 and ZnO, respectively.

Table (4.1): X-ray diffraction analysis data of zinc peroxide purchased.

Material	Crystal structure	Concentration	Space group
Zinc peroxide purchased	Cubic ZnO_2	88.6%	Pa-3 (205)
	Hexagonal ZnO	11.4%	P63mc (186)

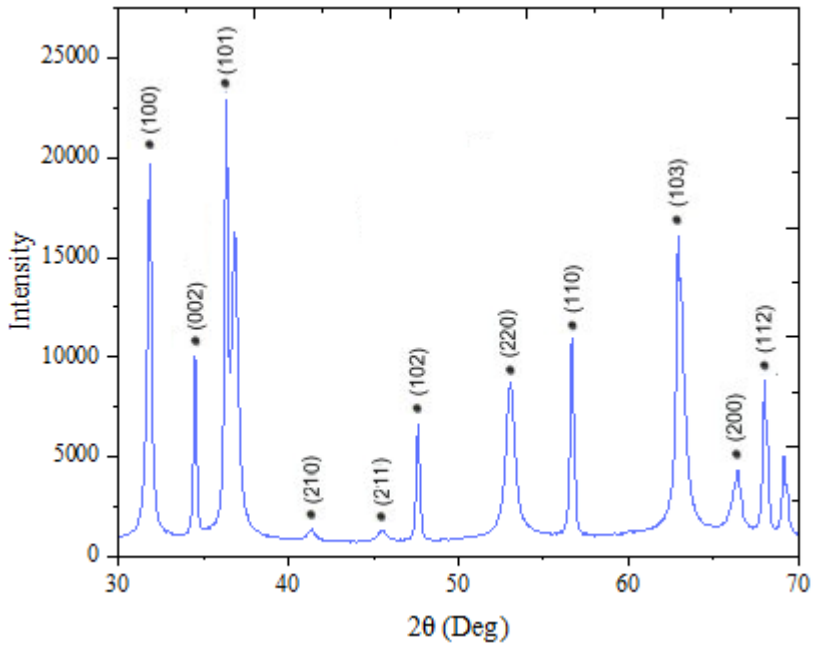

Figure (4.1): Experimental X-ray diffraction pattern of purchased zinc peroxide particles.

4.1.1.2 Synthesized zinc peroxide nanoparticles (ZnO_2 NP's)

The XRD pattern of the synthetized ZnO_2 nanoparticles produced by sol-gel and refluxing (with and without capping agent) were shown in the figure (4.2). All the diffraction peaks of synthesized ZnO_2 nanoparticles of the three methods were constituted by crystallites of cubic-ZnO_2 with space group $Pa3^-$ (no. 205) for sol-gel, reflux with and without of capping agent as shown in table (4.2).

XRD pattern reveals strong XRD reflections at 2θ = 31.0°, 36.5°, 53.0° and 63.0° are with indexes to 111, 200, 220 and 311 respectively for all synthesized nanoparticles, and did not detect any impurity peak that revealed a pure single-phase structure that coincided with that of standard cubic ZnO_2 crystal structure, suggesting the formation of ZnO_2 nanoparticles with high crystal quality. (Hussein, et al, 2021) (Ali, et al, 2017)

Table (4.2): X-Ray diffraction analysis data of synthetized zinc peroxide nanoparticles.

Materials	Crystal structure	Space group	Remark
A1	Cubic	Pa-3 (205)	without PEI
A2	Cubic	Pa-3 (205)	with PEI
B	Cubic	Pa-3 (205)	--

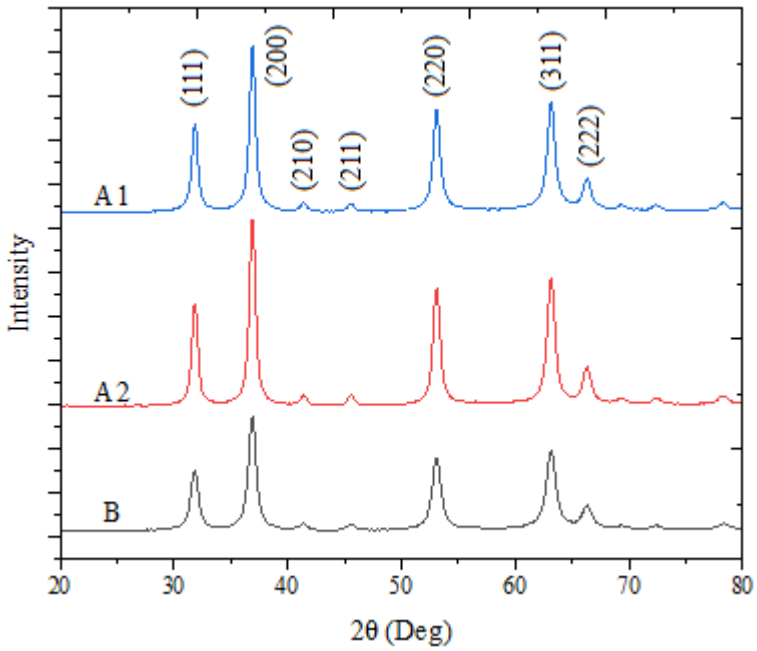

Figure (4.2): X-ray diffraction pattern of synthesized zinc peroxide nanoparticles.

4.1.2 Morphological Characterization

4.1.2.1 Zinc peroxide purchased material.

In order to study the morphology and size of the ZnO_2 that used to prepare composites, SEM was used. Figures (4.3) showed the SEM images of the ZnO_2. The SEM images showed that the size and morphology of particles cannot be precisely determined from these images, it is possible to see agglomerated and the particles not in a dispersed manner with a size outside the nanometer range.

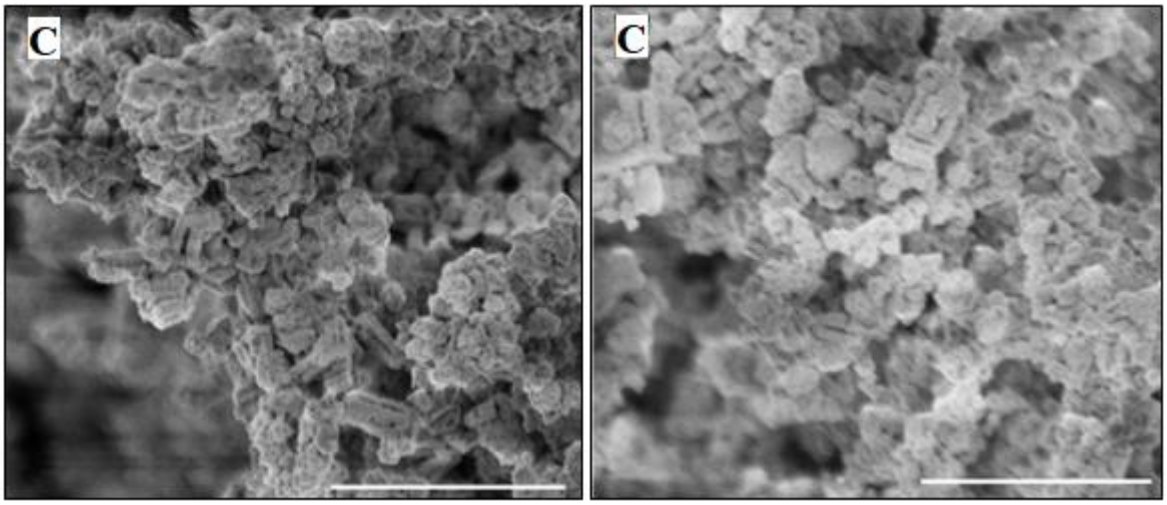

(Scale bar 2 μm).

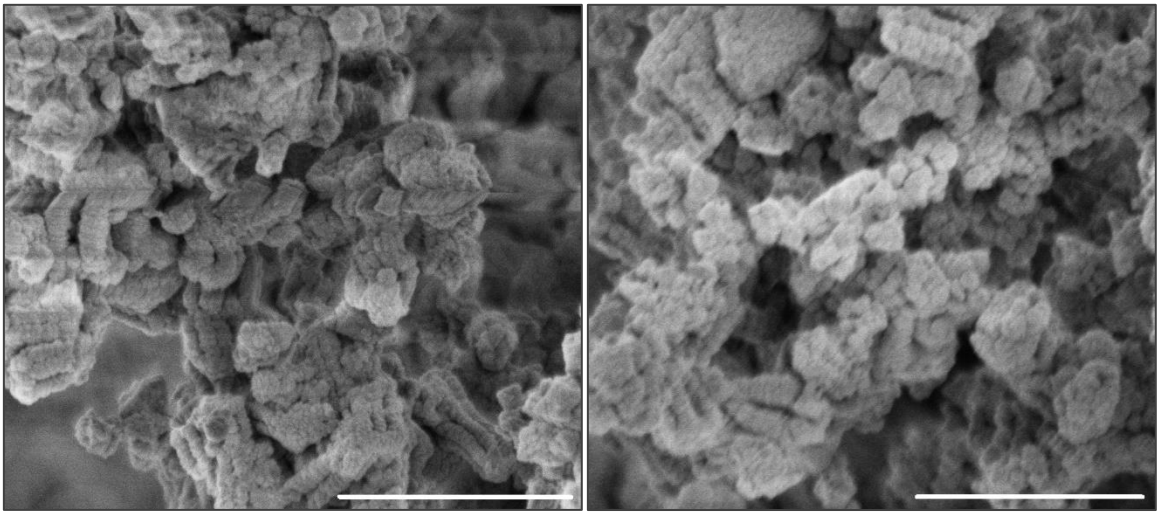

(Scale bar 1 μm)

Figures (4.3): SEM images of the purchased zinc peroxide particles.

4.1.2.2 Synthetized zinc peroxide nanoparticles (ZnO_2 NP's)

The nanoparticle sizes and morphologies were determined via SEM images of the ZnO_2 NP's that produced by sol-gel and reflux with and without capping agent. Figures (4.4, 4.5, and 4.6) shows the SEM images of the ZnO_2-NP's prepared by three different methods as mentioned.

The SEM shows that the ZnO_2-NPs for the three sample have grown in a near- spherical shape nanoparticles with a range of nanometer diameter which demonstrates the good quality of the ZnO_2-NPs. The SEM image reveals that the observed particles are smaller crystals and well dispersed in the powder form with small number of nanoaggregates**.**

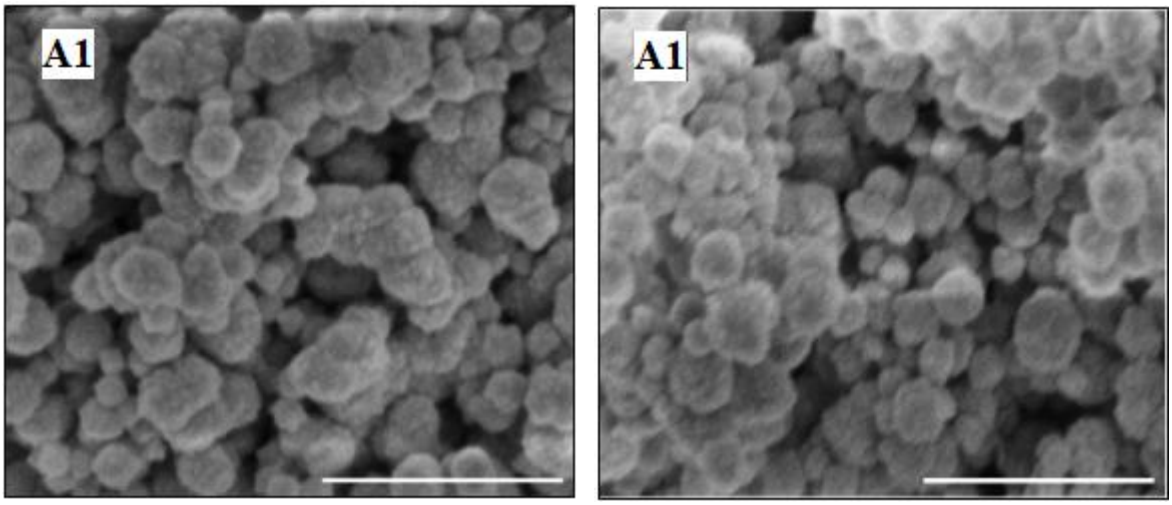

Figure (4.4): SEM images of the ZnO_2 nanoparticles by reflux method without PEI, (Scale bar 500 nm).

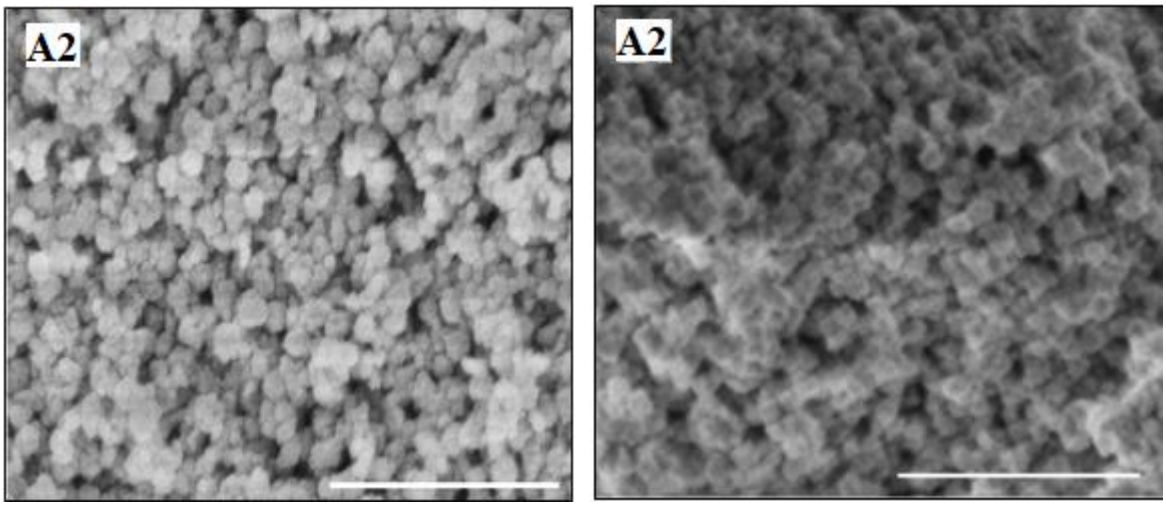

Figure (4.5): SEM images of the ZnO_2 nanoparticles by reflux method with PEI. (Scale bar 500 nm).

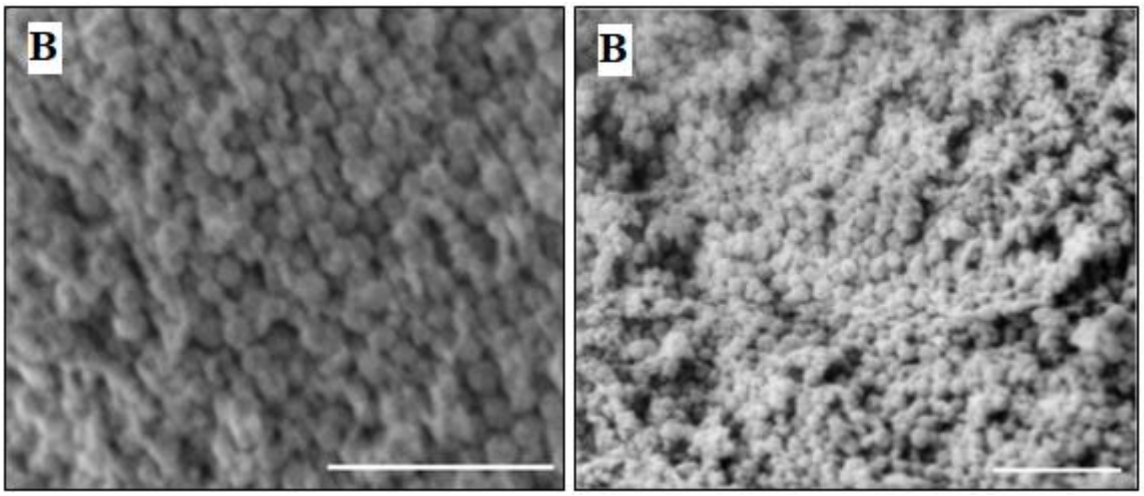

Figure (4.6) SEM images of the ZnO_2 nanoparticles by Sol-gel method. (Scale bar 500 nm).

As it is confirmed by the SEM images of ZnO_2 nanoparticles as showed in (Fig. 4.4 to 4.6), the particles size of all the method is in nanoscale which was implied by achieving such fine and small sizes with relatively few aggregations, a satisfying result was gained.

The average measured size and the size distribution of synthesized nanoparticles showed in Table (4.3) , the ZnO_2-NPs made by the sol-gel method is about 55 nm with polydispersity equal to 1.11 and the average particle sizes of the ZnO_2-NPs made by the reflux method using the capping agent is about 48 nm with polydispersity equal to 0.77 indicate that the sample has a narrow particle size distribution and the nanoparticles synthesized by reflux method without using capping agent give average particle size 82 nm with polydispersity equal to 1.33.

Table (4.3): Characteristic parameter of ZnO_2 NP's obtained from analysis of their SEM micrograph.

Materials	Average Size of NP's(nm)	Rn (nm)	Rv (nm)	Polydispersity (PDI)
A1	81.50	40.70	54.30	1.33
A2	47.50	23.70	18.30	0.77
B	54.80	27.40	30.50	1.11

The term of polydispersity index is used to describe the degree of non-uniformity of a size distribution of particles, PDI values bigger than 0.7 indicate that the sample has a very broad particle size distribution. (Bera, et al, 2015) The size histograms of the ZnO_2-NPs of the samples are shown in figure (4.7), The size distribution and nanoparticle diameter size were determined by counting the grains and crystals with an (J image,2015) software processing.

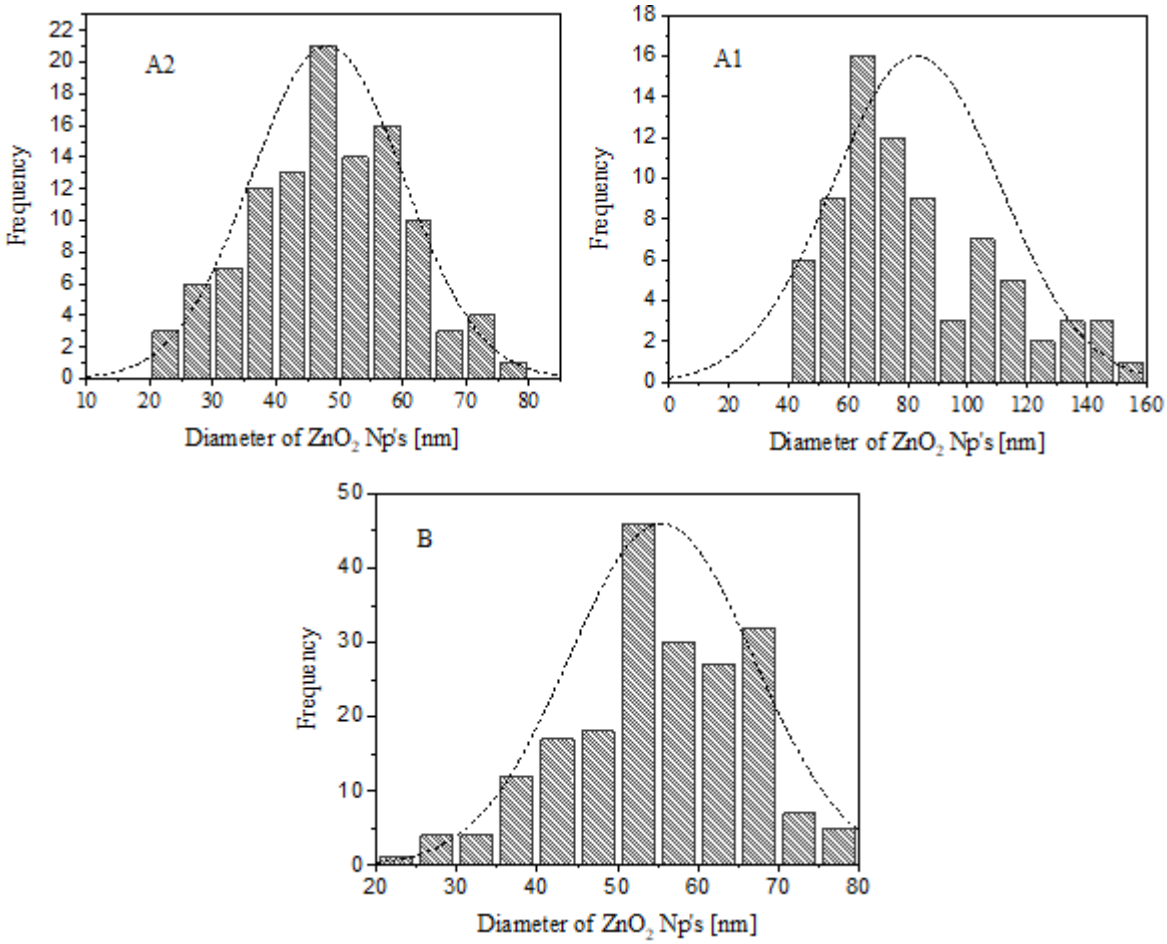

Figure (4.7): Particle size histograms obtained from image analysis of the SEM micrograph, where A1: reflux without PEI, A2: reflux with PEI and B: sol-gel method.

Table (4.4) shows the three methods for synthesized ZnO_2 nanoparticles and their percentage yield of reaction, as it was mentioned previously one of the methods used capping agent to enhance their properties such as stability and inhibit uncontrolled or over-growth of nanoparticles and controls physico-chemical characteristics in a precise way. (Javed, et al, 2020)

Table (4.4): Characteristic parameter of ZnO_2 NP's and their percentage yields of reactions.

Materials	Av Size of NP's(nm)	% Yield of reaction	Using of capping agent
A1	81.50	09.7 %	×
A2	47.50	10.9 %	✓ PEI
B	54.80	05.6 %	×

The variation of size of different synthesis method is related to several reason such as reaction temperature, concentration of reactants, time of reaction, and using of capping agent. (Shaba, et al, 2021) The more uniform distributions and smaller nanoparticle sizes were obtained when capping agent polyethyleneimine was used in comparison to the methods that do not use the capping agent. This finding because the role of capping agent centered on the prevention of agglomeration and control particle size. (Restrepo, et al, 2021)

According to (Javed, et al, 2016) and (Ibrahim, et al, 2017), the antibacterial activities of nanoparticles depicted a significant change possessed by capped nanoparticles as compared to the uncapped nanoparticles as a result of the effect of capping agent on the growth of bacteria. Many literatures support the positive effects of capping agent on the antimicrobial potential of nanoparticles. (Nithya, et al, 2015) (Javed, et al, 2017) For this study the method that used polyethyleneimine as capping agent was excluded due to the external effect of capping agent in the bacteria growth and not being used in nanocomposite materials applications for this study.

As previously shown in table (4.4), sol-gel method with average size 54.80 nm that did not use polyethyleneimine was excluded due to the low percentage yield compared to other methods. The lower percentage yields means that not much of the reactants that used has become products or there are incomplete reactions, this may be attributed to lower temperature of reaction that decrease the rate of reaction compare with other methods. The reflux method without PEI with average size of 81.50 nm was selected in the applications of nanocomposite materials for this study, because it has the good percentage yield compared to other methods and there is no external influence such as capping agent that affects its properties when distributed within the matrix.

4.1.2.3 Composite and Nanocomposite

In order to evaluate the dispersion and distribution of ZnO_2 and ZnO_2 NP's within the composite and nanocomposite, the morphological structure of the LDPE/ ZnO_2 composite and nanocomposite were investigated via SEM. Figure (4.8) are SEM micrograph images taken from the surfaces of the virgin low-density polyethylene without any of ZnO_2 filler, the surface area appears smooth and clear.

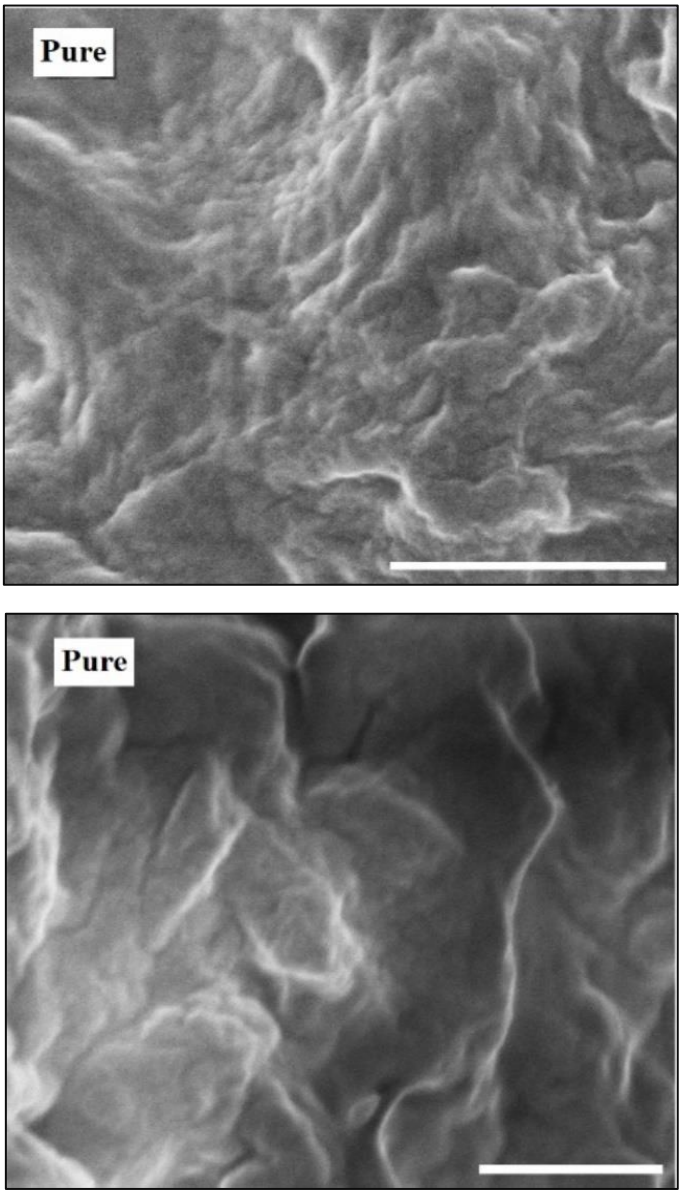

(Scale bar 1 μm)

Figure (4.8): SEM micrographs from the surface of pure LDPE prepared by solution method.

Figures (4.9, 4.10 and 4.11) show the morphological structure of LDPE/ ZnO_2 composite materials with different concentration of ZnO_2, comparing with the micrographs of pure LDPE, there are some of bright spots on the surface of composite, which indicate that ZnO_2 particles and it's embedded in the matrices of the composite. The ZnO_2 particles in polyethylene matrix with concentration of 1 % were present in smaller clusters and agglomerates with the size up to 5 μm and a little distribution can be seen in the upper right corner. While the ZnO_2 fillers with 3 % concentration do not appear clearly on the surface of composite. And the micrograph of composite with 5 % concentration shows a distribution of ZnO_2 in the LDPE matrix with little signs of agglomerates.

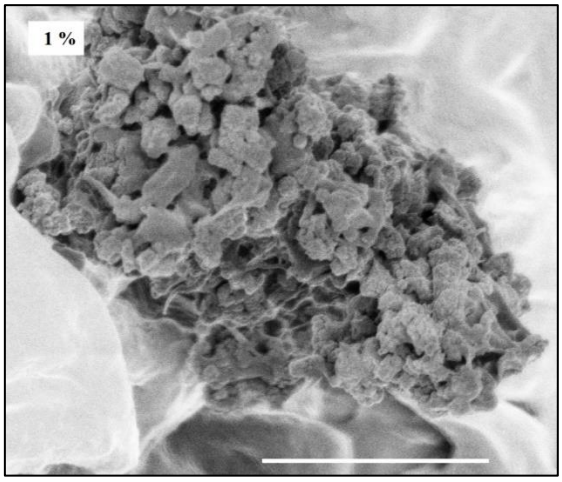

(Scale bar 2 μm)

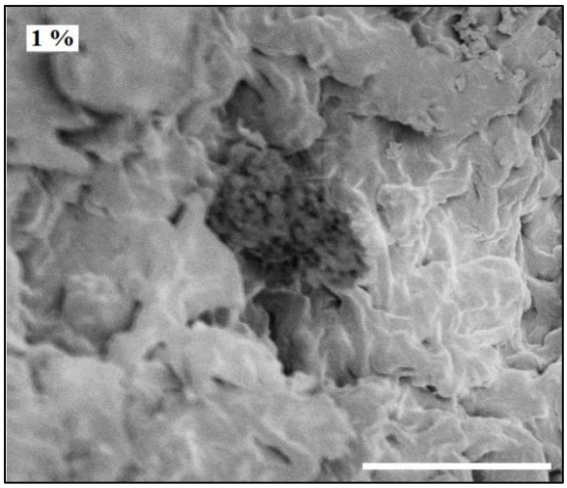

(Scale bar 5 μm)

Figure (4.9): SEM micrographs from the surface of the LDPE composite with 1% concentration of ZnO_2 particles.

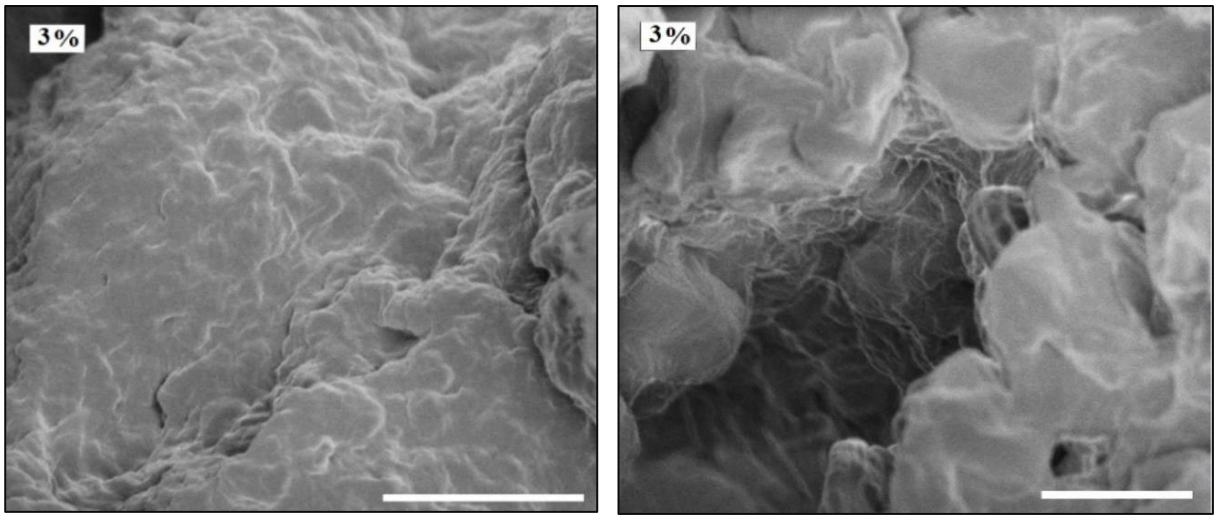

(Scale bar 5 μm).

Figure (4.10): SEM micrographs from the surface of the LDPE composite with 3% concentration of ZnO_2 particles.

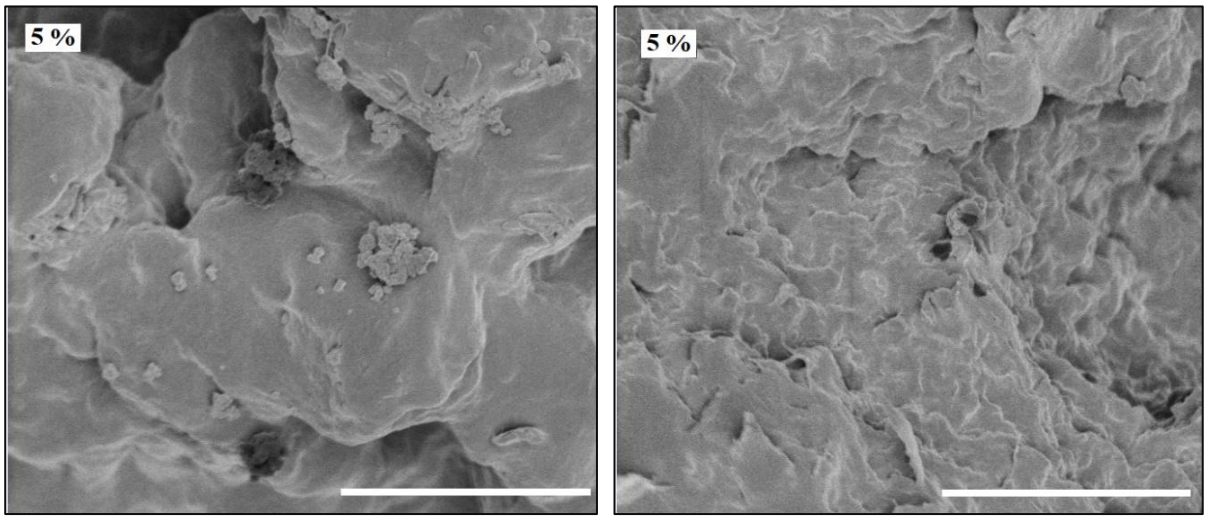

(Scale bar 5 μm).

Figure (4.11): SEM micrographs from the surface of the LDPE composite with 5% concentration of ZnO_2 particles.

Figures (4.12 to 4.16) shows the morphological structure of LDPE/ ZnO_2 nanocomposite materials, one of the main challenges in nanocomposites was to achieve an even distribution of nanoparticles that dispersion in the LDPE, a higher concentration of fillers causes a poor distribution with high number of particles in some areas and lower number of particles in another area. (Kim, et al,2007) (Pallon, 2016)

The SEM micrograph shows that the nanoparticles well distributed within the whole polymer matrix. The micrograph of the nanocomposite with ZnO_2 nanoparticles filler showed distinct dispersion behavior as that of the composite containing the ZnO_2 filler, On the other hand the nanocomposite showed not only smaller particles fillers than the composites that containing ZnO_2 filler but it also proved to be better dispersed in the LDPE matrix. Smaller agglomeration was present in some micrograph, and this affects the properties of the nanocomposite but in general, the micrographs show that the nanoparticles distributed better than composite samples. At a high concentration of nanoparticles (5%), it appears that the nanoparticles covered the surface significantly as a result of the huge number of nanoparticles, which is considered as a very high concentration compared to ZnO_2 particle within composite.

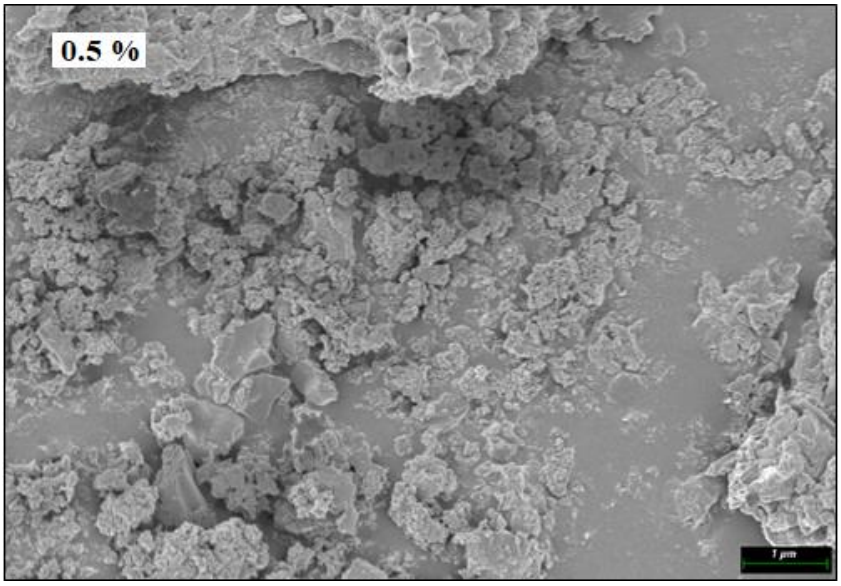

Scale Bar (1 μm)

Figure (4.12): SEM micrographs from the surface of the LDPE nanocomposite with 0.5% concentration of ZnO_2 NP's.

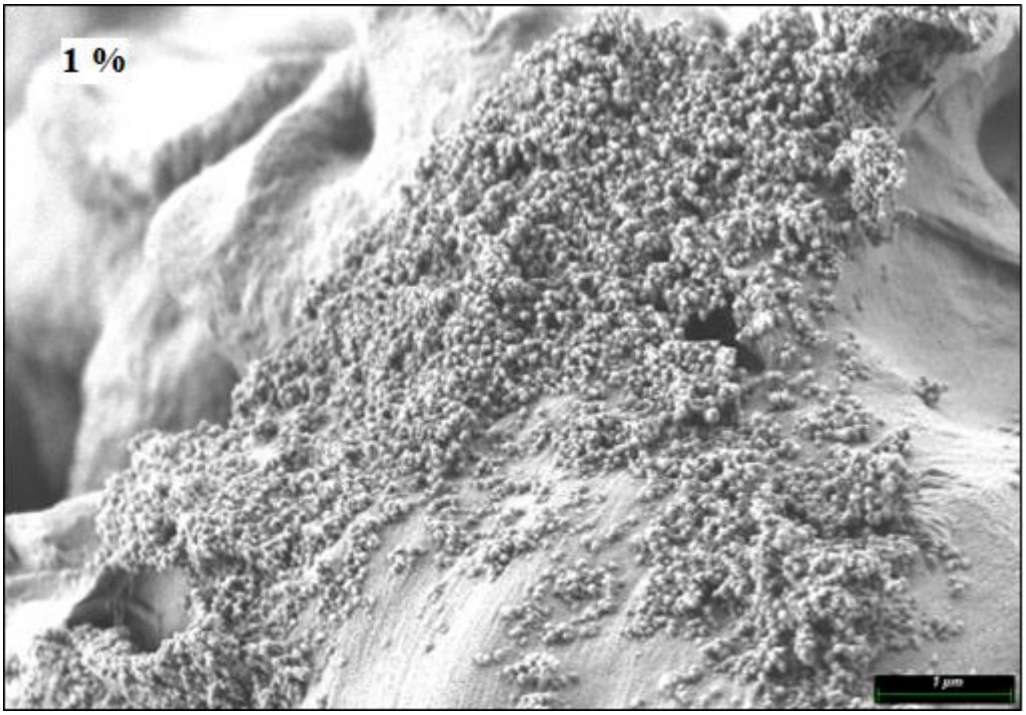

Scale Bar (1 μm)

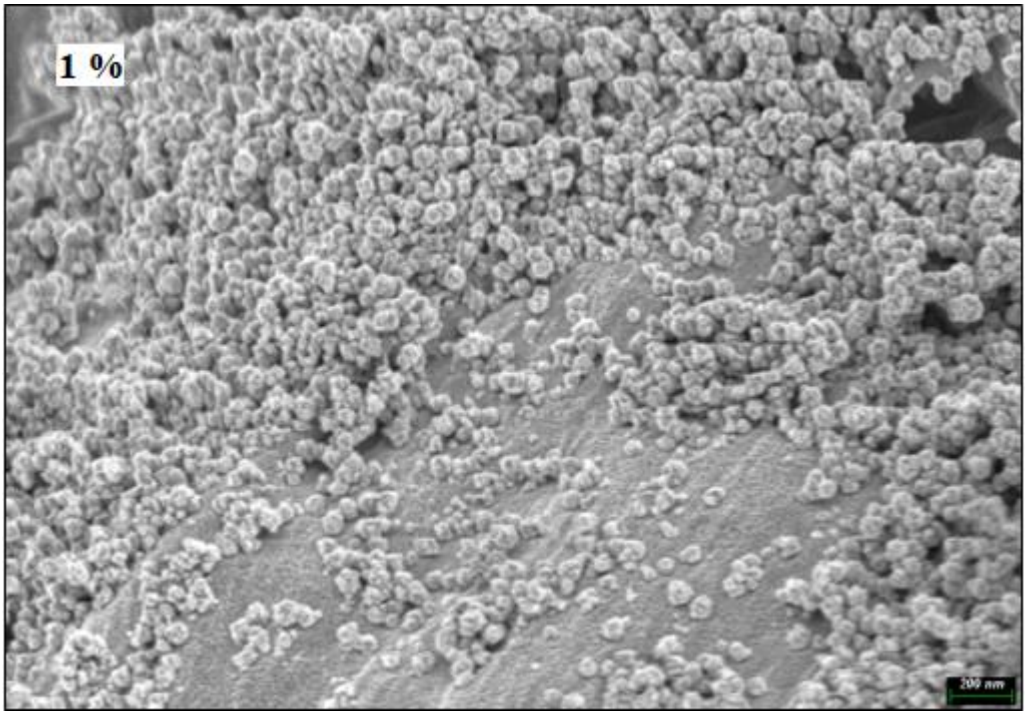

Scale Bar (200 nm)

Figure (4.13): SEM micrographs from the surface of the LDPE nanocomposite with 1% concentration of ZnO_2 NP's.

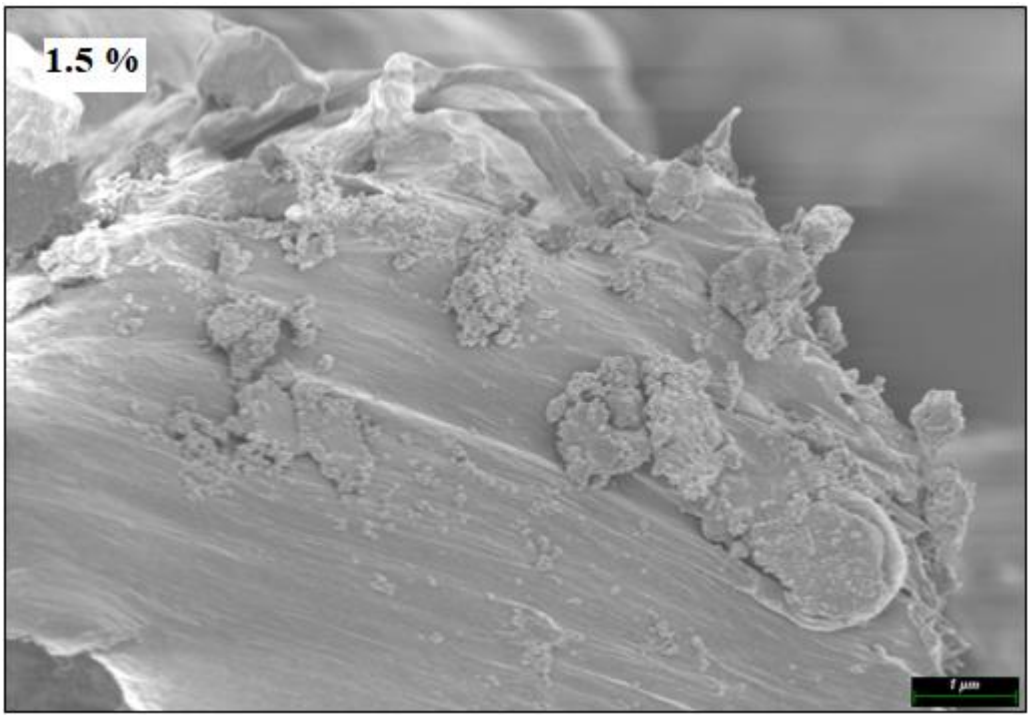

Scale Bar (1 μm)

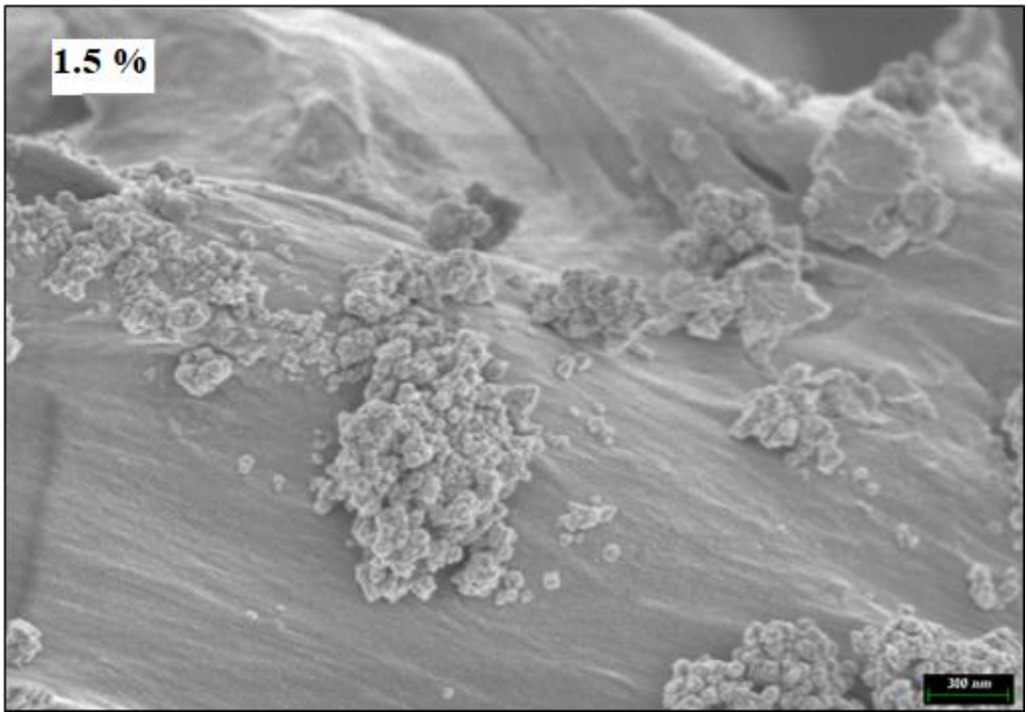

Scale Bar (200 nm)

Figure (4.14): SEM micrographs from the surface of the LDPE nanocomposite with 1.5% concentration of ZnO_2 NP's.

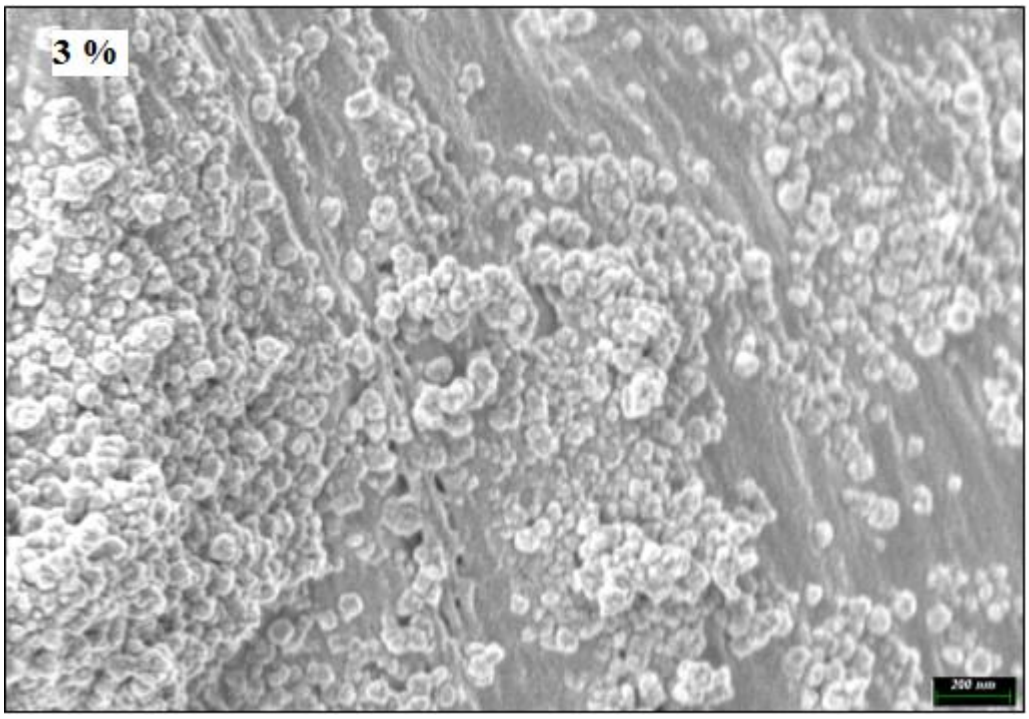

Scale Bar (200 nm)

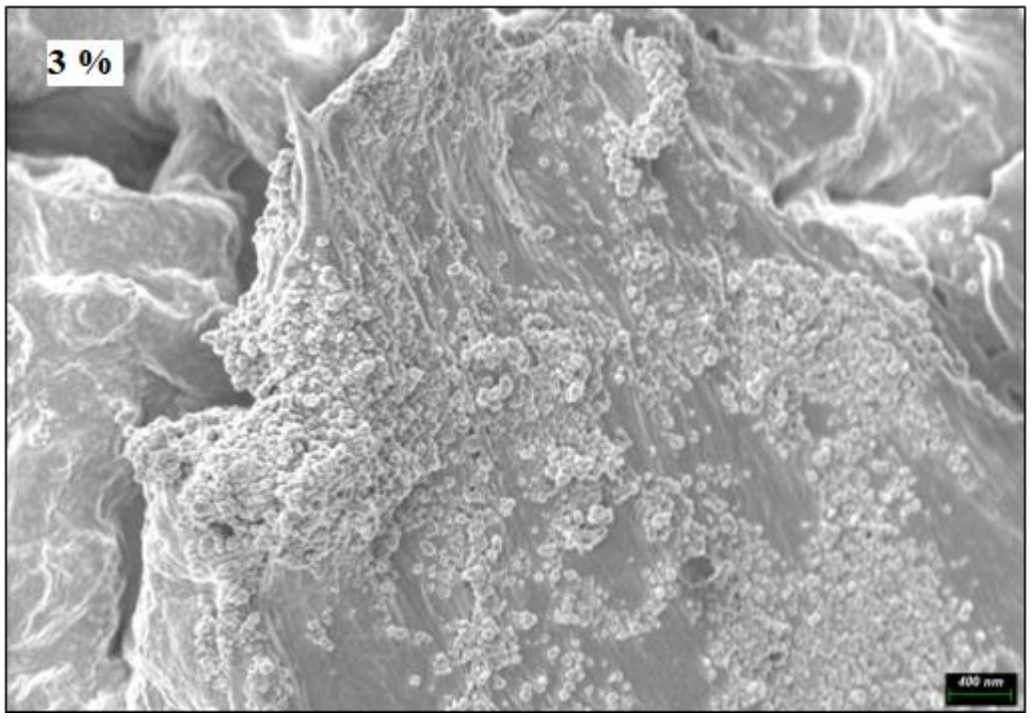

Scale Bar (400 nm)

Figure (4.15): SEM micrographs from the surface of the LDPE nanocomposite with 3% concentration of ZnO_2 NP's.

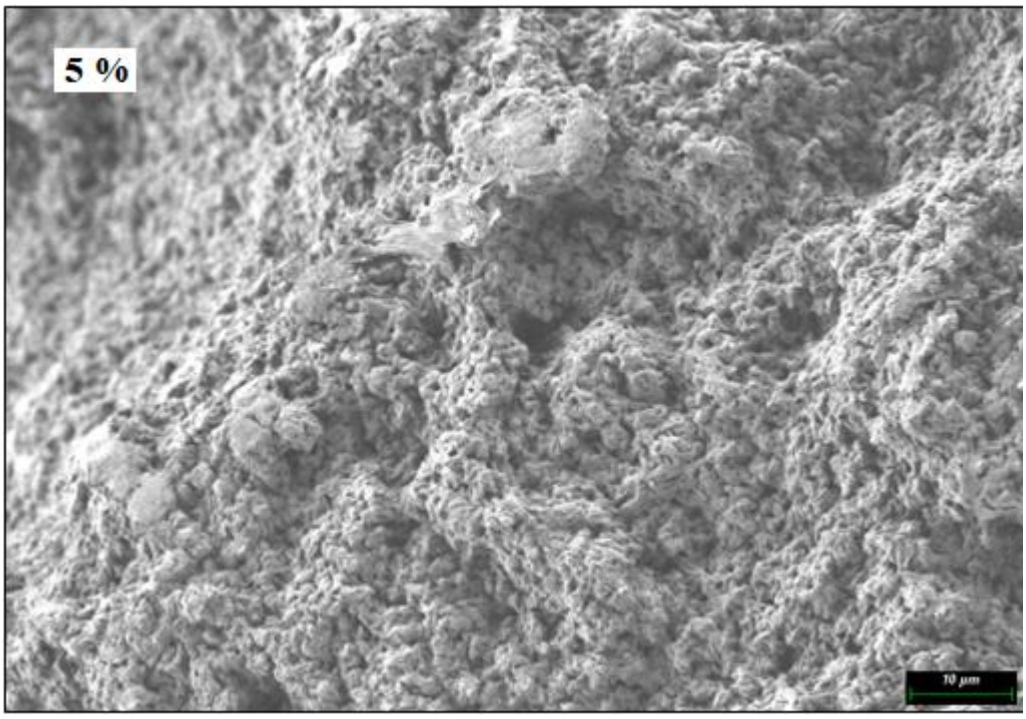

Scale Bar (10 μm)

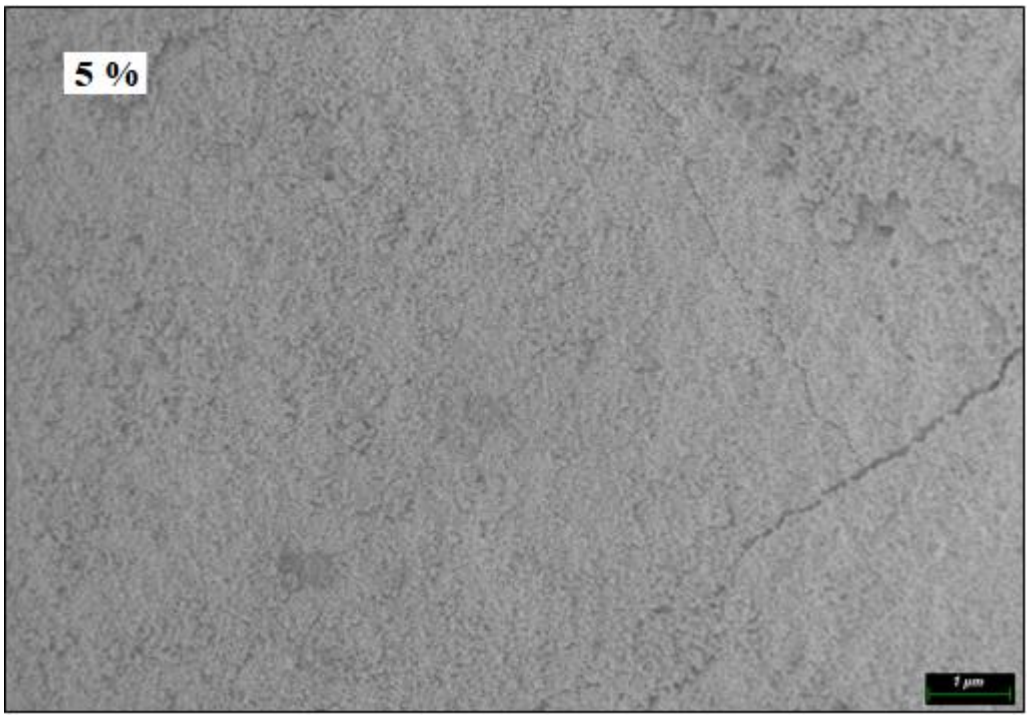

Scale Bar (1 μm)

Figure (4.16): SEM micrographs from the surface of the LDPE nanocomposite with 5% concentration of ZnO_2 NP's.

4.1.3 Fourier-transform infrared spectroscopy analysis

4.1.3.1 Synthesized zinc peroxide nanoparticles (ZnO_2 NP's)

The FT-IR is the powerful technique based on vibrational spectroscopy for the analysis of structure of compounds which allows the identification and determination of functional groups present. (Shameer, et al, 2019) The FTIR spectrum of synthetized ZnO_2 nanoparticles that produced by reflux with and without PEI and sol-gel is shown in figure (4.17).

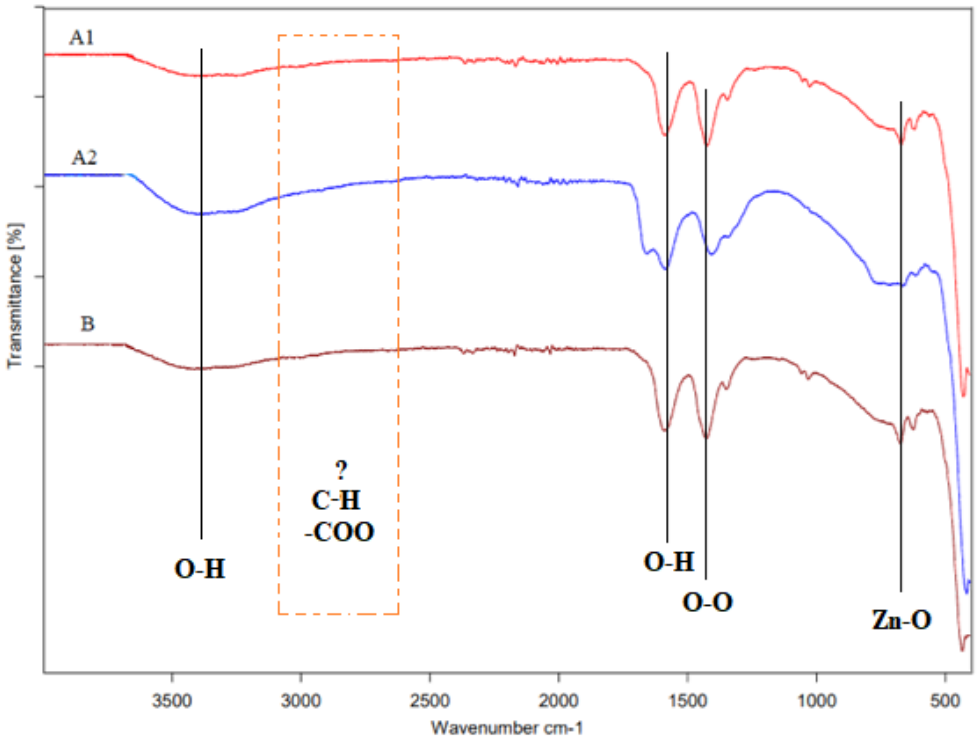

Figure (4.17): Fourier-transform infrared spectrum of the synthetized ZnO_2 -NPs.

The spectrum of the all- ZnO_2 samples that synthesized revealed almost similar absorption characteristic infrared absorption. A broad absorption peak is present in all the figures at 3404 cm^{-}, [1]3388 cm^{-1}, 3434 cm^{-1} for A1, A2 and B respectively, which can be attributed to the characteristic absorption of hydroxyl groups (O–H) corresponds to characteristic stretches of the water molecule. And other peak located at 1584, 1592,1579 cm^{-1} are attributed to the stretching vibration of the O–H bond and the bending vibration of H–O–H from water molecules. (Escobedo Morales, et al, 2011)

The bands located at 1421, 1414, and 1418.8 cm^{-1} for A1, A2 and B respectively, could be assigned to the vibrational modes of O-O bands corresponding to the peroxide (O_2) ions of ZnO_2 nanoparticles. Another sharp absorption bands of the synthesized ZnO_2 are observed located around 650 cm^{-1} for all three samples method, which corresponds to Zn–O vibration. (Hussein, et al 2021)

The FTIR peaks confirms presence of functional groups on the surface of ZnO_2 and formation of ZnO_2 nanoparticle FT-IR spectrum does not show any of absorption bands at 2924 and 2853 cm^{-1} of stretching modes of C–H bonds or -COO groups of zinc acetate, suggesting the purity of synthetized ZnO_2 nanoparticles from the reactants. (Aguilar, et al, 2011) Finally, the infrared band with wave number lower than 500 cm^{-1} is attributed to Zn–O bond; similar strong absorption band for three samples of synthesized ZnO_2 has been already reported. (Cheng, Yan, et al 2009)

4.2 Thermal Characterization

4.2.1 Zinc peroxide purchased material.

Figure (4.18) shows the obtained DSC thermograms of used ZnO_2, the thermograms show exothermic peak at 208.27 °C that attributed to oxygen release during heating and decomposition of ZnO_2 to ZnO according to the following chemical equation (Sebok, et al, 2009). The decomposition temperature close to the data sheet of ZnO_2 used powder which has a decomposition point 212 °C.

$$\mathbf{2\,ZnO_2 \rightarrow 2ZnO + O_2}$$

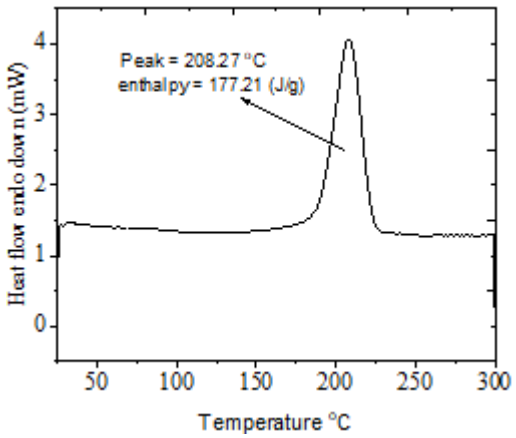

Figure (4.18): Differential scanning calorimetric curve of used zinc peroxide.

4.2.2 Synthetized zinc peroxide nanoparticles

DSC characterization was performed to the synthesized ZnO_2 nanoparticles powder. Figures (4.19) shows the thermal analysis of the samples. The figure shows the thermal behavior of synthesized ZnO_2-NPs by reflux with and without PEI, sol-gel, from room temperature 25 ^oC to 300 ^oC.

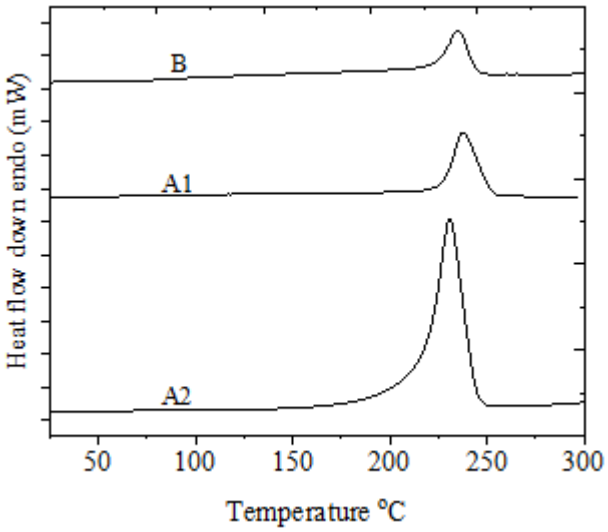

Figure (4.19): Differential scanning calorimetric curves of the synthetized ZnO_2

Based on the DSC thermograph, each sample show an exothermic peak at 238.03 °C, 230.80 °C and 235.20 °C for A1, A2 and B respectively as showed in table (4.5), which is attributed to oxygen release due to decomposition of ZnO_2 molecules to ZnO and oxygen, according to the following chemical reaction equation:

$$2\ ZnO_2 \rightarrow 2ZnO + O_2$$

Table (4.5): Thermal properties of zinc peroxide obtained from differential scanning calorimetry.

Sample Code	Decomposition temperature (^oC)	Enthalpy (J/g)
A1	238.03	51.62
A2	230.80	787.15
B	235.20	42.59

So thermal analysis revealed that the ZnO_2 samples is stable up to the exothermic peak at mentioned temperatures for all the samples, after decomposition temperature the product was zinc oxide (ZnO) with hexagonal structure and remaining which is almost constant up to 300 ^oC and remains after cooling to ambient temperature. (Cheng, et al, 2009)

Table (4.5) showed a little decrease of decomposition temperature was found for ZnO_2 nanoparticles that synthesized by refluxing with using polyethylenimine as capping agent and have the highest enthalpy value may be explained by the combustion reaction that takes place between the remaining agent matter of capping agent when oxygen is released due to the decomposition of ZnO_2. The reason of lower decomposition temperature may be due to this method having lower size than other method, so the decomposition temperature exhibits a strong size-dependence for particle size because of nano scale material have a much larger surface area to volume ratio than bulk material, means the surface energy will be increased. (Schlexer, et al, 2019)

4.2.3 Composite and Nanocomposite

Figures (4.20 & 4.21) shows the DSC curves of composite and nanocomposite samples. These figures declare that all the investigated samples were heated twice from room temperature to 130°C and subsequent cooling in nitrogen atmosphere for the first and second time, this step to remove the effect of residual solvents within the samples, and to eliminate any thermal history that the polymer may have gone through during its synthesis and post processing steps.

It will be noted that all samples are characterized by % degree of crystallinity, enthalpy, melting temperature and crystallization temperature. The values for these transitions along with measured endotherms and exotherms are recorded in Tables (4.6 &4.7). It is worthy to find the area under the melting peaks to find heat of fusion which is an indication on the percentage of crystalline regions.

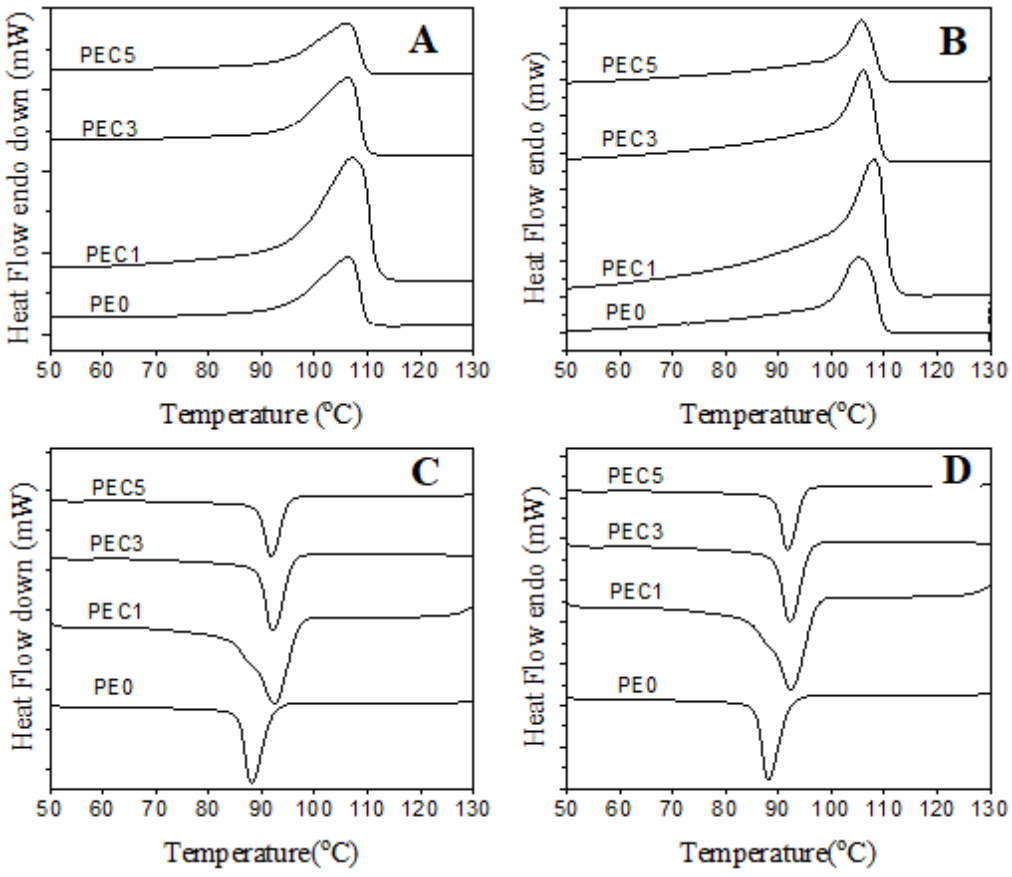

Figure (4.20): DSC scans of composites where (A): Heating 1st scan, (B): Heating 2nd scan, (C): Cooling 1st scan and (D) Cooling 2nd scan.

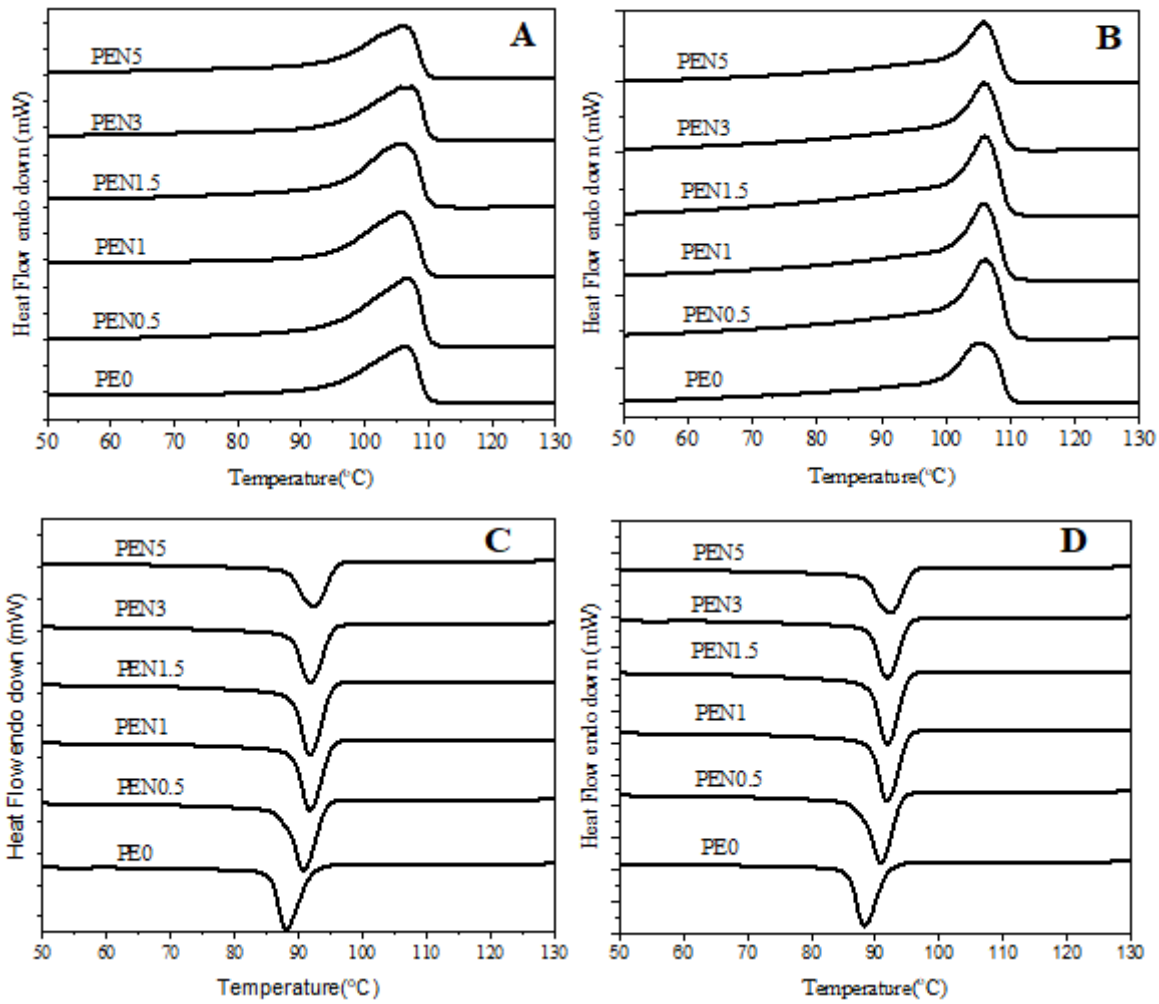

Figure (4.21): DSC scans of nanocomposites where (A): Heating 1st scan, (B): Heating 2nd scan, (C): Cooling 1st scan and (D): Cooling 2nd scan.

The DSC scan in figure (4.20 & 4.21) shows an exothermic peak of all concentration of composite and nanocomposite that observed around 88-93°C, indicating an exothermic reaction caused by crystallization and endothermic peaks observed at around 105-108°C refers to an endothermic reaction caused by melting. Table (4.6) lists the melting temperature and crystallization temperature of the composite and nanocomposite based on the DSC scanning curves.

Table (4.6): Melting and crystallization temperature as a function of zinc peroxide concentration obtain from DSC curves for composite and nanocomposite.

Materials	**Melting Temperature (°C)**		**Crystallization Temperature (°C)**	
	First scan	**Second scan**	**First scan**	**Second scan**
PE	106.4	105.2	88.1	88.1
PEC1	107.1	108.1	92.4	92.4
PEC3	106.2	106.1	92.1	92.1
PEC5	106.2	105.7	91.9	91.9
PEN0.5	106.9	106.1	90.8	90.9
PEN1	105.8	105.9	91.8	91.9
PEN1.5	105.8	106.1	91.8	91.9
PEN3	105.9	107.4	91.8	91.8
PEN5	105.9	106.1	92.5	92.4

The melting temperature of pure polyethylene without ZnO_2 loading was 106.4 ^oC,105.2 ^oC for first and second scan, respectively. The results showed that there are slight variations between the melting temperature of different concentration of composite and nanocomposite samples, the possible reason is there no strong chemical or intermolecular bonding between polymer and ZnO_2 that occurs, therefore melting temperature are not affected. While slight elevations compared to the pure LDPE sample are due to that ZnO_2 filler may restrict the flow ability of low-density polyethylene molecules during the melting process. (Anzoyar, et al, 2019)

For the exothermic peak for crystallization temperature, it is obvious that the pure low-density polyethylene has lower crystallization temperature at 88.1 ^{o}C than all filled ZnO_2 sample for composite and nanocomposite that exceed 90 ^{o}C. It is clear that the exothermic peaks shift to higher temperatures, which indicates that the crystallization rate of composite and nanocomposite have become faster due to the fact that the filler act as nucleating agent and the filler allow for polymer chain to rearrangement easily and speed in the crystallization process. Similar results have also been reported in the paper of wang. (Wang, et al, 2009)

Table (4.7) shows the percentage degree of crystallinity and melting, cooling enthalpy for the first and second time by DSC for the composite and nanocomposites, the incorporation of filler is observed to have little effect on the enthalpy of fusion and degree of crystallinity.

Table (4.7): DSC data analysis obtained from DSC scans for composite and nanocomposite.

Materials	**% Degree of Crystallinity (Xc)**		**Enthalpy(J/g)**			
			For Heating		**For Cooling**	
	First scan	**Second scan**	**First scan**	**Second scan**	**First scan**	**Second scan**
PE	20.2	17.9	58.2	51.8	55.7	55.7
PEC1	20.2	18.8	57.7	53.2	55.8	56.1
PEC3	23.3	21.1	65.1	58.8	59.8	59.6
PEC5	19.2	16.7	52.5	45.6	47.2	47.2
PEN0.5	20.6	18.9	58.9	54.3	51.7	50.9
PEN1	21.6	20.2	61.5	57.5	48.8	48.9
PEN1.5	21.8	21.1	61.9	59.9	56.3	56.2
PEN3	23.2	24.1	64.8	67.2	60.3	60.3
PEN5	23.3	25.4	63.7	69.6	57.1	57.7

Crystallization happens in many stages in LDPE composites and nanocomposite. Nucleation considered as the first stage, where new small particles can be formed with new phase. Incorporation of some ZnO_2 particle and nanoparticle to the pure polyethylene can change the percentage crystallization because of the change in the nucleating agents.

For the composite the melting and cooling enthalpy of composite is increased even by adding small concentration of ZnO_2 up to 3 %, and then decrease for high concentration of ZnO_2 at 5%, as showed in table (4.7). The value of melting enthalpy is commonly used to calculate the degree of crystallinity, so the melting enthalpy change is an indicator of the variation in the degree of crystallinity and behaving similarly when the zinc peroxide concentration increase.

Increasing in percentage of crystallinity of ZnO_2 as showed in figure (4.22 a), it's could be to the addition of ZnO_2 loading to the polyethylene composite leads to a reduced in mobility of the crystalline regions causes slow crystal formation and reduces the size of crystallites, hence results in an increase of the degree of crystallinity. (Tjong, et al, 2003)

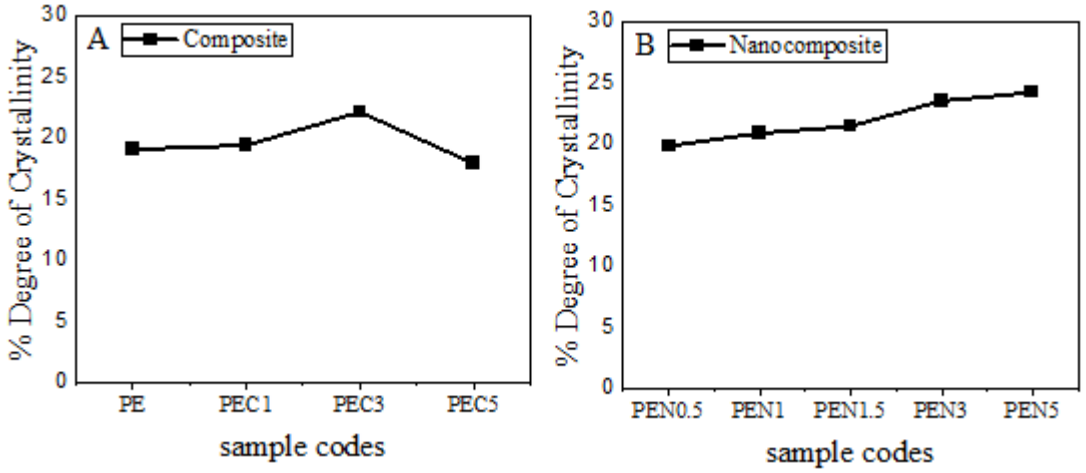

Figure (4.22): % Degree of crystallinity trend for: (a) Composite, (b) Nanocomposite.

Figure (22 b) demonstrated that for the nanocomposite, the degree of crystallinity increased approximately as ZnO_2 nanoparticles concentration increased. This can be explained by the fact that the nanoparticles act as nucleating agent and accelerate formation of crystalline, decrease spherulites dimensions and increase crystallinity. Many studies had indicated that nano filler could act as a nucleating agent. (Aswathy, et al, 2008) (Zaman, et al, 2012)

Figure (4.22 c) shows the different trend in percentage of crystallization between composite and nanocomposite. The degree of crystallization of nanocomposite relatively higher than composite. In nanocomposites, the loading level of 3% nano ZnO_2 induced a high crystallinity of all concentration of the composites, the increased surface area of ZnO_2 nanoparticles contributes to the shift of the percentage crystallinity. The reason can be explained to the disruption and the nature of the interaction between the particles and the low-density polyethylene matrix. (Zaman, et al, 2012)

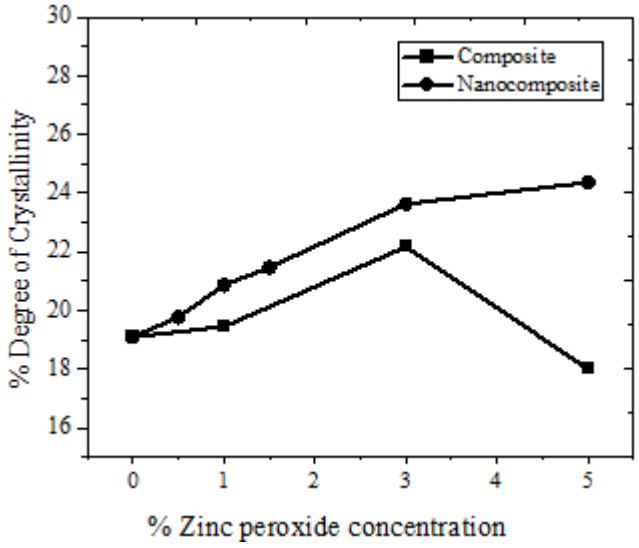

Figure (4.22 c): % Degree of crystallinity trend for: Composite and Nanocomposite.

Additionally, the increased degree of crystallinity is expected, since the nano-fillers will act as nucleating agents in polymer crystallization, the nanofiller contributes more towards nucleation, the nucleating agent that influence polymer crystallization depends on several aspects, such as the size and the geometry of the particles, the surface structure with the polymer matrix, increasing crystallinity leads to more regularly aligned polymer chains, therefore increasing the degree of crystallinity increases hardness and density of nanocomposite compared to composite. (Sanporean, et al, 2014)

4.3 Mechanical charactrization

Generally, incorporation of ZnO_2 / ZnO_2 nanoparticles into the polymer matrix has shown a significant effect on the tensile properties of the composite and nanocomposite samples, which include tensile strength, young's modulus, stress at yield, strength at break and percentage elongation at fracture. Figure (4.23) show the stress-strain curves behavior of composites and nanocomposites.

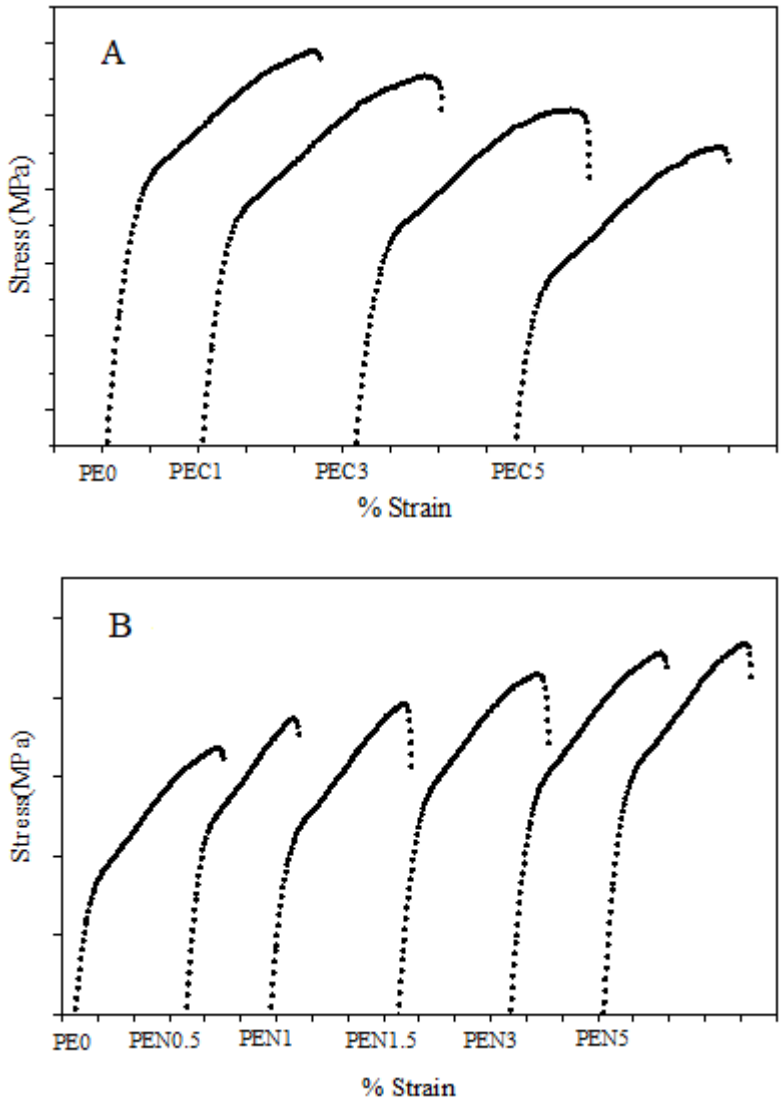

Figure (4.23): Stress-strain curves behavior, where A: composite samples and B: nanocomposite samples.

The effect of varies concentration of filler on the tensile properties of composites and nanocomposites were significant by increasing concentration of ZnO_2 in polymer matrix, either higher, lower or vice versa for all the tensile properties. Table (4.8 & 4.9) gives a summary of the tensile properties for all studied compositions of composites and nanocomposites.

Table (4.8): Tensile properties of composites materials.

Sample code	Tensile strength (MPa)	E modulus (GPa)	Yield strength (MPa)	Fracture strength (MPa)	% Elongation at fracture
PE	4.94 ±0.38	0.103 ±0.005	1.22 ±0.16	3.19 ±0.64	0.39 ±0.03
PEC1	4.76 ±0.80	0.110 ±0.009	1.24 ±0.17	3.74 ±0.25	0.36 ±0.04
PEC3	4.53 ±0.46	0.115 ±0.012	1.26 ±0.07	3.81 ±0.40	0.33 ±0.02
PEC5	4.35 ±0.56	0.117 ±0.010	1.27 ±0.21	3.39 ±0.21	0.29 ±0.02

Table (4.9): Tensile properties of nanocomposites materials.

Sample code	Tensile strength (MPa)	E modulus (GPa)	Yield strength (MPa)	Fracture strength (MPa)	% Elongation at fracture
PE	4.94 ±0.38	0.103 ±0.005	1.22 ±0.16	3.19 ±0.64	0.39 ±0.03
PEN0.5	4.98 ±0.79	0.109 ±0.006	0.81 ±0.15	4.28 ±0.33	0.48 ±0.03
PEN1	5.01 ±0.71	0.112 ±0.007	0.83 ±0.20	4.41 ±0.23	0.42 ±0.03
PEN1.5	5.16 ±0.93	0.114 ±0.006	0.89 ±0.23	4.40 ±0.36	0.42 ±0.07
PEN3	5.22 ±0.28	0.121 ±0.008	0.90 ±0.04	4.73 ±0.32	0.41 ±0.02
PEN5	5.28 ±0.73	0.124 ±0.010	1.06 ±0.20	4.90 ±0.54	0.42 ±0.05

4.3.1 Tensile strength

ZnO_2 plays an important role as a filler in plastics to impart various mechanical and novel functional properties. Herein, ZnO_2 powder and ZnO_2 nanoparticle that synthesized by reflux method were used as a filler in LDPE for prepared composite and nanocomposite.

At the beginning of the examination, the concentration of ZnO_2 in the low-density polyethylene matrix was 0% and it achieved a tensile strength of 4.94 MPa without any influence from the ZnO_2 filler concentration. The tensile strength of ZnO_2 /LDPE nanocomposites as a function of increasing ZnO_2 concentration are shown in figure (4.24).

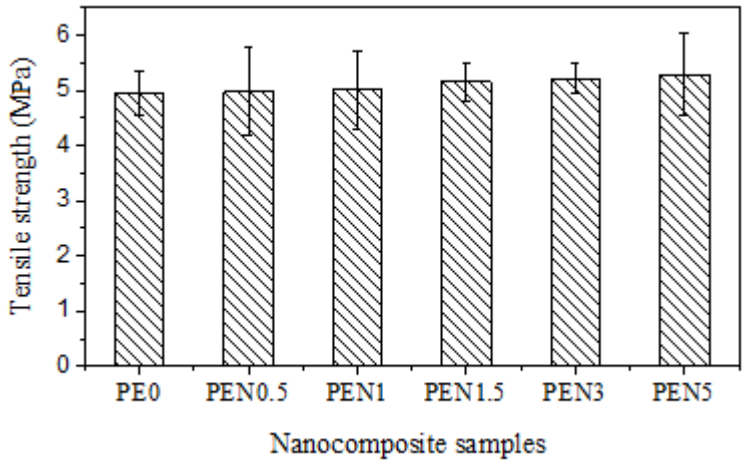

Figure (4.24): Tensile strength of nanocomposite, with different concentration of zinc peroxide NP's.

For nanocomposite the tensile properties improve by adding fillers to a polymer matrix since fillers have much higher strength and stiffness values than those of the matrices and the increasing trend in tensile strength be explained by the large surface area of the nanofillers, which makes it stronger bonding with the matrix. And as it is confirmed by the thermal properties of nano composite that the crystallinity of a polymer increases with the concentration of nano filler increases. This, in turn, also increases the tensile strength of the nanocomposite. (Haydar, et al, 2012) (Ahmad, et al, 2017)

For composite based on ZnO_2 powder, it is observed that the presence of filler in the polymeric matrix decrease the composite strength, and it can be seen in figure (4.25) that the tensile strengths of the composites decrease with increase concentration of ZnO_2 powder, this behavior can be attributed to the agglomeration of ZnO_2 particles as shown from some SEM micrographs for ZnO_2 and high loading of ZnO_2 hence creating more stress concentration and reducing the effectiveness of ZnO_2 as reinforcement. Similar results are shown in Abou-Kandil et al study. (Abou-Kandil, et al, 2015)

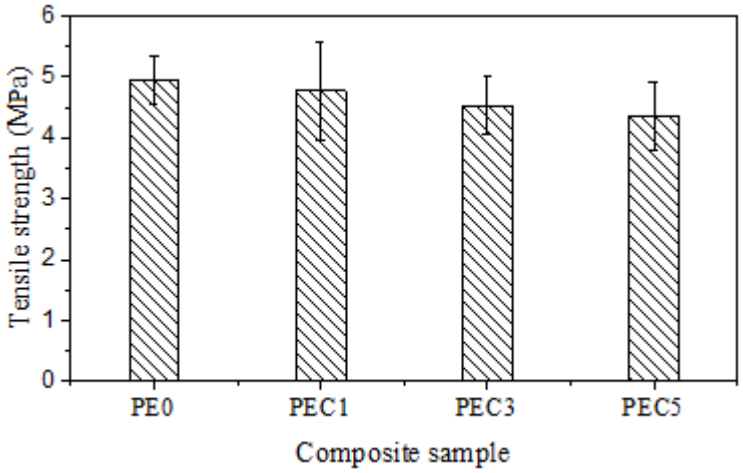

Figure (4.25): Ultimate tensile strength of composite, with different concentration of zinc peroxide.

As well the gradual drop from 0% to 5 % for composite in tensile strength may be related to the larger volume of voids which may be formed within the blend which would serve as flaws and stress concentration for crack initiation, which adversely affects the interfacial adhesion between the particles and the polymeric matrix resulting in poor tensile properties. (Dhawan, et al, 2013)

The maximum tensile strength for the composite and nanocomposite reached a maximum at 5 % ZnO_2 concentration of nanocomposite "5.25 MPa" as shown in the figure (4.26). This result suggests that high loading of the zinc peroxide nanoparticles improve tensile properties better than larger particle that produce low interfacial/interphase properties and poor tensile strength, so the nanoparticle contributed to the increase of tensile strength of the nanocomposite with the addition of ZnO_2 particles.

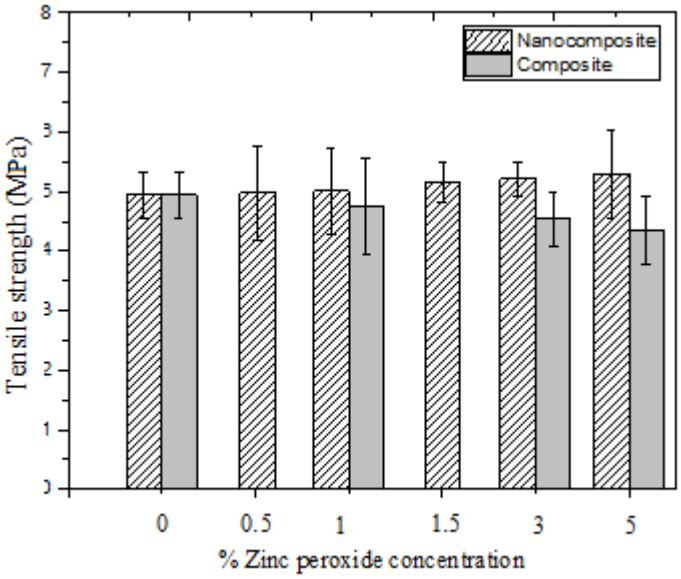

Figure (4.26): Ultimate tensile strength of composite and nanocomposite, with different concentration of zinc peroxide.

Comparing the tensile properties of the composite materials with nanocomposite in this study statistically significant differences were observed. ZnO_2 nanocomposites have a higher strength to weight ratio than ZnO_2 reinforced composites and a homogenous distribution of nano filler within the matrix hence reduce the stress concentrations within the composite structure, The nanoparticles with a high surface area to volume ratio. These make it to react at much faster rates than bulk filler materials because more surface area makes stronger bonding with the matrix. (Hanemann, et al, 2010) Here the difference is apparent that the tensile strength of nanocomposite at 1%, 3% and 5 % nanoparticles concentration are 5.01, 5.21 and 5.28 MPa respectively, while the tensile strength of composite at same concentration filler at 1 %, 3 % and 5 % is 4.76,4.53 and 4.43 MPa respectively.

4.3.2 Elastic modulus

The elastic Modulus of LDPE- ZnO_2 composite and nanocomposite samples with different concentration of ZnO_2 powder and ZnO_2 nanoparticles are presented in figure (4.27). Elastic modulus was found to increase with ZnO_2 concentration for composite and nanocomposite samples. The highest set of values was obtained for 5 wt% concentration of ZnO_2 for nanocomposite with the modulus value 0.124 GPa as compared to the composite.

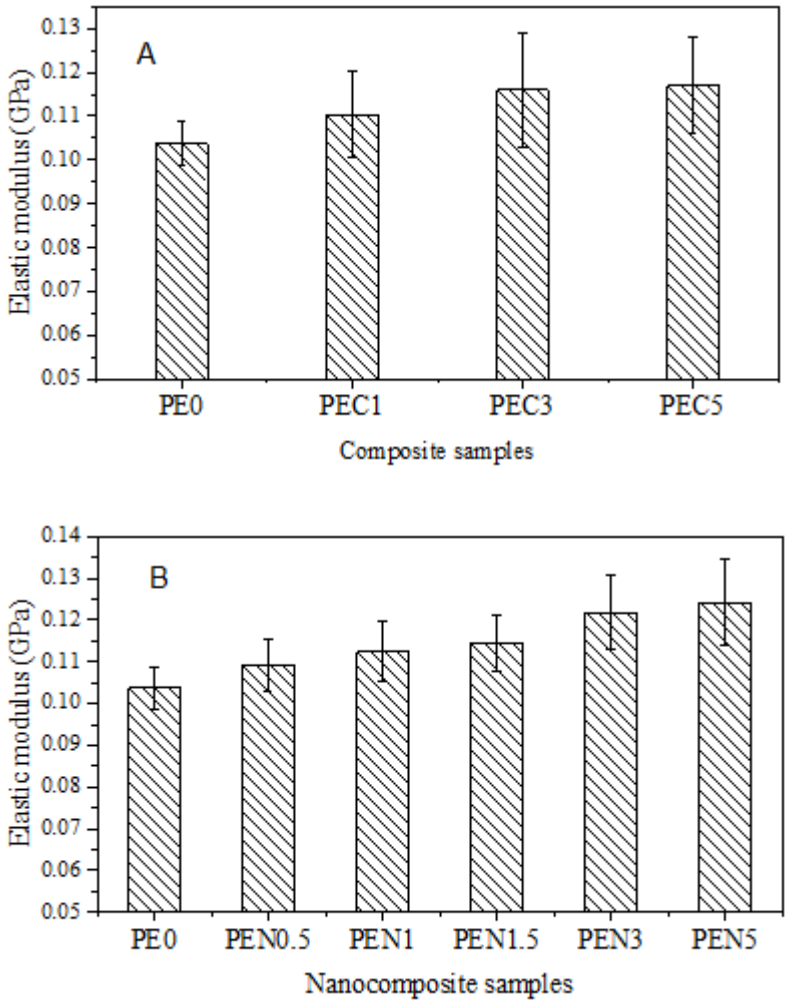

Figure (4.27): Elastic modulus of composite and nanocomposite, with different concentration of ZnO_2.

Elastic modulus is an indicator of the stiffness of a material. The incorporation of ZnO_2 into the polymer matrix improves the stiffness of the composites when filler concentration increased. This could be attributed to the distribution of the filler within the matrix, which efficiently hinders chain movement during deformation and the filler is stiffer than the polymer matrix. Many of researchers have reported a similar trend in Young's modulus with the increasing filler concentration. (Pantani, et al, 2013) (Díez-Pascual, et al, 2014).

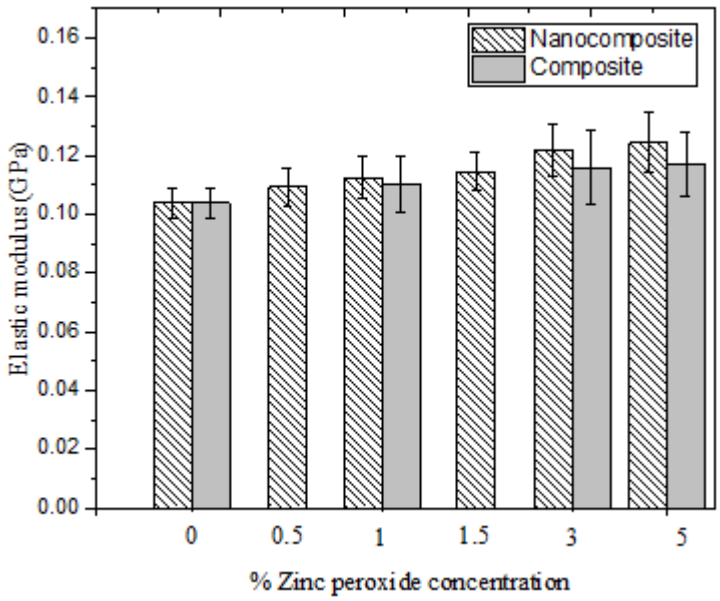

Figure (4.28): Elastic modulus of composite and nanocomposite, with different concentration of ZnO_2

Figure (4.28) shows that the nanocomposites based on ZnO_2 NP's show better elastic modulus and stiffness than the composite with ZnO_2 filler concentration. Therefore, the modulus of the nanocomposite is observed to be significantly enhanced even with a low concentration of ZnO_2 nanoparticles. In general, the improvement is due to higher contact surface area due to the small size of nanoparticles and strong interfacial bonding of nanoparticles-polymer. On the other hand, it was found that degree of crystallinity for nanocomposite was higher than composite. This in turn increases the stiffness (elastic modulus) and strength of the nanocomposite compare to composite. (Basu, ghadi, et al, 2017)

4.3.3 Yield Strength

Results of the yield strength of LDPE/ZnO_2 composite and nanocomposite with ZnO_2 concentration are presented in and figure (4.29). It is clearly shown that, the yield strength of composite and nanocomposite increased slightly with increased ZnO_2 concentration.

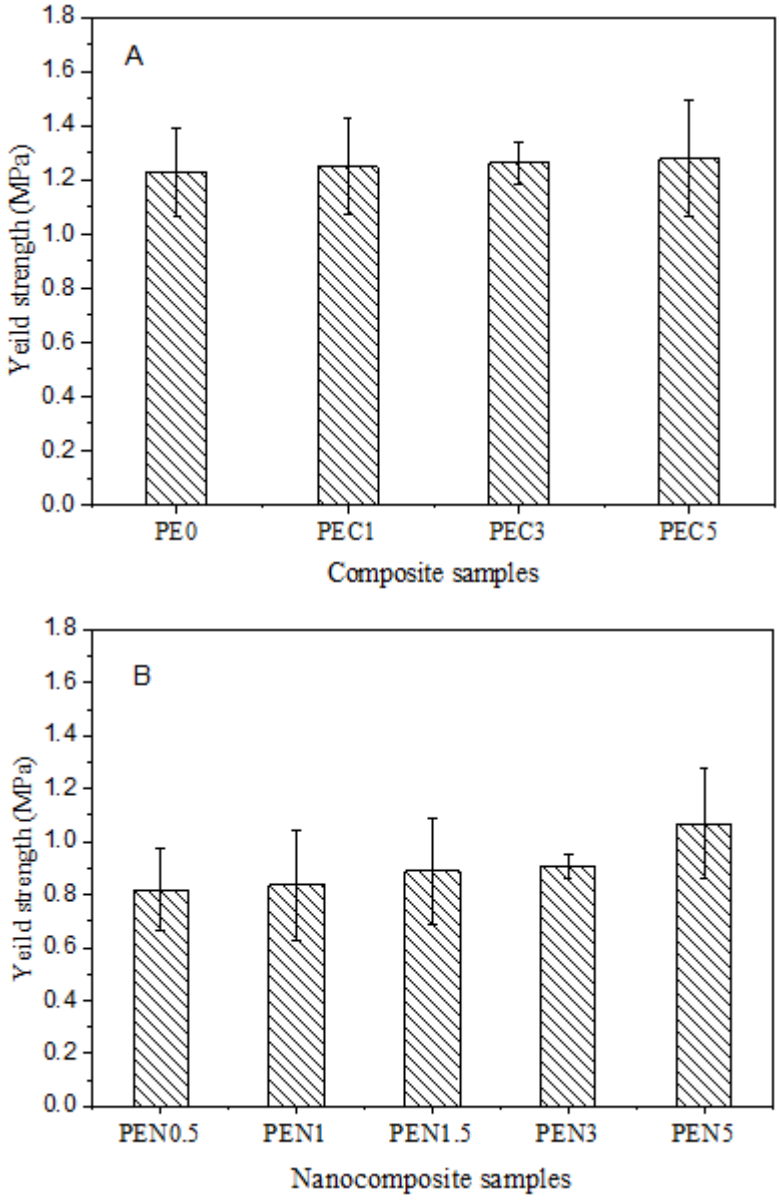

Figure (4.29): Yield strength of composite and nanocomposite, with different concentration of ZnO_2.

Yield strengths obtained of nanocomposite were found to be lower than the control (0 % filler) as shown in figure (4.30). It could be observed that yield strength increased progressively with increase in ZnO_2 concentration for composite and nanocomposite. For composite and nanocomposite there is no apparent increased change in yield strength from 0 % to 5 %, and the increase no more than 0.13 and 0.25 MPa for composite and nanocomposite respectively and it is not considered as significant change in yield properties.

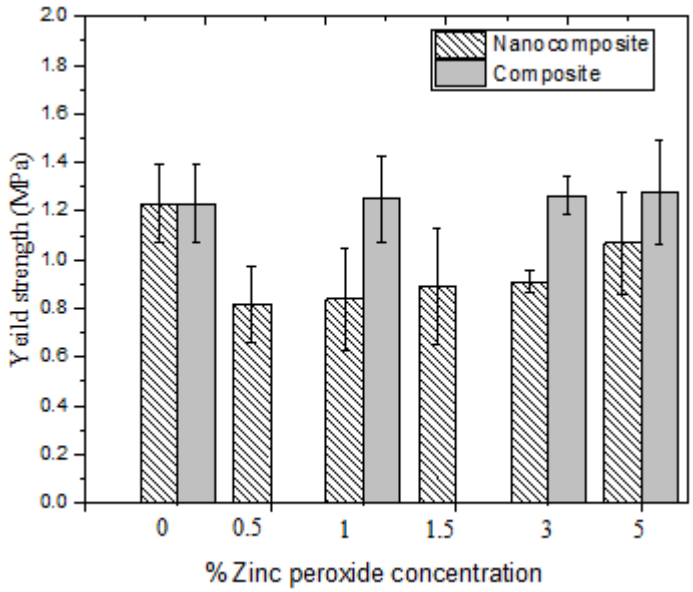

Figure (4.30): Yield strength of composite and nanocomposite, with different concentration of ZnO_2

The little increased of yield strength may be related to the strength effect of the filler due to the dispersion of ZnO_2 in the polymer matrix, that increasing restrictions on the movement of the polymer chain. The maximum yield strength value was recorded for the composite at 5 % of ZnO_2 concentration with yield value 1.27 MPa. (Onuoha, et al, 2017)

However, at similar concentration of ZnO_2 loading, ZnO_2 nanocomposite with nano particle size has lower yield strength, than similar composites with larger particle size of ZnO_2. This means, that the composite can withstand high stress without permanent a plastic deformation as compared to nanocomposite that the deform starts to appear early as plastic deformation due to rigidity of nanoparticles.

4.3.4 Fracture strength

Figures (4.31 & 4.32) show the effect of ZnO_2 concentration on fracture strength of LDPE/ ZnO_2 composite and nanocomposite samples. As shown in figure (31) nanocomposites can not only improve stiffness and strength, but also fracture strength. The results observed that the fracture strength of nanocomposites increases as the concentration of ZnO_2 increases, this could be attributed to the fact that the ZnO_2 nanoparticles impede the formation of porosity within nanocomposite and enhanced fracture properties. (Karapappas, et al, 2009)

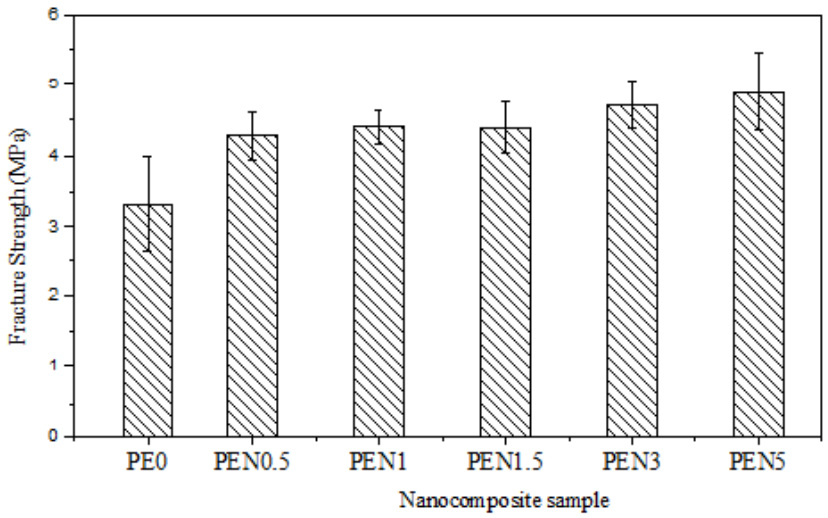

Figure (4.31): Fracture strength of nanocomposite with different concentration ZnO_2

For composite the fracture strength improved as the zinc concentration increased up to 3 % and then decreased at higher concentration at 5 % as shown in figure (4.32), it's could be to the ZnO_2 filler formation stress concentration and higher percentage of ZnO_2 concentration reducing the ductility of composite and produce a brittle fracture, which is reflected in the decrease of fracture strength.

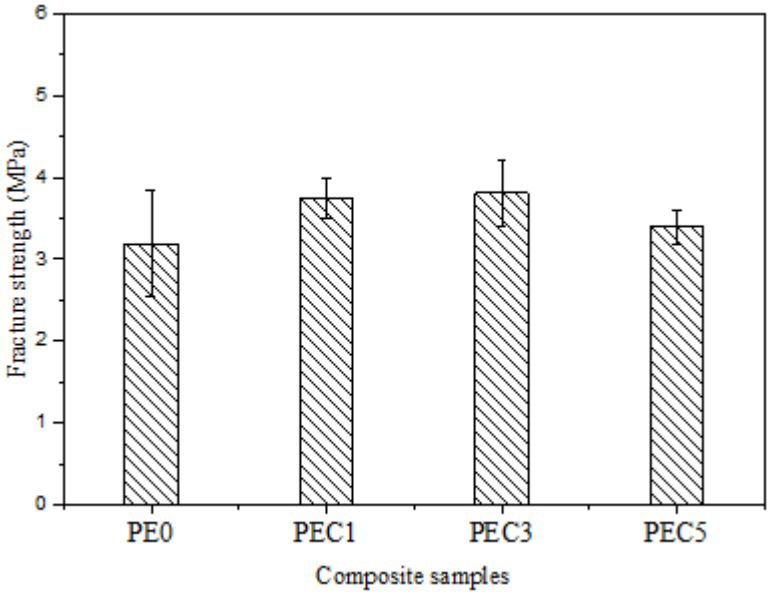

Figure (4.32): Fracture strength of composite, with different concentration ZnO_2

In the case of nanocomposites as shown in figure (4.33), the highest fracture strength at 5 % concentration of 4.90 MPa, and in the case of composite, the fracture strength at 5 % concentration of 3.93 MPa. The zinc peroxide nanoparticles concentration affected the fracture strength more than high concentration of ZnO_2 in composite, so fracture strength increases as the nanofiller size decreases to nano sized as compare to composite and the nanocomposite have higher ability to resist failure.

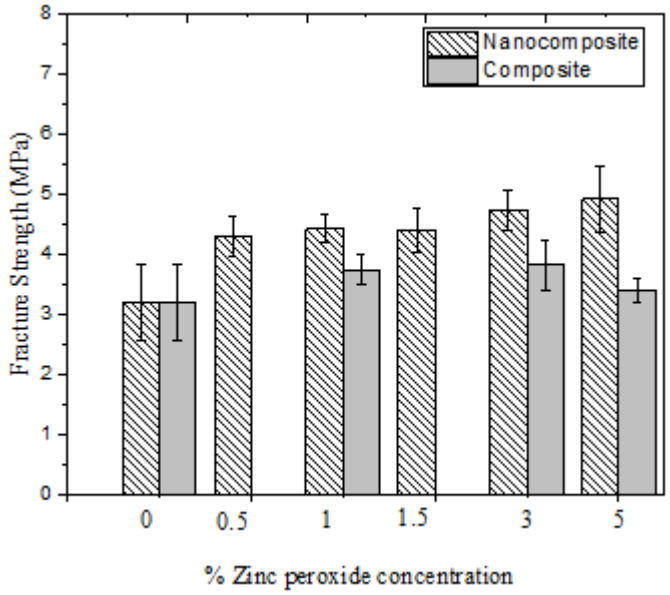

Figure (4.33): Fracture strength of composite and nanocomposite, with different concentration ZnO_2

4.3.5 % Elongation at fracture

Tables (4.8 & 4.9) shows the variation of the elongation at fracture for the LDPE/ ZnO_2 composite and LDPE/ ZnO_2 nanocomposite. It is obvious from the data that elongation decreased steadily with zinc ZnO_2 peroxide concentration increased for composite and nanocomposite. which is attributed to the brittle nature imparted by the zinc peroxide filler in the composites and nanocomposite.

For composite as shows in figure (4.34), the % elongation of fracture at lower concentration of zinc peroxide is slightly higher than those using high concentration of the ZnO_2 as reinforcement. For example, the % elongation of the composite made from LDPE with 1% ZnO_2 concentration is 36% as compared to that made with 5 wt.% ZnO_2 concentration which is only about 29 %, it's could be related to the fact that a weaker interfacial region between the filler surface and the LDPE matrix are formed and the cracks travel more easily through the weaker interfacial regions.

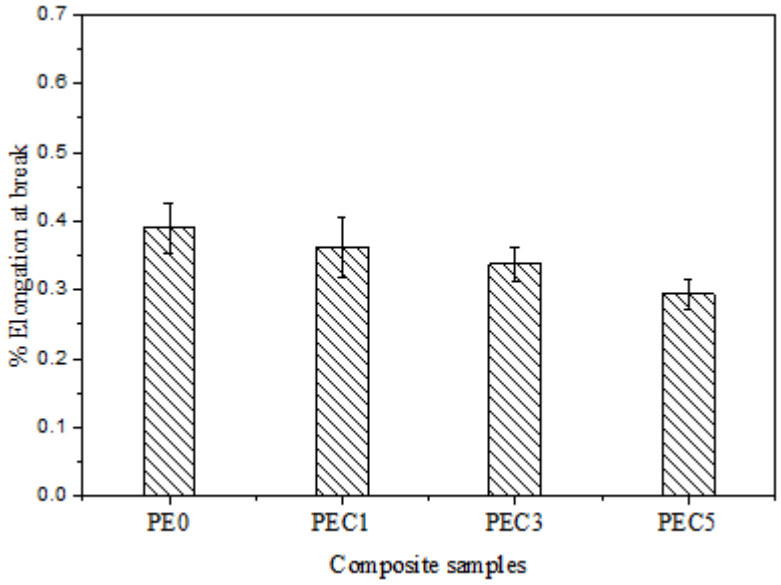

Figure (4.34): % Elongation at fracture of composite, with different concentration ZnO_2.

For nanocomposite, the elongation at fracture decreased with increased of ZnO_2 nanoparticle concentration as showed in figure (4.35), the reduction of elongation might be due to the ZnO_2 nanoparticles incorporation into a low-density polyethylene matrix increased the stiffness and strength of the composite. This increase in stiffens resulted in decrease in % elongation at fracture and ductility of the material. Hence, as filler concentration increases, the ductility decreases. Such decreasing elongation with filler loading**.** (Prasert, et al, 2020)

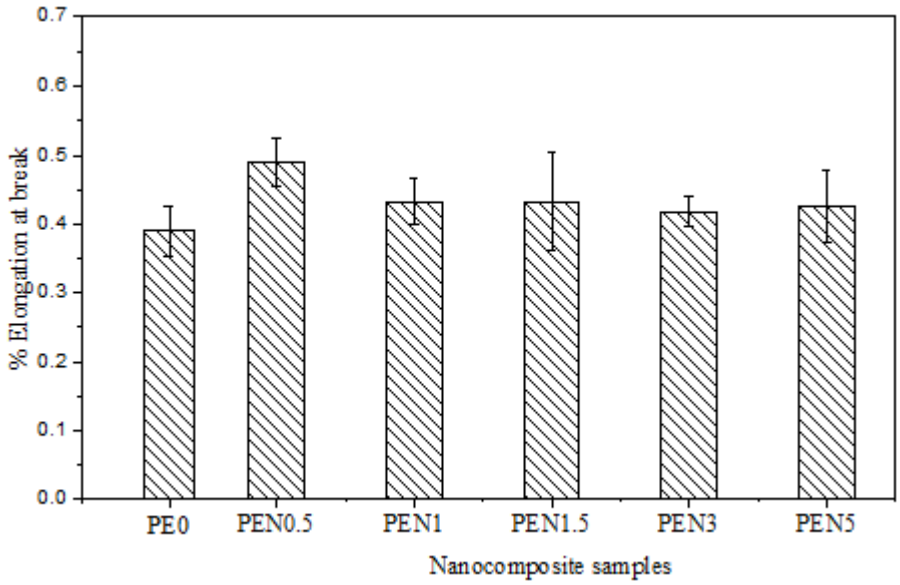

Figure (4.35): % Elongation at fracture of nanocomposite, with different concentration ZnO_2 NP's.

Moreover, the reduction of elongation at fracture when increasing ZnO_2 concentration is due to several reasons, the most important of which is aggregates of particles within the matrix due to high filler loading. Aggregates of particles lead to lower ductile behavior. The dispersion could be an important factor in this threshold, when large aggregates are present the voids that are created by de-bonding are not stable and grow to a size where initial crack occurs. According to Awad study the other reason that the elongation decreases is due to the increase in the degree of crystallinity of composite and nano composite as estimated from DSC results. (Awad, et al, 2015)

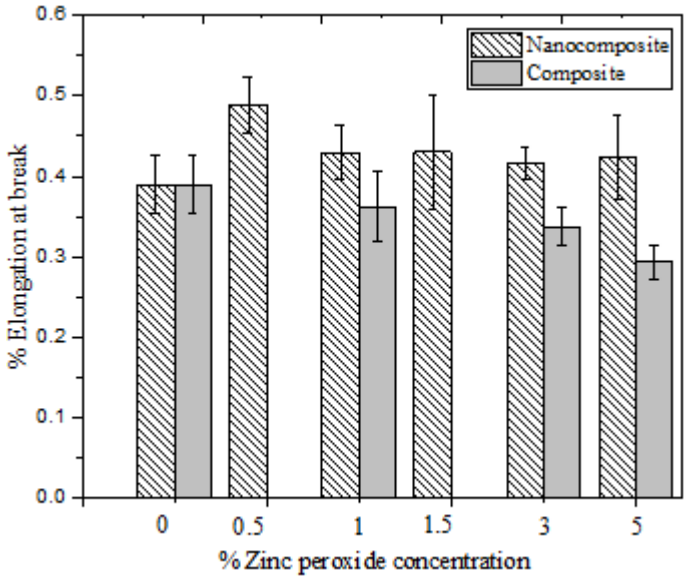

Figure (4.36): % Elongation at fracture of composite and nanocomposite, with different concentration ZnO_2.

The above figure shows that the elongation at fracture of nanocomposite with different concentration of ZnO_2 nanoparticles was found to be higher than the pure low-density polyethylene. The nanocomposite evidence better improvement of elongation at fracture than composite, its due to that the nanocomposite with higher elongation at fracture percentage have higher ductility, and its indicates that a nanocomposite will be more likely to deform and not break, while the composite with lower ductility indicates that a material is brittle and will fracture before deforming much under a tensile load.

4.4 Antibacterial characterization

4.4.1 Composite and nanocomposite

The recent development of nanotechnology increases the number of potential applications of synthetic nano-scale materials such as nanocomposites, to prepare antibacterial nanocomposites, the two most common methods are coating antimicrobial agents into polymers surface or incorporating of antimicrobial agents into the polymers such as our study. (Kim, et al, 2019)

In our study the antimicrobial activity of different concentrations of composites and nanocomposites were investigated by disc diffusion method against aerobic bacteria such as Staphylococcus aureus (MRSA), Escherichia coli (E. coli) and Pseudomonas aeruginosa and against anerobic bacteria such as anerobic gram-positive streptococcus and anaerobic gram-negative bacilli.

Figure 4.37 and 4.38 did not show any zone of inhibition on the agar plates for composites and nanocomposite against aerobic bacteria tested for all different concentation of ZnO_2 filles. This mean that the composite and nanocomposite within ZnO_2 filler did not have an antibacterial property against strain of bacteria that studied and indicated to there are no antibacterial properties effects of ZnO_2 filles when incorporated into LDPE in our study. In addition, figure (4.37 B & C) shows zone of inhibition around positive control (antibiotic) that used and it's particularly useful for validating the experimental procedure, if the test go well.

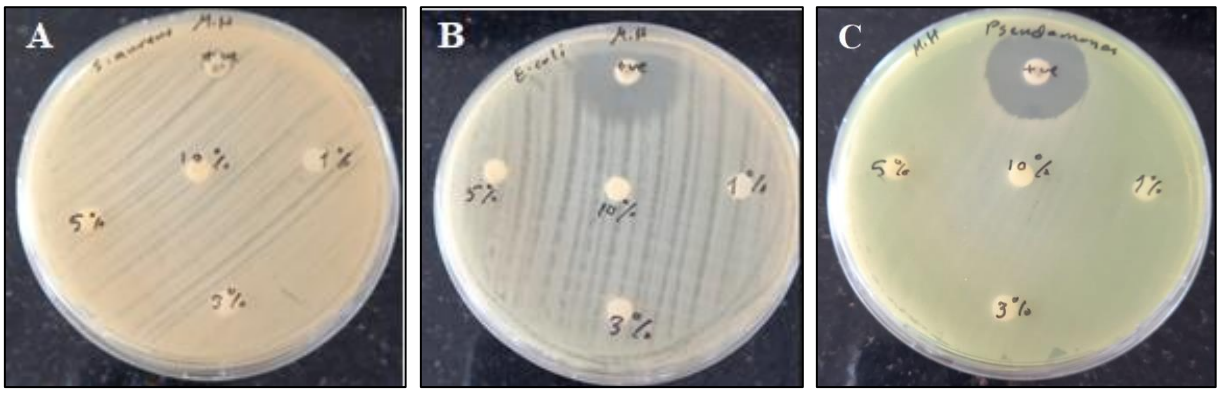

Figure (4.37): Disc diffusion tests for the evaluation of antimicrobial activity of different concentration of composite against aerobic strains where A: Staphylococcus aureus, B: Escherichia coli and C: pseudomonas aeruginosa.

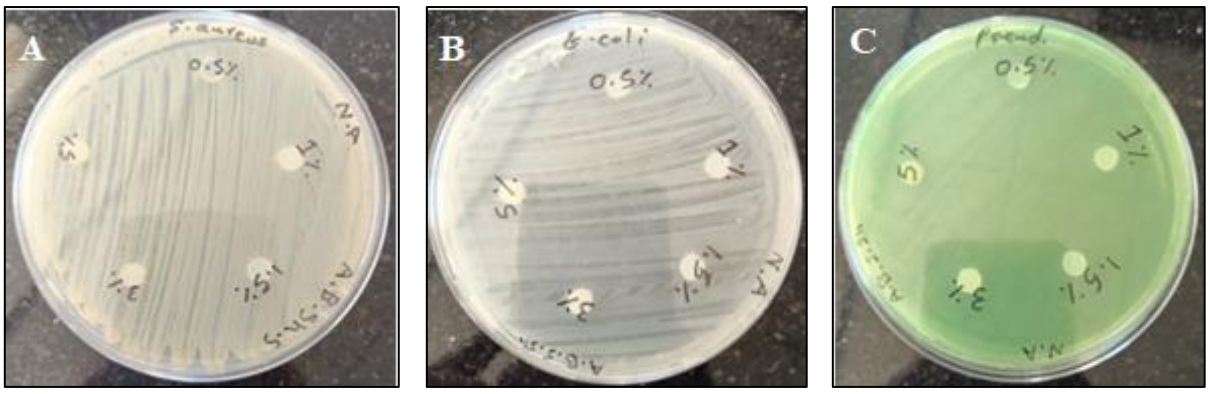

Figure (4.38): Disc diffusion tests for the evaluation of antimicrobial activity of different concentration of nano composite against aerobic strains where A: Staphylococcus aureus, B: Escherichia coli and C: pseudomonas aeruginosa.

Figure 4.39 and 4.40 shows the effect of composite and nanocomposite samples with different concentration of fillers against anerobic bacteria strain, the figure shows that the composite and nanocomposite sample does not show any zone of inhibition around sample disk that located on blood agra medium that allow to the anerobic bacteria to growth as shows in figure 4.39 E where the upper region shows the growth of anerobic gram-positive streptococcus and the lower region shows the growth of anaerobic gram-negative bacilli.

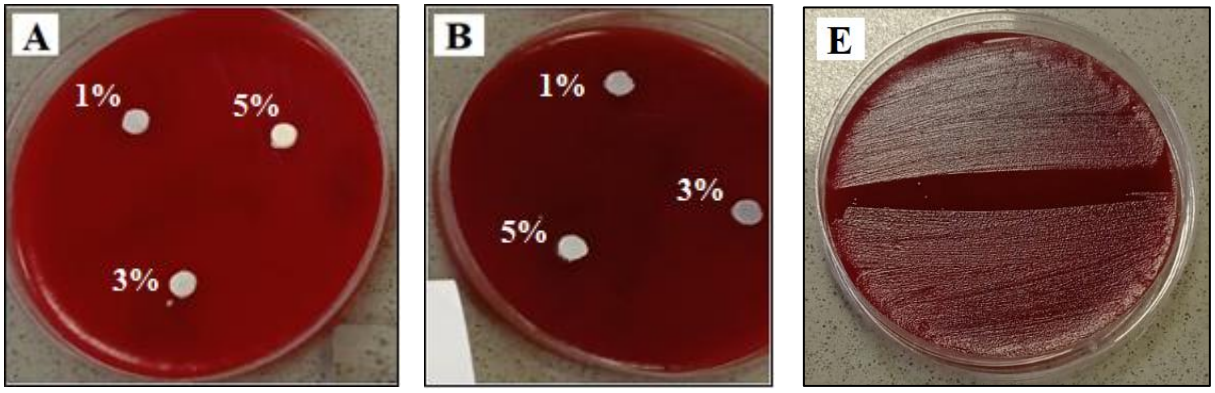

Figure (4.39): Disc diffusion tests for the evaluation of antimicrobial activity of different concentration of composite against anerobic bacteria strain where A: anerobic gram-positive streptococcus and B: anaerobic gram-negative bacilli.

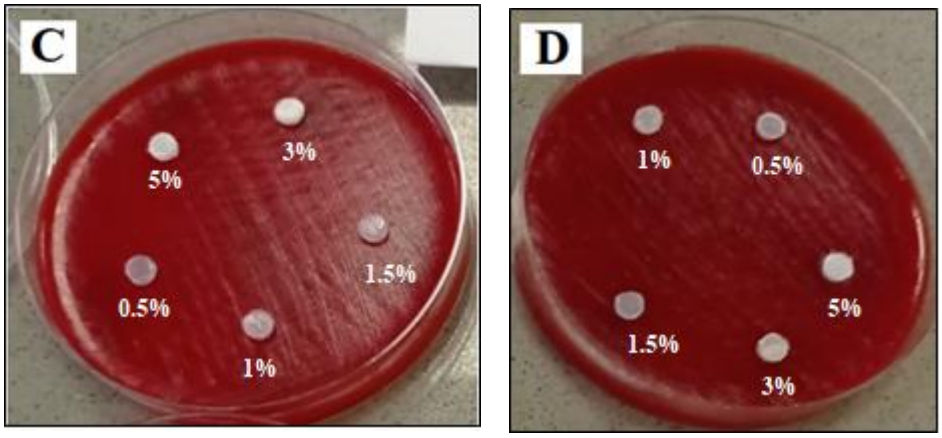

Figure (4.40): Disc diffusion tests for the evaluation of antimicrobial activity of different concentration of nanocomposite against anerobic bacteria strain where: C: anerobic gram-positive streptococcus and D: anaerobic gram-negative bacilli.

In our study the result of antibacterial properties of the composite and nanocomposite against aerobic and anerobic bacteria show the same behavior with no effect of our samples that contain different concentration of ZnO_2 and ZnO_2 nanoparticles .In composite and nanocomposites the main mechanism of inhibit bacteria to growth is related with the ZnO_2 since plastic has no anti-bacterial activity, as previously discussed before, two possible routes of the effect of ZnO_2 as antibacterial agent in polymer matrix, one route is the metal nanoparticles when they have in direct contact with a bacteria cell which causes changes in microenvironment within the contact area of the organism and particle or the second route is the released of metal ions and ROS from the particles. (Prabhu, et al, 2012) (Dimapilis, et al ,2018)

In LDPE matrix with embedded antibacterial agent (ZnO_2 and ZnO_2 nanoparticles) fillers, the ion release is the main mechanism behind their bacteriadal activity due to the nanoparticles incorporation into the polymer and it does not exist entiely on the surface which puts it in direct contact with bacteria and the concentrations of antibacterial agent in the surface lower than the bulk of the material so the polymer interacts more with bacteria compared antibacterial agent (Palza, 2015) Therefore, the only suitable mechanism for the release of metal ions and this explains why it has no effect against bacteria as we expect.

Chapter Five

Conclusion and future work

5.1 Conclusion

In this study, ZnO_2 nanoparticles were chemically prepared by reflux with capping agent polyethyleneimine as a surface modifier to prevent agglomeration of NP's and by reflux without capping agent and the last one by sol-gel method and then incorporated one of these ZnO_2 nanoparticles in LDPE**,** The XDR pattern of ZnO_2 nanoparticles confirmed a pure single phase with cubic ZnO_2 crystal for all prepared method, which compared with previous reports. FT-IR spectrum does not show any of absorption bands of reactant groups of zinc acetate, suggesting the purity of synthetic ZnO_2-NPs and it was found by DSC that the synthesized ZnO_2 samples decomposes into ZnO at about 230-238 ^oC. SEM revealed synthesis of non-agglomerated ZnO_2 nanoparticles having spherical shape with sizes of 82 nm ,48 nm and 55 nm for reflux without PEI, reflux with PEI and sol-gel respectively. Composite and nanocomposite materials were prepared by compounding LDPE with ZnO_2 particles and nanoparticles by solution mixing techniques. Dogbone specimens according to *IV ASTM D-638* type of the composites and nanocomposites were prepared. The influence of ZnO_2 concentration on the morphology, thermal, mechanical and, and antibacterial properties of the obtained composite and nanocomposites was investigated. SEM images showed that the ZnO_2 particles were dispersed and embedded in the matrices with little sign of agglomeration for the composite but it does not appear well on the surface of composite and the nanocomposite showed not only smaller particles fillers than the composites that containing ZnO_2 filler but it also proved to be better dispersed in the LDPE matrix. Characterizations of the mechanical properties show that the tensile strength improved by increasing concentration of ZnO_2 nano fillers to a polymer matrix of nanocomposites while the tensile strength decrease with increasing ZnO_2 concentration to composite. Elastic modulus, yield strength, fracture strength showed improvement when increasing concentration of ZnO_2 particles and nanoparticles. While percentage elongation at fracture decreased steadily with ZnO_2 concentration increased for composite and nanocomposite due to the brittle nature imparted by the ZnO_2 and increase in the stiffness and strength of the composite resulted in decrease in elongation at fracture of the material. Moreover, the thermal analysis results of composite and nanocomposite showed there are slight variations between the melting temperature of different concentration of composite and nanocomposite samples while imparts significant improvements in the degree of crystallinity that mean the crystallization rate of composite and nanocomposite have become faster due the filler act as nucleating agent. The

antibacterial characterization of the composite and nanocomposite against aerobic and anerobic bacteria show the same behavior with no effect of our samples that contain different concentration of ZnO_2 particles and ZnO_2 nanoparticles.

5.2 Future work

Many possibilities for future work for this study still remain, this work mainly focus on the influence of ZnO_2 on the mechanical, thermal, antibacterial properties of polyethylene. So, we suggest focusing on:

1- The photodegradation resistant properties of composite and nanocomposite to ultraviolet irradiation, some study showed that the nanoparticle act as screens for this type of radiation.
2- Water uptake and oxygen permeability properties of composite and nanocomposite by incorporating inorganic filler into polymer matrix causes a change in these properties.
3- Enhance the compatibility and dispersion of the LDPE matrix polymer and the inorganic filler.
4- Enhance the antibacterial activity properties of composites and nanocomposites by developing new methods.
5- Investigations of different nano particles with the development of new nanoparticles production methods, new possibilities are created.

References

- Klein, R. (2012). Laser welding of plastics: materials, processes and industrial applications. John Wiley & Sons .
- Scharff, R. L. (2012). Economic burden from health losses due to foodborne illness in the United States. *Journal of food protection*, *75*(1), 123-131.
- Lagaron, J., Sanchez-Garcia, M., & Gimenez, E. (2008). Thermoplastic nanobiocomposites for rigid and flexible food packaging applications.
- AlMaadeed, M. A., Ouederni, M., & Khanam, P. N. (2013). Effect of chain structure on the properties of Glass fibre/polyethylene composites. Materials & Design, 47, 725-730.
- Ebewele, R. O. (2000). *Polymer science and technology*. CRC press.
- Brown EN, Willms RB, Gray GT III, Rae PJ, Cady CM, Vecchio KS, Flowers J, Martinez MY (2007) Influence of molecular conformation on the constitutive response of polyethylene: a comparison of HDPE, UHMWPE, and PEX. Exp Mech 47(3):381–393
- Omar, M. F., Akil, H. M., & Ahmad, Z. A. (2012). Effect of molecular structures on dynamic compression properties of polyethylene. *Materials Science and Engineering: A*, *538*, 125-134.
- Jordan, J. L., Casem, D. T., Bradley, J. M., Dwivedi, A. K., Brown, E. N., & Jordan, C. W. (2016). Mechanical properties of low-density polyethylene. *Journal of dynamic behavior of materials*, *2*(4), 411-420.
- Mwafy, E. A., Abd-Elmgeed, A. A., Kandil, A. A., Elsabbagh, I. A., Elfass, M. M., & Gaafar, M. S. (2015). High UV-shielding performance of zinc oxide/high-density polyethylene nanocomposites. Spectroscopy Letters, 48(9), 646-652.
- Chae, D. W., & Kim, B. C. (2005). Characterization on polystyrene/zinc oxide nanocomposites prepared from solution mixing. *Polymers for advanced technologies*, *16*(11-12), 846-850.
- Zeng, C., Hossieny, N., Zhang, C., & Wang, B. (2010). Synthesis and processing of PMMA carbon nanotube nanocomposite foams. *Polymer*, *51*(3), 655-664.
- Seo, J., Jeon, G., Jang, E. S., Bahadar Khan, S., & Han, H. (2011). Preparation and properties of poly (propylene carbonate) and nanosized ZnO composite films for packaging applications. Journal of Applied Polymer Science, 122(2), 1101-1108.

- Khashaba, U. A. (2013). Drilling of polymer matrix composites: a review. *Journal of composite materials*, *47*(15), 1817-1832.
- Rajak, D. K., Pagar, D. D., Kumar, R., & Pruncu, C. I. (2019). Recent progress of reinforcement materials: a comprehensive overview of composite materials. *Journal of Materials Research and Technology*, *8*(6), 6354-6374.
- Sharma, A. K., Bhandari, R., Aherwar, A., & Rimašauskienė, R. (2020). Matrix materials used in composites: A comprehensive study. *Materials Today: Proceedings*, *21*, 1559-1562.
- Roylance, D. (2000). Introduction to composite materials. *Department of material science and engineering, Massachusetts Institute of Technology, Cambridge*
- Cantor, B., Dunne, F. P., & Stone, I. C. (2003). *Metal and ceramic matrix composites*. CRC Press.
- Zhang, C. (2014). Understanding the wear and tribological properties of ceramic matrix composites. In *Advances in ceramic matrix composites* (pp. 312-339). Woodhead Publishing.
- Kutz, M. (2015). Mechanical engineers' handbook, volume 1: Materials and engineering mechanics. John Wiley & Sons.
- Wypych, G. (2016). *Handbook of fillers* (Vol. 938). Toronto: ChemTec Publishing.
- Sharma, A. K., Bhandari, R., Aherwar, A., & Rimašauskienė, R. (2020). Matrix materials used in composites: A comprehensive study. *Materials Today: Proceedings*, *21*, 1559-1562
- Davim, J. P., & Reis, P. (2003). Study of delamination in drilling carbon fiber reinforced plastics (CFRP) using design experiments. *Composite structures*, *59*(4), 481-487.
- Rastelli, A. N., Jacomassi, D. P., Faloni, A. P. S., Queiroz, T. P., Rojas, S. S., Bernardi, M. I. B., ... & Hernandes, A. C. (2012). The filler content of the dental composite resins and their influence on different properties. *Microscopy research and technique*, *75*(6), 758-765.
- Khan, W. S., Hamadneh, N. N., & Khan, W. A. (2016). Polymer nanocomposites–synthesis techniques, classification and properties. Science and applications of Tailored Nanostructures, 50.

- Gul, S., Kausar, A., Muhammad, B., & Jabeen, S. (2016). Research progress on properties and applications of polymer/clay nanocomposite. Polymer-Plastics Technology and Engineering, 55(7), 684-703.
- Patel, H. A., Somani, R. S., Bajaj, H. C., & Jasra, R. V. (2006). Nanoclays for polymer nanocomposites, paints, inks, greases and cosmetics formulations, drug delivery vehicle and waste water treatment. *Bulletin of Materials Science*, *29*(2), 133-145.
- Xanthos, M. (2005). Polymers and polymer composites. *Functional fillers for plastics*, 1-16.
- L. Ibarra, A. Marcos-Fernandez, M. Alzorriz, Mechanistic approach to the curing of carboxylated nitrile rubber (XNBR) by zinc peroxide/zinc oxide, Polymer 43 (2002) 1649–1655
- Ohno, S., Aburatani, N., & Ueda, N. (1980). Foam products from a high-melting synthetic resin. *DE Patent*, *2914058*.
- Hagel, R., & Redecker, K. (1981). Use of zinc peroxide as an oxidizing agent for explosives and pyrotechnical mixtures. *DE Patent*, *2952069*
- Hussein, H. M., Ghafoor, D. D., & Omer, K. M. (2021). Room temperature and surfactant free synthesis of zinc peroxide (ZnO2) nanoparticles in methanol with highly efficient antimicrobials. *Arabian Journal of Chemistry*, *14*(4), 103090.
- Bergs, C. (2017). *Syntheses, Characterizations and Applications of Zinc Peroxide Nanoparticles* (Doctoral dissertation, Universitätsbibliothek der RWTH Aachen).
- Ealia, S. A. M., & Saravanakumar, M. P. (2017, November). A review on the classification, characterisation, synthesis of nanoparticles and their application. In *IOP conference series: materials science and engineering* (Vol. 263, No. 3, p. 032019). IOP Publishing.
- Bergs, C., Brück, L., Rosencrantz, R. R., Conrads, G., Elling, L., & Pich, A. (2017). Biofunctionalized zinc peroxide (ZnO 2) nanoparticles as active oxygen sources and antibacterial agents. *RSC advances*, *7*(62), 38998-39010.
- Ali, S. S., Morsy, R., El-Zawawy, N. A., Fareed, M. F., & Bedaiwy, M. Y. (2017). Synthesized zinc peroxide nanoparticles (ZnO2-NPs): a novel antimicrobial, anti-

elastase, anti-keratinase, and anti-inflammatory approach toward polymicrobial burn wounds. *International journal of nanomedicine*, *12*, 6059.

- Kaushik, M., Niranjan, R., Thangam, R., Madhan, B., Pandiyarasan, V., Ramachandran, C., ... & Venkatasubbu, G. D. (2019). Investigations on the antimicrobial activity and wound healing potential of ZnO nanoparticles. *Applied Surface Science*, *479*, 1169-1177.
- Padmavathy N, Vijayaraghavan R. Enhanced bioactivity of ZnO nanoparticles – an antimicrobial study. Sci Technol Adv Mater. 2008; 9:035004.
- Kadiyala, U., Kotov, N.A., VanEpps, J.S. (2018) Antibacterial metal oxide nanoparticles: Challenges in interpreting the literature. Current Pharmaceutical Design, 24, 896-903.
- Chen, W., Lu, Y. H., Wang, M., Kroner, L., Paul, H., Fecht, H. J., ... & Jiang, J. Z. (2009). Synthesis, thermal stability and properties of ZnO2 nanoparticles. *The journal of physical chemistry C*, *113*(4), 1320-1324.
- Brown, H. P. (1963). Crosslinking reactions of carboxylic elastomers. *Rubber Chemistry and Technology*, *36*(4), 931-962.
- Uekawa, N., Mochizuki, N., Kajiwara, J., Mori, F., Wu, Y. J., & Kakegawa, K. (2003). Nonstoichiometric properties of zinc oxide nanoparticles prepared by decomposition of zinc peroxide. *Physical Chemistry*, *5*(5), 929-934.
- Rosenthal-Toib, L., Zohar, K., Alagem, M., & Tsur, Y. (2008). Synthesis of stabilized nanoparticles of zinc peroxide. *Chemical Engineering Journal*, *136*(2-3), 425-429.
- Lemire, J. A., Harrison, J. J., & Turner, R. J. (2013). Antimicrobial activity of metals: mechanisms, molecular targets and applications. *Nature Reviews Microbiology*, *11*(6), 371-384.
- Aoki, W., & Ueda, M. (2013). Characterization of antimicrobial peptides toward the development of novel antibiotics. *Pharmaceuticals*, *6*(8), 1055-1081.
- Guzmán, M. G., Dille, J., & Godet, S. (2009). Synthesis of silver nanoparticles by chemical reduction method and their antibacterial activity. *Int J Chem Biomol Eng*, *2*(3), 104-111.
- Dimapilis, E. A. S., Hsu, C. S., Mendoza, R. M. O., & Lu, M. C. (2018). Zinc oxide nanoparticles for water disinfection. *Sustainable Environment Research*, *28*(2), 47-56.

- Gold, K., Slay, B., Knackstedt, M., & Gaharwar, A. K. (2018). Antimicrobial activity of metal and metal-oxide based nanoparticles. *Advanced Therapeutics*, *1*(3), 1700033.
- Yamamoto, O. (2001). Influence of particle size on the antibacterial activity of zinc oxide. *International Journal of Inorganic Materials*, *3*(7), 643-646.
- Vega-Jiménez, A. L., Vázquez-Olmos, A. R., Acosta-Gío, E., & Álvarez-Pérez, M. A. (2019). In vitro antimicrobial activity evaluation of metal oxide nanoparticles. *Nanoemulsions Prop. Fabr. Appl*, 1-18.
- Kasemets K, Ivask A, Dubourguier HC, Kahru A. Toxicity of nanoparticles of ZnO, CuO and TiO2 to yeast Saccharomyces cerevisiae. Toxicol In Vitro 2009;23: 1116e22
- Vega-Jiménez, A. L., Vázquez-Olmos, A. R., Acosta-Gío, E., & Álvarez-Pérez, M. A. (2019). In vitro antimicrobial activity evaluation of metal oxide nanoparticles. *Nanoemulsions Prop. Fabr. Appl*, 1-18.
- Sirelkhatim, A., Mahmud, S., Seeni, A., Kaus, N. H. M., Ann, L. C., Bakhori, S. K. M., ... & Mohamad, D. (2015). Review on zinc oxide nanoparticles: antibacterial activity and toxicity mechanism. *Nano-micro letters*, *7*(3), 219-242.
- N. Padmavathy, R. Vijayaraghavan, Enhanced bioactivity of ZnO nanoparticles—an antimicrobial study. Sci. Technol. Adv. Mater. 9(3), 035004 (2008).
- Jones, N., Ray, B., Ranjit, K. T., & Manna, A. C. (2008). Antibacterial activity of ZnO nanoparticle suspensions on a broad spectrum of microorganisms. FEMS Microbiology Letters, 279(1), 71–76
- Dimapilis, E. A. S., Hsu, C. S., Mendoza, R. M. O., & Lu, M. C. (2018). Zinc oxide nanoparticles for water disinfection. *Sustainable Environment Research*, *28*(2), 47-56.
- Javed, R., Usman, M., Tabassum, S., & Zia, M. (2016). Effect of capping agents: structural, optical and biological properties of ZnO nanoparticles. *Applied Surface Science*, *386*, 319-326.
- Harper, C. A. (2006). *Handbook of plastic processes* (pp. 18-19). Hoboken, NJ, USA: John Wiley & Sons.
- Spaak, A. (1975). Processing of plastics. Environmental Health Perspectives, 11, 21-28
- Pavlidou, S., & Papaspyrides, C. D. (2008). A review on polymer–layered silicate nanocomposites. *Progress in polymer science*, *33*(12), 1119-1198.

- Shen, Z., Simon, G. P., & Cheng, Y. B. (2002). Comparison of solution intercalation and melt intercalation of polymer–clay nanocomposites. *Polymer*, *43*(15), 4251-4260.
- Ray, S. S., & Okamoto, M. (2003). Polymer/layered silicate nanocomposites: a review from preparation to processing. *Progress in polymer science*, *28*(11), 1539-1641.
- Araby, S., Meng, Q., Zhang, L., Kang, H., Majewski, P., Tang, Y., & Ma, J. (2014). Electrically and thermally conductive elastomer/graphene nanocomposites by solution mixing. *Polymer*, *55*(1), 201-210.
- Chen, W., Lu, Y. H., Wang, M., Kroner, L., Paul, H., Fecht, H. J., ... & Jiang, J. Z. (2009). Synthesis, thermal stability and properties of ZnO2 nanoparticles. *The journal of physical chemistry C*, *113*(4), 1320-1324.
- Ramírez, J. I. D. L., Villegas, V. A. R., Sicairos, S. P., Guevara, E. H., Brito Perea, M. D. C., & Sánchez, B. L. (2020). Synthesis and characterization of zinc peroxide nanoparticles for the photodegradation of nitrobenzene assisted by UV-light. *Catalysts*, *10*(9), 1041.
- Escobedo-Morales, A., Esparza, R., García-Ruiz, A., Aguilar, A., Rubio-Rosas, E., & Pérez, R. (2011). Structural and vibrational properties of hydrothermally grown ZnO2 nanoparticles. *Journal of Crystal Growth*, *316*(1), 37-41.
- Hussein, H. M., Ghafoor, D. D., & Omer, K. M. (2021). Room temperature and surfactant free synthesis of zinc peroxide (ZnO2) nanoparticles in methanol with highly efficient antimicrobials. *Arabian Journal of Chemistry*, *14*(4), 103090.
- Colonia, R., Solís, J. L., & Gómez, M. (2013). Bactericidal, structural and morphological properties of ZnO2 nanoparticles synthesized under UV or ultrasound irradiation. *Advances in Natural Sciences: Nanoscience and Nanotechnology*, *5*(1), 015008.
- El-Shounya, W. A., Moawad, M., Haider, A. S., Ali, S., & Nouh, S. (2019). Antibacterial potential of a newly synthesized zinc peroxide nanoparticles (ZnO2-NPs) to combat biofilm-producing multi-drug resistant Pseudomonas aeruginosa. *Egyptian Journal of Botany*, *59*(3), 657-666.

- Bergs, C., Brück, L., Rosencrantz, R. R., Conrads, G., Elling, L., & Pich, A. (2017). Biofunctionalized zinc peroxide (ZnO 2) nanoparticles as active oxygen sources and antibacterial agents. *RSC advances*, *7*(62), 38998-39010.
- Pasquet, J., Chevalier, Y., Pelletier, J., Couval, E., Bouvier, D., & Bolzinger, M. A. (2014). The contribution of zinc ions to the antimicrobial activity of zinc oxide. *Colloids and Surfaces A: Physicochemical and Engineering Aspects*, *457*, 263-274.
- Ali, S. S., Morsy, R., El-Zawawy, N. A., Fareed, M. F., & Bedaiwy, M. Y. (2017). Synthesized zinc peroxide nanoparticles (ZnO2-NPs): a novel antimicrobial, anti-elastase, anti-keratinase, and anti-inflammatory approach toward polymicrobial burn wounds. *International journal of nanomedicine*, *12*, 6059.
- Anžlovar, A., Primožič, M., Švab, I., Leitgeb, M., Knez, Ž., & Žagar, E. (2019). Polyolefin/ZnO composites prepared by melt processing. *Molecules*, *24*(13), 2432.
- Golcha, M. C., Sangawar, V. S., Bhagat, R. N., & Thakare, N. R. (2018). Structural and morphological analysis of ZnO nanoparticles filled low density polyethylene thin film. *Int. J. Innovat. Res. Sci. Technol*, *4*, 88-92.
- Prasert, A., Sontikaew, S., Sriprapai, D., & Chuangchote, S. (2020). Polypropylene/ZnO nanocomposites: Mechanical properties, photocatalytic dye degradation, and antibacterial property. *Materials*, *13*(4), 914.
- Li, S. C., & Li, Y. N. (2010). Mechanical and antibacterial properties of modified nano-ZnO/high-density polyethylene composite films with a low doped content of nano-ZnO. *Journal of applied polymer science*, *116*(5), 2965-2969.
- Seo, J., Jeon, G., Jang, E. S., Bahadar Khan, S., & Han, H. (2011). Preparation and properties of poly (propylene carbonate) and nanosized ZnO composite films for packaging applications. *Journal of Applied Polymer Science*, *122*(2), 1101-1108.
- Koerner, G. R., & Koerner, R. M. (2018). Polymeric geomembrane components in landfill liners. *Solid Waste Landfilling*, 313-341.
- Ebewele, R. O. (2000). *Polymer science and technology*. CRC press.
- https://www.worldofchemicals.com/chemicals/chemical-properties/zinc peroxide.html

- Ahmad, Z., Al Dajani, W. W., Paleologou, M., & Xu, C. (2020). Sustainable process for the depolymerization/oxidation of softwood and hardwood kraft lignins using hydrogen peroxide under ambient conditions. *Molecules*, *25*(10), 2329.
- Jäger, M., Schubert, S., Ochrimenko, S., Fischer, D., & Schubert, U. S. (2012). Branched and linear poly (ethylene imine)-based conjugates: synthetic modification, characterization, and application. Chemical Society Reviews, 41(13), 4755-4767.
- Escobedo-Morales, A., Esparza, R., García-Ruiz, A., Aguilar, A., Rubio-Rosas, E., & Pérez, R. (2011). Structural and vibrational properties of hydrothermally grown ZnO2 nanoparticles. *Journal of Crystal Growth*, *316*(1), 37-41.
- Bocharov, D., Chesnokov, A., Chikvaidze, G., Gabrusenoks, J., Ignatans, R., Kalendarev, R., ... & Purans, J. (2022). A comprehensive study of structure and properties of nanocrystalline zinc peroxide. *Journal of Physics and Chemistry of Solids*, *160*, 110318.
- http://polymerdatabase.com/Polymer/Polyethyleneimine.com
- Escobedo-Morales, A., Esparza, R., García-Ruiz, A., Aguilar, A., Rubio-Rosas, E., & Pérez, R. (2011). Structural and vibrational properties of hydrothermally grown ZnO2 nanoparticles. *Journal of Crystal Growth*, *316*(1), 37-41.
- Colonia, R., Solís, J. L., & Gómez, M. (2013). Bactericidal, structural and morphological properties of ZnO2 nanoparticles synthesized under UV or ultrasound irradiation. *Advances in Natural Sciences: Nanoscience and Nanotechnology*, *5*(1), 015008.

- Golchha, M. C., Sangawar, V. S., Bhagat, R. N., & Thakare, N. R. Structural and Morphological Analysis of ZnO Nanoparticles filled Low Density Polyethylene Thin Films.
- Dr. A. K. Ghatage, Prof. S. G. Kanitkar, 2019, Characterization of Materials by X-Ray Diffraction, International Journal of Engineering Research & Technology (IJERT) Volume 08, Issue 11 (November 2019).
- Akhtar, K., Khan, S. A., Khan, S. B., & Asiri, A. M. (2018). Scanning electron microscopy: Principle and applications in nanomaterials characterization. In Handbook of materials characterization (pp. 113-145). Springer, Cham.
- Baudot, C., Tan, C. M., & Kong, J. C. (2010). FTIR spectroscopy as a tool for nano-material characterization. *Infrared Physics & Technology*, *53*(6), 434-438.
- Koshy, O., Subramanian, L., & Thomas, S. (2017). Differential scanning calorimetry in nanoscience and nanotechnology. In Thermal and Rheological Measurement Techniques for Nanomaterials Characterization (pp. 109-122). Elsevier.
- Schick, C. (2009). Differential scanning calorimetry (DSC) of semicrystalline polymers. *Analytical and bioanalytical chemistry*, *395*(6), 1589-1611.
- Mirabella FM, Bafna A (2002) Determination of the crystallinity of polyethylene/α-olefin copolymers by thermal analysis: Relationship of the heat of fusion of 100% polyethylene crystal and the density. Journal of Polymer Science Part B: Polymer Physics 40: 1637–1643.
- Steinmann, W., Walter, S., Beckers, M., Seide, G., & Gries, T. (2013). Thermal analysis of phase transitions and crystallization in polymeric fibers. Applications of Calorimetry

in a Wide Context—Differential Scanning Calorimetry, Isothermal Titration Calorimetry and Microcalorimetry, 277-302.

- Kun, E., & Marossy, K. (2013). Evaluation methods of antimicrobial activity of plastics. In *Materials Science Forum* (Vol. 729, pp. 430-435). Trans Tech Publications Ltd.
- Hussein, H. M., Ghafoor, D. D., & Omer, K. M. (2021). Room temperature and surfactant free synthesis of zinc peroxide (ZnO2) nanoparticles in methanol with highly efficient antimicrobials. *Arabian Journal of Chemistry*, *14*(4), 103090.
- Ali, S. S., Morsy, R., El-Zawawy, N. A., Fareed, M. F., & Bedaiwy, M. Y. (2017). Synthesized zinc peroxide nanoparticles (ZnO2-NPs): a novel antimicrobial, anti-elastase, anti-keratinase, and anti-inflammatory approach toward polymicrobial burn wounds. International journal of nanomedicine, 12, 6059.
- Bera, B. Nanoporous silicon prepared by vapour phase strain etch and sacrificial technique. In Proceedings of the International Conference on Microelectronic Circuit and System (Micro), Kolkata, India, 11–12 July 2015; pp. 42–45.
- Javed, R., Zia, M., Naz, S., Aisida, S. O., & Ao, Q. (2020). Role of capping agents in the application of nanoparticles in biomedicine and environmental remediation: recent trends and future prospects. *Journal of Nanobiotechnology*, *18*(1), 1-15.
- Shaba, E. Y., Jacob, J. O., Tijani, J. O., & Suleiman, M. A. T. (2021). A critical review of synthesis parameters affecting the properties of zinc oxide nanoparticle and its application in wastewater treatment. *Applied Water Science*, *11*(2), 1-41.
- Restrepo, C. V., & Villa, C. C. (2021). Synthesis of silver nanoparticles, influence of capping agents, and dependence on size and shape: A review. *Environmental Nanotechnology, Monitoring & Management*, *15*, 100428.
- Javed, R., Usman, M., Tabassum, S., & Zia, M. (2016). Effect of capping agents: structural, optical and biological properties of ZnO nanoparticles. *Applied Surface Science*, *386*, 319-326.
- Ibrahim, N. A., Nada, A. A., Hassabo, A. G., Eid, B. M., Noor El-Deen, A. M., & Abou-Zeid, N. Y. (2017). Effect of different capping agents on physicochemical and antimicrobial properties of ZnO nanoparticles. *Chemical Papers*, *71*(7), 1365-1375.

- Nithya A, JeevaKumari HL, Rokesh K, Ruckmani K, Jeganathan K, Jothivenkatachalam K. A versatile effect of chitosan-silver nanocomposite for surface plasmonic photocatalytic and antibacterial activity. *J Photochem Photobiol, B.* 2015;**153**:412–422. doi: 10.1016/j.jphotobiol.2015.10.020.
- Javed R, Ahmed M, Haq IU, Nisa S, Zia M. PVP and PEG doped CuO nanoparticles are more biologically active: antibacterial, antioxidant, antidiabetic and cytotoxic perspective. *Mater Sci Eng C Mater Biol Appl.* 2017;**79**:108–115.
- Pallon, L. (2016). Polyethylene/metal oxide nanocomposites for electrical insulation in future HVDC-cables: probing properties from nano to macro (Doctoral dissertation, KTH Royal Institute of Technology).
- Kim, D., Lee, J. S., Barry, C. M., & Mead, J. L. (2007). Microscopic measurement of the degree of mixing for nanoparticles in polymer nanocomposites by TEM images. Microscopy research and technique, 70(6), 539-546.
- Shameer, P. M., & Nishath, P. M. (2019). Exploration and enhancement on fuel stability of biodiesel: A step forward in the track of global commercialization. In *Advanced biofuels* (pp. 181-213). Woodhead Publishing.
- Escobedo-Morales, A., Esparza, R., García-Ruiz, A., Aguilar, A., Rubio-Rosas, E., & Pérez, R. (2011). Structural and vibrational properties of hydrothermally grown ZnO2 nanoparticles. *Journal of Crystal Growth*, *316*(1), 37-41.
- Hussein, H. M., Ghafoor, D. D., & Omer, K. M. (2021). Room temperature and surfactant free synthesis of zinc peroxide (ZnO2) nanoparticles in methanol with highly efficient antimicrobials. *Arabian Journal of Chemistry*, *14*(4), 103090.
- Aguilar, A., Rubio-rosas, E., Pe, R., 2011. Structural and vibrational properties of hydrothermally grown ZnO2 nanoparticles. 316, 37–41.
- Cheng, S., Yan, D., Chen, J. T., Zhuo, R. F., Feng, J. J., Li, H. J., ... & Yan, P. X. (2009). Soft-template synthesis and characterization of ZnO2 and ZnO hollow spheres. *The Journal of Physical Chemistry C*, *113*(31), 13630-13635.
- Sebők, D., Szabó, T., & Dékány, I. (2009). Optical properties of zinc peroxide and zinc oxide multilayer nanohybrid films. *Applied surface science*, *255*(15), 6953-6962.

- Cheng S, Yan D, Chen JT, et al. Soft template synthesis and characterization of ZnO2 and ZnO hollow spheres. J Phys Chem C. 2009; 113(31):13630.
- Schlexer, P., Andersen, A. B., Sebok, B., Chorkendorff, I., Schiøtz, J., & Hansen, T. W. (2019). Size-dependence of the melting temperature of individual Au nanoparticles. *Particle & Particle Systems Characterization*, *36*(3), 1800480.
- Anžlovar, A., Primožič, M., Švab, I., Leitgeb, M., Knez, Ž., & Žagar, E. (2019). Polyolefin/ZnO composites prepared by melt processing. *Molecules*, *24*(13), 2432.
- Wang, Y., Shi, J., Han, L., & Xiang, F. (2009). Crystallization and mechanical properties of T-ZnOw/HDPE composites. *Materials Science and Engineering: A*, *501*(1-2), 220-228.
- Li, X. H., Tjong, S. C., Meng, Y. Z., & Zhu, Q. (2003). Fabrication and properties of poly (propylene carbonate)/calcium carbonate composites. *Journal of Polymer Science Part B: Polymer Physics*, *41*(15), 1806-1813.
- Aswathy, V., & Rani, J. (2008). Nano ZnO filled polypropylene: thermal properties. *Int J Plast Technol*, *12*(1), 957-967.
- Zaman, H. U., Hun, P. D., Khan, R. A., & Yoon, K. B. (2012). Morphology, mechanical, and crystallization behaviors of micro-and nano-ZnO filled polypropylene composites. *Journal of Reinforced Plastics and Composites*, *31*(5), 323-329.
- Sanporean, C. G., Vuluga, Z., Radovici, C., Panaitescu, D. M., Iorga, M., Christiansen, J. D., & Mosca, A. (2014). Polypropylene/organoclay/SEBS nanocomposites with toughness–stiffness properties. *RSC Advances*, *4*(13), 6573-6579.
- Haydar U. Zaman, H. U., Hun, P. D., Khan, R. A., & Yoon, K. B. (2012). Morphology, mechanical, and crystallization behaviors of micro-and nano-ZnO filled polypropylene composites. *Journal of Reinforced Plastics and Composites*, *31*(5), 323-329.
- Ahmed, J.; Arfat, Y.A.; Al-Attar, H.; Auras, R.; Ejaz, M. Rheological, structural, ultraviolet protection and oxygen barrier properties of linear low-density polyethylene films reinforced with zinc oxide (ZnO) nanoparticles. Food Packag. Shelf Life 2017, 13, 20–26.
- Abou-Kandil, A. I., Awad, A., & Mwafy, E. (2015). Polymer nanocomposites part 2: Optimization of zinc oxide/high-density polyethylene nanocomposite for ultraviolet radiation shielding. *Journal of Thermoplastic Composite Materials*, *28*(11), 1583-1598.

- Dhawan, V., Singh, S., & Singh, I. (2013). Effect of natural fillers on mechanical properties of GFRP composites. *Journal of Composites*, *2013*.
- Hanemann, T., & Szabó, D. V. (2010). Polymer-nanoparticle composites: from synthesis to modern applications. *Materials*, *3*(6), 3468-3517.
- Pantani, R.; Gorrasi, G.; Vigliotta, G.; Murariu, M.; Dubois, P. PLA-ZnO nanocomposite films: Water vapor barrier properties and specific end-use characteristics. Eur. Polym. J. 2013, 49, 3471–3482
- Díez-Pascual, A.; Díez-Vicente, A. Poly (3-hydroxybutyrate)/ZnO bionanocomposites with improved mechanical, barrier and antibacterial properties. Int. J. Mol. Sci. 2014, 15, 10950–10973.
- Basu, A., Nazarkovsky, M., Ghadi, R., Khan, W., & Domb, A. J. (2017). Poly (lactic acid)-based nanocomposites. *Polymers for Advanced Technologies*, *28*(8), 919-930.
- Onuoha, C., Onyemaobi, O. O., Anyakwo, C. N., & Onuegbu, G. C. (2017). Effect of filler content and particle size on the mechanical properties of corn cob powder filled recycled polypropylene composites. *Am J Eng Res*, *6*, 72-79.
- Karapappas, P., Vavouliotis, A., Tsotra, P., Kostopoulos, V., & Paipetis, A. (2009). Enhanced fracture properties of carbon reinforced composites by the addition of multi-wall carbon nanotubes. *Journal of Composite Materials*, *43*(9), 977-985.
- Prasert, A., Sontikaew, S., Sriprapai, D., & Chuangchote, S. (2020). Polypropylene/ZnO nanocomposites: Mechanical properties, photocatalytic dye degradation, and antibacterial property. *Materials*, *13*(4), 914.
- Awad A, Abou-Kandil AI, El Sabbagh I, et al. Polymer nanocomposites part 1: structural characterization of ZnO nanoparticles synthesized via novel calcination method, Accepted, Journal of Thermoplastic Composite Materials 2015; 28(9): 1343–1358.
- Kim, I., Viswanathan, K., Kasi, G., Sadeghi, K., Thanakkasaranee, S., & Seo, J. (2019). Poly (lactic acid)/ZnO bionanocomposite films with positively charged ZnO as potential antimicrobial food 9packaging materials. *Polymers*, *11*(9), 1427.
- Prabhu, S., & Poulose, E. K. (2012). Silver nanoparticles: mechanism of antimicrobial action, synthesis, medical applications, and toxicity effects. *International nano letters*, *2*(1), 1-10.
- Palza, H. (2015). Antimicrobial polymers with metal nanoparticles. *International journal of molecular sciences*, *16*(1), 2099-2116

مادة مركبة ومادة مركبة نانوية من البولي إيثيلين منخفض الكثافة و بيروكسيد الزنك محضر بطريقة الصب: الخصائص الحرارية والميكانيكية والمورفولوجية (الشكلية) .

اعداد : هنبال موسى عيسى منصور .

اشراف : د. أحمد جبارين و أ.د. فؤاد الريماوي .

ملخص :

تعتبر المواد البلاستيكية المركبة والمواد البلاستيكية المركبة النانوية ذات الحشو غير العضوي مثل بيروكسيد الزنك مجالات بحثية جديدة ومحفزة بسبب مزيج مبتكر من الخصائص التي بين البوليمر والحشو الناشئة عن تطبيق حشو غير عضوي وحشو بحجم النانو متر داخل مصفوفة البوليمر. تبحث الدراسة الحالية في تأثير التركيز المختلف لجزيئات بيروكسيد الزنك (ZnO_2) والجسيمات النانوية على الخصائص الشكلية (المورفولوجيا) والحرارية والميكانيكية والخصائص المضادة للبكتيريا للمادة المركبة بولي إيثيلين منخفض الكثافة. تم تحضير تركيبات مختلفة من مركبات $LDPE / ZnO_2$ و $LDPE / nano\ ZnO_2$ بتقنية cast solution بتركيز بيروكسيد الزنك (1٪ ، 3٪ و 5٪) للمادة المركبة و (0.5٪ ، 1٪ ، 1.5٪ ، 3٪ و 5٪.) للمادة المركبة النانوية. تم تصنيع الجسيمات النانوية ZnO_2 باستخدام ثلاث طرق مختلفة ، الأولى بطريقة reflux method تستخدم البولي إيثيلين أمين capping agent والثانية ايضا بطريقة reflux method ولكن بدون استخدام capping agent والأخيرة بطريقة sol-gel method. تم اختيار reflux method بدون capping agent للمادة المركبة النانوية المحضرة لهذه الدراسة لأنها تحتوي على مردود جيد من التفاعل مقارنة بالطرق الأخرى ولا يوجد تأثير خارجي كعامل تغطية يؤثر على خصائصها عند توزيعها داخل مصفوفة البوليمر.

تم تحليل جسيمات الزنك بيروكسيد ZnO_2 النانوية المُصنَّعة بحيود الأشعة السينية (XRD) ، ومجهر المسح الإلكتروني (SEM) ، والتحليل الطيفي بالأشعة تحت الحمراء (FTIR) ، والمسح الحراري التفاضلي (DSC). تم الحصول على جزيئات نانوية مكعبة عالية البلورية نمت في شكل شبه كروي بمتوسط حجم حوالي 81 نانومتر لطريقة reflux بدون capping agent و 47 نانومتر لطريقة reflux مع capping agent و 55 نانومتر لطريقة sol-gel بناءً على بيانات SEM و XRD. وجد بواسطة DSC أن عينات ZnO_2 تحولت إلى ZnO عند حوالي 230-238 درجة مئوية. تمت مناقشة الاهتزازات المرصودة بواسطة FTIR في مسحوق نانو ZnO_2 ومقارنتها بالتقارير السابقة واقترحت نقاء جزيئات بيروكسيد الزنك النانوية الاصطناعية من المواد المتفاعلة. تشير نتائج التحليلات المورفولوجية للمادة المركبة إلى أن جزيئات بيروكسيد الزنك موزعة ومدمجة في مصفوفات المادة المركبة ولكنها لا تظهر بشكل جيد على السطح ، بينما يظهر التوزيع في المادة المركبة النانوية بشكل جيد على البولمير بشكل كلي مما يعني ان المادة المركبة النانوية افضل تشتتا من المادة المركبة . تؤدي إضافة حشو ZnO_2 في المواد المركبة والمركبة النانوية إلى تحسينات كبيرة في درجة التبلور بسبب ان الحشو يمكن أن يعمل كعامل نواة و تظهر نتائج الخصائص الميكانيكية أن tensile properties

للمادة المركبة النانوية ZnO_2 / LDPE أعلى من تلك الخاصة بالمادة المركبة ZnO_2 / LDPE باستثناء yield strength مما يعني أن المادة المركبة يمكن أن تتحمل الضغط العالي دون تشوه دائم للبلاستيك مقارنة بالمادة المركبة النانوية. وجد أن البولي إثيلين منخفض الكثافة بدون أي حشو حقق tensile strength قدره 4.94 ميجا باسكال وزادت للمادة المركبة النانوية ZnO_2 / LDPE مع زيادة تركيز بيروكسيد الزنك (ZnO_2) حتى الوصول إلى أعلى قيمة tensile strength 5.28 ميجا باسكال عند 5٪ من الجسيمات النانوية. بينما تنخفض tensile strength للمركبات مع زيادة تركيز مسحوق ZnO_2 وتنخفض إلى 4.35 ميجا باسكال عند 5٪ جزيئات بيروكسيد الزنك. وجد أن Elastic modulus للمادة المركبة ZnO_2 / LDPE والمادة المركبة النانوية تزداد تدريجياً مع تركيز ZnO_2 ، وتم الحصول على أعلى مجموعة من القيم لتركيز 5٪ من بيروكسيد الزنك للمادة المركبة النانوية بقيمة معامل 0.124 جيجا باسكال مقارنة بـ 0٪ بقيمة 0.103 جيجا باسكال. علاوة على ذلك ، انخفضت نسبة elongation at fracture بشكل طردي مع زيادة تركيز بيروكسيد الزنك للمادة المركبة من 36٪ إلى 29٪ وللمادة المركبة النانوية من 48٪ إلى 42٪. لسوء الحظ ، لم يُظهر التوصيف المضاد للبكتيريا للمادة المركبة والمركبة النانوية أي منطقة من التثبيط على اقراص أجار للمركبات والمركبات النانوية ضد البكتيريا الهوائية واللاهوائية التي تمت دراستها. يشير هذا إلى أن جزيئات بيروكسيد الزنك والجسيمات النانوية لا تأثير لخصائصها المضادة للبكتيريا عند دمجها مع البولي إيثيلين منخفض الكثافة في دراستنا.